THESIS ON CIVIL ENGINEERING F32

Discrete Analysis of Single-Pylon Suspension Bridges

MARTTI KIISA

TUT
PRESS

TALLINN UNIVERSITY OF TECHNOLOGY
Faculty of Civil Engineering
Department of Transportation

The dissertation was accepted for the defence of the degree of Doctor of Philosophy in Engineering on 02.05.2011.

Supervisor: Professor Siim Idnurm (PhD)
Chair of Bridge Construction, Department of Transportation, Faculty of Civil Engineering, Tallinn University of Technology, Estonia

Adviser: Associate Professor Juhan Idnurm (PhD)
Chair of Bridge Construction, Department of Transportation, Faculty of Civil Engineering, Tallinn University of Technology, Estonia

Opponents: Associate Professor Algirdas Juozapaitis (PhD)
Department of Bridges and Special Structures, Faculty of Civil Engineering, Vilnius Gediminas Technical University, Lithuania

Senior Research Scientist Arvi Ravasoo (PhD)
Mechanics and Applied Mathematics Department, Institute of Cybernetics, Tallinn University of Technology, Estonia

Defence of the thesis: 10.06.2011.

Declaration:
Hereby I declare that this doctoral thesis, my original investigation and achievement, submitted for the doctoral degree at Tallinn University of Technology has not been submitted for any academic degree.

Martti Kiisa 

Euroopa Liit
Euroopa Sotsiaalfond

Eesti tuleviku heaks

ISSN 1406-4766
ISBN 978-9949-23-104-1 (publication)
ISBN 978-9949-23-105-8 (PDF)

EHITUS F32

Ühe pülooniga rippsildade diskreetne analüüs

MARTTI KIISA

TTÜ
KIRJASTUS

CONTENTS

List of tables

List of figures

INTRODUCTION

The aim of the thesis. The overall aim of this doctoral thesis is to present an algorithm to calculate the internal forces and deformations of a statically loaded single-pylon suspension bridge by use of discrete analysis. The more detailed aims of the thesis are the following:

- to present an analytical solution to the internal forces and deformations of an elastic cable in the case of static loading, using discrete analysis and describing the corresponding calculation problems;
- to work out a numerical design method, which can be applied in the practical work of engineers, and to compare the result with the analytical solution;
- combining discrete and, to a small extent, continuous mathematical structures (to exploit the advantages of both of them) to describe the co-operation of a cable and stiffening girder as a two-span suspension bridge;
- to check the results experimentally.

Topicality of the problem. Worldwide, suspension bridges are structures with the longest span – almost two kilometres, however, suspension structures with several times longer spans are being planned. Therefore, it is topical to develop the corresponding calculation methods, since the traditional geometrically linear calculation methods are not adequately precise to be applied for structures with extra long spans and large deformations. Cable-supported structures usually have large deformations and to obtain sufficiently precise calculation results, it is inevitable to consider geometric non-linearity.

Although discrete analysis requires high computational efficiency, it is possible (unlike with continuous model) to consider more precisely the complicated load combinations and types. Therefore, the main cable is regarded as a discrete mathematical structure, where concentrated loads affect a cable through hangers. To a small extent, a continuous method in the form of a universal equation of a stiffening girder's elastic curve has been used, because it enables a considerable reduction of the calculation capacity related to a stiffening girder. As the novelty of the work is primarily related to the development of discrete analysis, the title of the doctoral thesis is also in direct association.

The author believes that preference can be given to some calculation methods over others or they will be abandoned in practice (e.g. because of problems with preciseness and calculation capacity) only after achieving a level, in which the methods can be adequately compared. Computational capacity is a fast advancing area, whereas a calculation technique abandoned ten years ago as being impractical, may prove the most efficient one after some minor

improvements. As long as the contrary has not been proved, it is reasonable and necessary to develop calculation techniques in a stable and consistent way.

Novelty of the thesis. The novelty of the thesis is most obvious in two fields:

- development of the numerical method of discrete analysis to find out the internal forces and deformations of the elastic cable;
- elaboration of the calculation algorithm to describe the behaviour of a single-pylon suspension bridge.

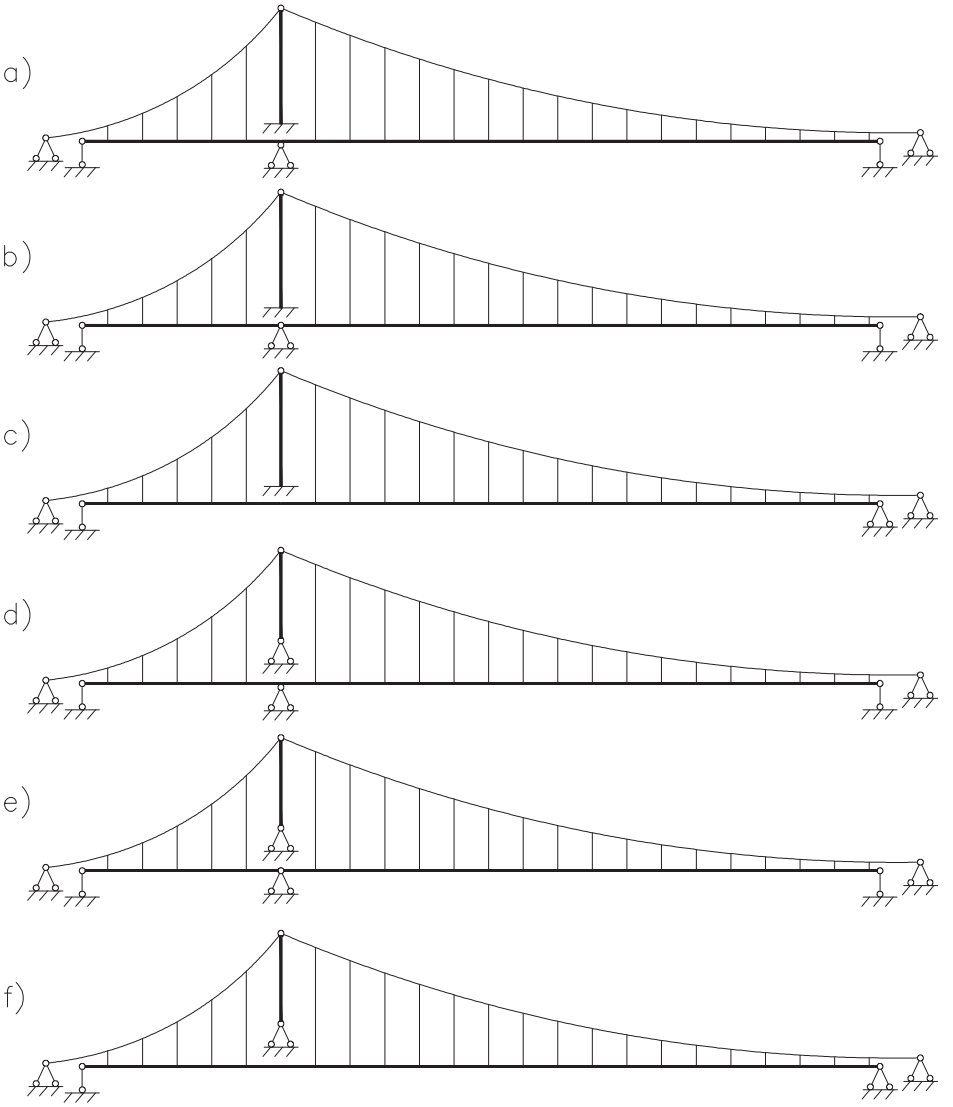

Figure 1. Design schemes of the suspension bridges under examination in this thesis

Short overview of the thesis. The behaviour of a suspension structure under static loading has been investigated, whereas dynamical behaviour and detailed dimensioning of components have not been covered. Since this thesis examines the classical suspension bridges with the main cables anchored in the ground (not in the ends of stiffening girders), the hangers being vertical and the main cables stiffened only by stiffening girders, the emphasis is upon design schemes described in Figure 1.

In addition, the thesis includes calculation examples to illustrate and explain the theoretical part. A model test in scale 1:25 has been carried out to check the validity of the developed calculation method. The calculation examples are interrelated, comprising a step-by-step solution process of the girder-stiffened suspension structure. To characterise the interrelations and tendencies of functions, the calculation examples are supplemented by reference data for different parameters (e.g. cable's different moduli of elasticity.) For the sake of entirety, the model test parameters proceed from the calculation examples. A short overview of the history and types of cable-supported bridges is also provided.

Background of the topic. In this thesis, the most general term "cable-supported structures" has been used, including different suspension and cable-stayed structures as well as their combinations. In the structures like these, most of the loads are received by the cables that are mostly tensioned. A cable-supported structure is often stiffened, using stiffening girders (trusses) and/or combined cable systems for this purpose. In a different field of study, the utilization of cables with flexural rigidity and development of the corresponding calculation methods are covered [Fürst, Marti, Ganz 2001; Grigorjeva, Juozapaitis, Kamaitis 2004, 2006, 2010a, 2010b; Juozapaitis, Idnurm, S., Kaklauskas, Idnurm, J., Gribniak 2010].

The present thesis is a continuation of the research on cable-supported structures (roofs, hoisting masts, bridges), which started at the end of the 1950s at Tallinn University of Technology (hereinafter: TUT). Designing, testing and erecting of the hoisting masts of reactors and song festival tribunes in Tallinn and Tartu, as well as working out solutions of the fixed link of Saaremaa are only a few examples of the projects. Research work has been conducted (theoretical investigations and experimental investigations on large-scale models), publications issued and master's and doctor's degrees defended during the decades [Kulbach 2007a, 2007b]. Therefore, reference is made to continuity of research in TUT, as well as to the existence of different schools of thought and calculation methods in this field. In the course of fifty years, many fields of cable-supported structures have been investigated by Valdek Kulbach [Kulbach 1973, 2007a][1], Johannes Aare [Aare, Kulbach 1984], Heinrich Laul, Karl Õiger [Õiger 1992], Allan Sumbak, Jüri Engelbrecht [Engelbrecht 1968], Arvi Ravasoo [Ravasoo 1971], Urmas Mänd [Mänd 1974], Andres Talvik [Talvik,

[1] Here only a selection of the most significant publications is presented.

A. 1982], Tiina Hallang, Ahti Lääne, Ivar Talvik [Talvik, I. 1990], Peeter Paane, Indrek Tärno, Siim Idnurm, Juhan Idnurm [Idnurm, J. 2004], Egon Kivi [Kivi 2009].

International and regional publications on cable-supported structures provide a comprehensive coverage of thorough research conducted by K. Õiger and V. Kulbach [Õiger 1992; Kulbach 2007a].

The discrete analysis for calculating cable-supported bridges has been developed in TUT mostly by Juhan Idnurm and Valdek Kulbach, whose earlier investigations provided an initial source for this thesis.

My most sincere thanks belong to my supervisor Professor Siim Idnurm, a good advisor and consultant, Assistant Professor Juhan Idnurm and Mr Evald Kalda, who assisted in carrying out the model test. I am very thankful to my family, whose support and encouragement has helped me greatly throughout my studies.

1. OVERVIEW OF CABLE-SUPPORTED BRIDGES

1.1 Suspension bridges

As far as the span length is concerned, cable-supported bridges are indisputable leaders nowadays. Most of the carrying elements are tensioned and this enables slender structures to be achieved. Cable-supported bridges can be divided into suspension, cable-stayed and combined systems.

Suspension bridges were first built at the beginning of our era in China, India and probably in South America, but the span length was limited because of insufficient qualities of natural building materials (bamboo, leather) and the lack of stiffening elements [Chen, Duan 1999; Matve 1978; Tang 2010; Virola 1999a]. Up to the 19th century, designing of suspension bridges was art rather than science [Gimsing 1997]. The first substantial calculation techniques were developed by the end of the 19th century, and since then the development has been continuous (J. A. Roebling, W. J. M. Rankine, M. Levy, J. Melan, L. S. Moisseiff, F. Lienhard etc.). Main emphasis has been placed on the studies of the geometrically non-linear behaviour of structures, as well as on the improvement of aerodynamics.

Figure 2. The Akashi-Kaikyo Bridge in Japan (photo: Kim Rötzel)

At the beginning of the 19th century, USA became the greatest developer of suspension bridges. In 1809 and 1816, the suspension bridges with the main span lengths of 74 m and 124 m were built in Philadelphia. In 1926 the limit of 500 m was exceeded (the Benjamin Franklin Bridge – 533 m) and only five years later the George Washington Bridge was built, the main span length of

which was more than 1 km (1067 m). After the length records had been gained by the Golden Gate Bridge (in 1937; 1280 m) and the Verrazano-Narrows Bridge (in 1964; 1298 m), it was time for Europeans to stand out. The longest suspension bridges in Europe (after completion, these were also the longest ones worldwide) are the Humber Bridge in Great Britain (a span of 1410 m; built in 1981) and the Great Belt Bridge in Denmark (1624 m; 1998). The latter could enjoy the status of the longest bridge for less than a year: in the same year, the Akashi-Kaikyo Bridge with the longest-ever span of 1991 m was built in Japan (Figure 2). A historical overview of the development of suspension bridges is presented in Table 1.

Table 1. Span records[2] of the suspension bridges since 1705 [Chen, Duan 1999; Tang 2010; Virola 1999a]

Period	**Bridge**	**Span [m]**	**Location**
1705-1816	Luding	103	China
1816-1820	Schuylkill	124	USA
1820-1826	Union	137	Great Britain
1826-1834	Menai	176	Wales
1834-1849	Grand Pont	273	Switzerland
1849-1866	Wheeling	308	USA
1866-1869	Cincinnati-Covington (Roebling)	322	USA
1869-1883	Niagara Clifton (Falls View)	386	USA
1883-1903	Brooklyn	486	USA
1903-1924	Williamsburg	488	USA
1924-1926	Bear Mountain	497	USA
1926-1929	Benjamin Franklin	533	USA
1929-1931	Ambassador	564	USA
1931-1937	George Washington	1067	USA
1937-1964	Golden Gate	1280	USA
1964-1981	Verrazano-Narrows	1298	USA
1981-1998	Humber	1410	Great Britain
1998	Great Belt (East)	1624	Denmark
1998-	Akashi-Kaikyo (Pearl)	1991	Japan

The carrying elements of a suspension bridge are the following: parabolic main cable(s), stiffening girder(s) or trusses connected to the main cable by hangers (hangers are mostly vertical), pylon(s) and anchoring blocks where cables are anchored (Figure 3).

Bridges may be either single-span or multi-span. The main cable is commonly anchored to separate-standing anchor blocks, or seldom to a stiffening girder – the so-called self-anchoring system (e.g. the Konohana Bridge in Japan with a main span of 300 m completed in 1990).

[2] According to different sources span lengths and dates may differ.

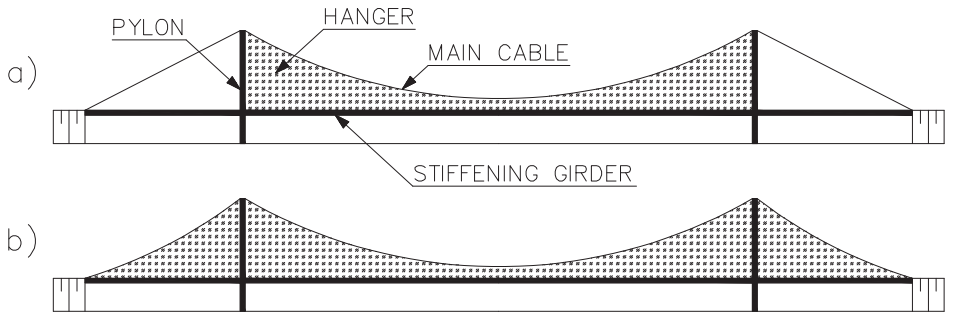

Figure 3. The most popular types of a suspension bridge: a) with non-supported and b) supported side spans [Idnurm, J. 2004]

The ratio of the sag of the main cable and the span length is between 1/12...1/8 [Kulbach 2007a]. Most frequently, the main cables are placed on the edges of the bridge deck. Mostly, long-span suspension bridges have two cables placed side by side; few have four cables (e.g. the George Washington Bridge). Suspension bridges with shorter spans may have one cable (the Konohana Bridge) or three cables (the Rodenkirchen Bridge in Germany, with 378-m span after widening in 1995). Although there is some evidence of using iron chains in ancient China and India, it was only after two millenniums that improvement of industrial manufacturing of wrought iron enhanced the development of suspension bridges. The main load-carrying elements of the first modern suspension bridges of the 18th and 19th centuries were mostly made of chains. One of the most outstanding examples was the Menai Bridge with a span of 176 m, designed in 1826 by engineer T. Telford [Gimsing 1997], which had chains assembled from wrought iron eye-bars. Worldwide, the longest span (339 m) of the suspension bridge made of chains is the Hercilio Luz Bridge in Florianopolis (Brazil) built in 1926 [Virola 1999a]. It was only in 1823 when the first known modern suspension bridge with cables composed of drawn iron wires designed by engineer M. Seguin was built in Geneva [Gimsing 1997]. In 1883, the Brooklyn Bridge was completed in the USA, having the longest span of 486 m in the world. Then the supporting cables were made of steel wires with the tensile strength up to 1100 MPa, whereas today the tensile strength of wires has nearly doubled – the cables of the Akashi-Kaikyo Bridge, completed in 1998, are made of the wires with the tensile strength of 1800 MPa [Virola 1999a]. Nowadays, engineers are trying to develop a steel wire with the tensile strength of 2000 MPa, also potential use of carbon fibre cables is being studied [Gimsing 1997; Virola 1999a]. For the first time in the world the diameter of the main cable exceeded 1-metre limit in 1988, when the Minami Bisan-Seto Bridge with a span of 1100 m was built (for comparison: the Akashi-Kaikyo Bridge – 1122 mm).

A stiffening girder (truss) plays an essential role not only in stiffening the main cable(s), but also in ensuring the stability of the whole bridge when vibration occurs (both longitudinal and torsional vibrations). It is high

slenderness and small rigidity of a stiffening girder that has caused the collapse of bridge constructions due to wind. In the middle of the 19th century engineer John A. Roebling was one of the first to succeed in stabilising the suspension bridge to wind load [Tang 2010]. In the middle of the 20th century S. Hardesty, H. E. Wessmann, F. Bleich, F. Farquharson, T. Von Karman, A. Selberg and others studied the aerodynamic problems of suspension bridges and worked out solutions [Gimsing 1997]. One of the most well-known accidents was the collapse of the Tacoma Narrows Bridge in 1940. The bridge was finished four months before the collapse, and with its 853 m main span it was the third longest bridge in the world. The main reason of the collapse was the bridge deck, which was too slender, had small rigidity and rectangular cross-section [Virola 2002b]. While the bridge had a span length of $L = 853{,}44\,\text{m}$, superstructure height $H = 2{,}44\,\text{m}$ and width $B = 11{,}89\,\text{m}$, the corresponding ratios were $L/H = 350$ and $L/B = 72$. The Golden Gate Bridge (the main span 1280 m), which was finished in 1937, was also considered to be a relatively slender structure, but the corresponding characteristics were $L/H = 168$ and $L/B = 47$ [Virola 2002b]. To avoid similar disasters, bridge decks of higher rigidity and/or streamlined superstructure have been constructed later. The Severn Bridge in Great Britain (the main span 988 m, completed in 1966) was the first long-span suspension bridge in the world, which had a streamlined box girder bridge deck to withstand wind loads [Virola 1999a]. The ratios were $L/H = 324$ and $L/B = 43$ [Virola 2002b]. Improvement of the streamlined stiffening box girder has resulted in the characteristics $L/H = 497$ and $L/B = 43$ for the Runyang South Bridge (the main span 1490 m), which was built in China in 2005 [Virola 2002b].

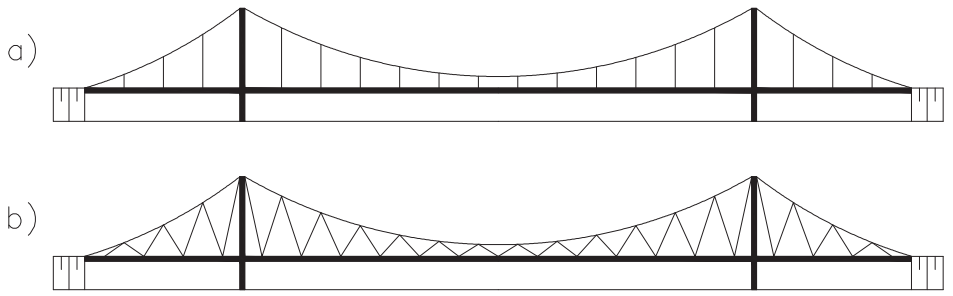

Figure 4. Hangers can be a) vertical or b) inclined [Idnurm, J. 2004]

The main cable and the stiffening girder are connected by hangers (Figure 4). The hangers are usually placed at distances of 6...50 m and the number of them is mostly between 8...30 [Kulbach 2007a]. Anchoring cables can be connected to stiffening girders by hangers (but not always); neither should hangers always be vertical. Inclined hangers have higher capacity of suppressing vibration due to traffic and wind load. The most well-known recent bridge of this type is the Humber Bridge (built in 1981). To increase rigidity, grid layout of hangers has

been used – e.g. the San Marcos Bridge in El Salvador (finished in 1952, span lengths 76+159+204+159+76 m).

The function of pylons is to fix the cable. Pylons are made either of steel (the height record belongs to the Akashi-Kaikyo Bridge with 283 m) or reinforced concrete (the Great Belt Bridge – 254 m). The support of the pylon can be fixed or hinged. In suspension bridges, the optimum ratio of pylon height and span is ~0,10 [Gimsing 1997].

1.2 Cable-stayed bridges

The history of cable-stayed bridges dates back to the beginning of the 17th century, when a chain-supported timber bridge was built in Venice [Idnurm, J. 2004]. Insufficient understanding of calculation methods hindered the development of cable-stayed bridges, and after a few cable-stayed bridges had collapsed in the first quarter of the 19th century, the development stopped. In the first half of the 20th century an essential advance in the method of design took place (F. Dischinger, F. de Miranda, R. Morandi, F. Leonhardt and others), and this triggered the construction of cable-stayed bridges with increasingly longer spans.

The Strömsund Bridge (main span 183 m), constructed in Sweden by the design of a German engineer Franz Dischinger in 1956, is considered to be the first contemporary cable-stayed bridge [Tang 2010]. Since then, the popularity of cable-stayed bridges has constantly been growing and span lengths increasing. In the following period, slightly longer than a decade, several outstanding cable-stayed bridges were constructed in Germany. A 200-metre span limit was exceeded in 1959 (the Theodor Heuss Bridge in Germany with a 260-m span), and a 300-m limit in 1961 (the Severin Bridge in Germany – 302 m). Before the Saint-Nazaire Bridge in France exceeded a 400-m limit (404 m), span length records belonged to the bridges constructed in Germany – the Knie Bridge (in 1969; 320 m) and the Duisburg-Neuenkamp Bridge (1970; 350 m).

The last decade of the 20th century is featured by an active construction of outstanding cable-stayed bridges. First, the Ikuchi Bridge was completed in Japan (in 1991; 490 m), followed by the Skarnsund Bridge in Norway (1991; 530 m), which was the first bridge to exceed the limit of half a kilometre. The next record-holders were the Yangpu Bridge in China (1993; 602 m), the Normandy Bridge in France (1995; 856 m), and finally, the Tatara Bridge in Japan (1999), which held the record with its 890 metres for almost a decade.

It was only 17 years after the span length of a cable-stayed bridge exceeded a limit of 500 metres that the record span length had doubled. This was due to extremely fast economic development in China. The first cable-stayed bridge to exceed a span length of 1000 m was the Sutong Bridge in 2008 – 1088 m (Figure 5). Table 2 shows an overview of the development of the longest spans of cable-stayed bridges.

Table 2. Span records of the cable-stayed bridges since 1955 [Chen, Duan 1999; Tang 2010; Virola 1999b]

Period	Bridge	Span [m]	Location
1956-1959	Strömsund	183	Sweden
1959-1961	Theodor Heuss	260	Germany
1961-1969	Severin	302	Germany
1969-1970	Knie	320	Germany
1970-1975	Duisburg-Neuenkamp	350	Germany
1975-1983	Saint-Nazaire	404	France
1983-1986	Casado (Luna)	440	Spain
1986-1991	Alex Fraser (Annacis)	465	Canada
1991	Ikuchi	490	Japan
1991-1993	Skarnsund	530	Norway
1993-1995	Yangpu	602	China
1995-1999	Normandy	856	France
1999-2008	Tatara	890	Japan
2008-	Sutong	1088	China

Figure 5. The Sutong Bridge in China (photo: ANR2008)

With span lengths up to 1000 metres, cable-stayed bridges are considered even more economical than suspension bridges [Chen, Duan 1999]. The structure of a cable-stayed bridge is the following: cables attached to the pylons support a

stiffening girder. The cables are connected to the stiffening girders and massive anchorage in the ground becomes unnecessary (although a scheme with partially anchored cables has also been used). Cables can be placed on the vertical plane (or at a small angle to this) in parallel or as radials, as well as in a combination of these (Figure 6). Traditionally, cables are placed on both edges of the bridge deck, although a single cable line (on the longitudinal axis of the bridge deck) is becoming popular. This sets higher demands on the torsional rigidity of the bridge deck. While in the first contemporary cable-stayed bridges rather sparsely installed cables were used (e.g. the Strömsund Bridge), more closely installed cables have been preferred in the bridges constructed after the Friedrich Ebert Bridge was completed in 1967 [Tang 2010].

The pylons of cable-stayed bridges are usually higher than those of suspension bridges. For fan-shaped cable systems with light stiffening girders of steel the optimal pylon height and span ratio is about 0,16; with heavier concrete stiffening girders the ratio may increase to 0,25 [Gimsing 1997].

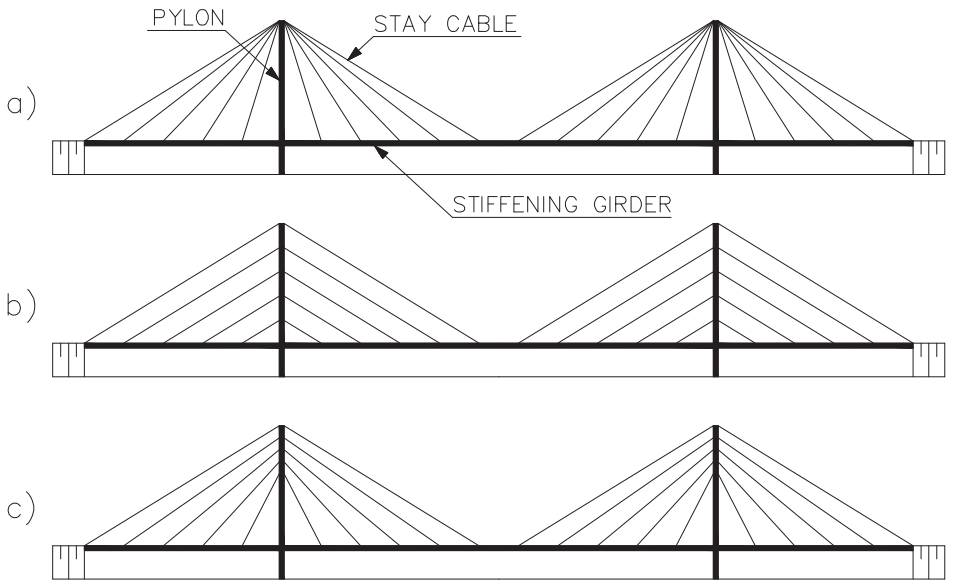

Figure 6. Types of the cable-stayed bridges: a) fan-type; b) harp-type; c) modified fan-type [Idnurm, J. 2004]

For architectural reasons curvilinear bridge decks and inclined pylons have been used – mainly on bridges, which are not designed for heavy traffic. Still, skilful experiments have been made with modern structure types. For example, a rigid connection of a pylon and a bridge deck (e.g. the Erasmus Bridge in Holland) and a massive inclined pylon (e.g. the Alamillo Bridge in Spain) have been constructed.

1.3 Combined cable-supported bridges

Combined systems of cable-stayed and suspensions bridges have also been used (Figure 7).

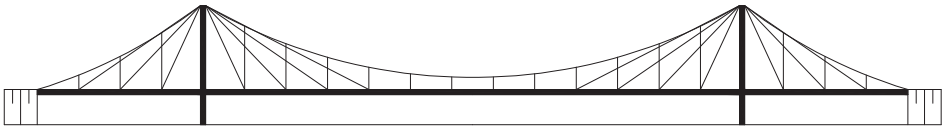

Figure 7. Combined cable-supported bridge [Idnurm, J. 2004]

One of the first known strengthenings of a suspension bridge with stay cables dates from the middle of the 19th century and it was used to cross the Niagara Falls [Chen, Duan 1999; Gimsing 1997]. This bridge, the span of which was 246 metres, was completed in 1855. It was designed by engineer J. A. Roebling who initiated studies and development of combined systems. The longest span of this bridge type, completed in Roebling's lifetime, was the Cincinnati-Covington Bridge (in 1866; span – 322 m). He also led the designing process of the longest bridge of this type so far – the Brooklyn Bridge (Figure 8), the spans of which are 286+486+286 m. However, the bridge was completed only 14 years after Roebling's death in 1883. In the period to follow, construction of combined systems stopped. Interest in combined systems was raised again due to the rapid development of calculation techniques, because a complicated cable system requires an excessive capacity of mathematical work. So far simplified calculations and an engineer's intuition have been used. Numerous studies have been dedicated to combined systems, although no spectacular designs have been realised yet.

The majority of the load is carried by a suspension cable; the main function of the stay cable is to facilitate the construction process of a bridge (a bridge is constructed as a cable-stayed bridge and a suspension cable is installed from the already existing bridge deck), as well as to be an additional stiffening element during service. However, the following scheme has also been used: first, a suspension cable is installed, and the rest of the structure, stay cables included, is hung on it. As for the longer bridges, it was in the construction of the Brooklyn Bridge, where a combined system was last used. However, a combined system should enable materials use more economically, since carrying loads with stay cables require less material than in the case of a suspension bridge with parabolic main cable and hangers, and it also makes it possible to use more efficiently the optimised pylon height [Gimsing 1997].

Another advantage of such a combined system is that on the one hand (concerning the horizontal forces of a suspension structure) it is a self-anchoring system (stay cables) and on the other hand, a ground-anchored system (parabolic cable). However, primarily due to constructional complexity, this structure type has been used in relatively rare cases.

Figure 8. The Brooklyn Bridge (photo: Jeffrey Bary)

It is also worth mentioning that the cable-supported bridges can have non-traditional design solutions. Here are some examples:

- one-pylon bridges (Figure 9), both with symmetrical and non-symmetrical spans (e.g. the Erasmus Bridge in Holland);
- multi-span bridges (the Hitsuishijima Bridge in Japan);
- different lengths of side spans (the Humber Bridge in Great Britain);
- pylons of different heights (the Minami Bisan-Seto Bridge);
- suspension and cable-stayed bridges, the pylon tops of which are connected with a horizontal cable (repeatedly used in the 19th century in France).

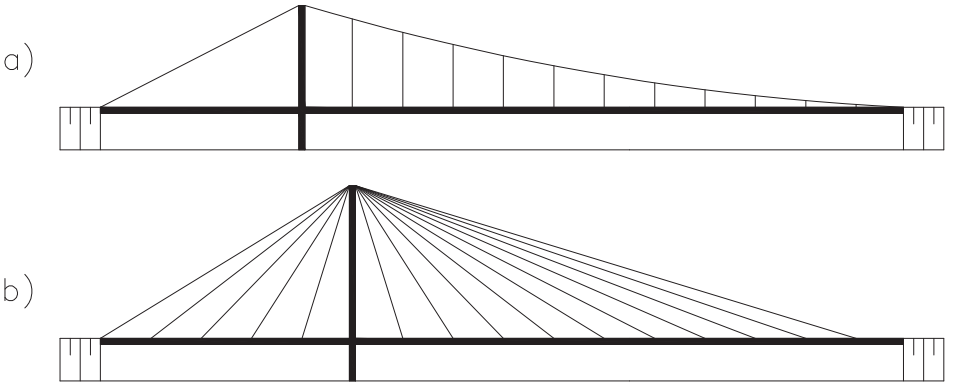

Figure 9. Single-pylon cable-supported bridges: a) suspension bridge and b) cable-stayed bridge

Today it is planned to construct bridges with considerably longer suspension spans. In 2005, Messina Bridge's design with a 3300-metre main span was completed [Tang 2010]. The proposed solutions for a bridge over the Strait of Gibraltar, which would connect Spain and Morocco, are the following: a suspension bridge with two successive 5-kilometre spans, and a huge cable-stayed bridge with an 8,4-kilometre span [Virola 2002a]. In Japan, plans have been made to build a bridge over the Tsugaru Strait, consisting of two successive suspension and cable-stayed bridges with 4-kilometre spans [Virola 2002a]. With the materials available, today it is possible to construct cable-stayed bridges with spans up to 3500 metres and suspension bridges with spans up to 7000 metres [Tang 2010].

2. DISCRETE ANALYSIS
2.1 Introduction

Mathematical structures may be divided into two groups: continuous and discrete.

Continuous structures rely on the concept of the real number and main attention is paid to the values of continuity and limit.

Discrete structures are based on the natural number. The branch of mathematics which investigates discrete structures is called discrete mathematics[3] (in contrast to continuous mathematics[4]). Because these structures are mostly finite, discrete mathematics is also called finite mathematics. [Palm 2003]

Continuous analysis does not require high computational efficiency, but it is complicated to describe the boundary conditions and to calculate the concentrated and asymmetric loads. Therefore, continuous analysis is most suitable for uniformly distributed loads to obtain exact results. In applied mathematics simplified formulas have also been developed for different distributed loads (e.g. the shape of square parabola, sinusoid) [Kulbach 2007a].

In discrete analysis the whole structure is separated to small pieces and mutual influences between them are described. The word "discrete" is used in the sense of "separated from each other", the opposite of "continuous"; it is also often used in the more restrictive sense of "finite" [Lovasz, Pelikan, Vesztergombi 2003]. The advantages of discrete analysis are that it is easy to describe different load types and combinations and to change the parameters of the structural elements (e.g. flexural rigidity). The most important disadvantage is the necessity to calculate complicated systems of equations and very often these systems converge slowly. At the same time the huge amount of equations may reduce the precision of the calculation results. Using analogous initial data, discrete analysis gives almost the same results as continuous analysis [Idnurm, J. 2004; Leonard 1988].

Mathematical methods can be analytic or numerical. The analytic function can be described using exact formulas. Very often in science the solution of the problem can not be expressed in an exact analytic form, or it is too complicated

[3] The keywords of discrete mathematics are: logic, sets, graphs, algebraic structures, relations, logical algebra, logical functions, combinatorial analysis [Lensen, Kruus 2006].

[4] Continuous mathematics is related to the continuous functions of the mathematical analysis, differential calculus, integral calculus [Lensen, Kruus 2006].

to be used in practice. In that case the approximated numerical methods can be used to solve the problem. [Vaarmann 2005]

Numerical methods are techniques by which mathematical problems are formulated so that they can be approximately solved with arithmetic operations. All numerical methods have one common characteristic: they invariably involve large numbers of tedious arithmetic calculations. With the development of fast, efficient digital computers, the role of numerical methods in engineering problem solving has increased dramatically in recent years. [Chapra, Raymond 2006; Janno 2008]

One of the most popular numerical discrete methods is a finite element method (FEM). The idea of FEM is that the continuous function, which describes some property of the structure, can be replaced with the approximated discrete structure. These "small pieces" are continuous and the functions of these bounded subregions can be linear, quadratic or cubic polynomial for example. Minimising the preassigned functional of the nodal points is the basis of calculating the value of the whole consistent function. [Kirs, Arjassov 1999; Lahe 1998]

In this thesis both analytic and numerical discrete analysis are used to describe the behaviour of the elastic cable. The purpose of the development of the numerical discrete analysis is to simplify the calculations in practice. The behaviour of the cable is described using the conditions of equilibrium for the nodal points and the deformations of the cable's segments. The universal equation of the elastic curve enables us to calculate the deflections and internal forces of the stiffening girder using the continuous analysis.

The process of stepwise approximation, known as an iterative method, is worked out to characterise the cooperation of the cable(s), stiffening girder(s) and pylon(s). The idea is to start with a reasonable initial approximation reflecting the problem and to proceed with a corrective procedure, producing an improved approximation. Thus, one iteration is completed. In the next iteration, the same corrective procedure is applied to the improved approximation, generating an even better one; and so on. [Breuer, Zwas 1993]

The following assumptions have been made in this thesis:

- stress-strain dependence of the material is linear;
- flexural rigidity of the cable is neglected;
- tension rigidity of the cable is invariable;
- cable segments between the nodal points are straight lines;
- hangers are vertical;
- flexural rigidity of the stiffening girder is invariable.

2.2 Behaviour of the cable

2.2.1 Initial balance of the cable

The initial balance (state) of the cable is the situation before deflection and it is marked with subscript "0".

The cable is loaded with concentrated forces (through the hangers) – i.e. the cable takes the configuration of a string polygon and cable segments between the nodal points are straight lines.

The source data for calculations are the coordinates of the starting and end point of the cable and the characterization of the loads (the value and the location). In addition it is necessary to describe another parameter – the total length of the cable or the coordinates of a random nodal point (mostly in the middle of the span).

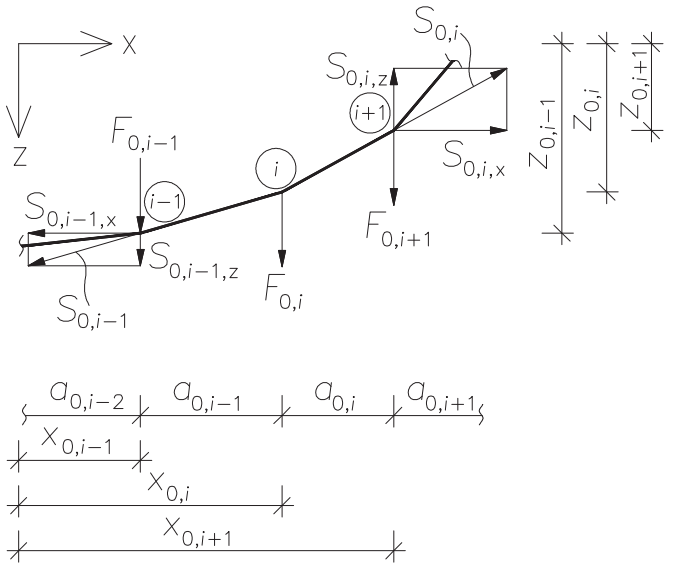

Figure 10. Initial discrete scheme of the cable [Idnurm, J. 2004]

Let us have a cable whose neighbouring nodes are denoted by indices $i-1$, i and $i+1$ (Figure 10) and observe the nodal point i of the cable. The nodal point is in equilibrium under the action of the internal forces of the two consecutive cable segments and the external concentrated load. Then the condition of equilibrium for the initial state may be presented in a vector form [Kulbach, Õiger 1986]:

$$\vec{F}_{0,i} + \vec{S}_{0,i} + \vec{S}_{0,i-1} = 0, \tag{1}$$

where

$\vec{F}_{0,i}$ – initial nodal load;

$\vec{S}_{0,i}$, $\vec{S}_{0,i-1}$ – initial internal forces of the cable segments.

The projections of the initial internal forces of each cable segment on the coordinate horizontal *x*-axis are equal. The projections of each force of the node on the coordinate vertical *z*-axis are

$$F_{0,i,z} = F_{0,i}, \tag{2}$$

$$S_{0,i,z} = H_0 \frac{z_{0,i+1} - z_{0,i}}{a_{0,i}} \text{ and} \tag{3}$$

$$S_{0,i-1,z} = H_0 \frac{z_{0,i-1} - z_{0,i}}{a_{0,i-1}}, \tag{4}$$

where

$F_{0,i,z}$ – projection of the initial nodal load on the coordinate *z*-axis;

$S_{0,i,z}$, $S_{0,i-1,z}$ – projections of the initial internal forces of the cable segments on coordinate *z*-axis;

H_0 – the projection of the initial internal force of the cable on the coordinate *x*-axis (the horizontal component);

$z_{0,i-1}$, $z_{0,i}$, $z_{0,i+1}$ – initial ordinates of the nodes of the cable (the ordinate and the abscissa of the point are the distances from the horizontal and the vertical axis in this thesis);

$a_{0,i-1}$, $a_{0,i}$ – initial horizontal distances between the nodes of the cable.

The algebraic sum of all the forces of the node *i* projected on the arbitrary axis must be zero if the nodal point is in equilibrium. After summing up the projections of all the forces of the node *i*, the equilibrium of the node can be presented as follows [Kulbach, Õiger 1986]:

$$F_{0,i} + H_0 \frac{z_{0,i+1} - z_{0,i}}{a_{0,i}} + H_0 \frac{z_{0,i-1} - z_{0,i}}{a_{0,i-1}} = 0 \tag{5}$$

or [Idnurm, J. 2004]

$$\frac{H_0 z_{0,i-1}}{a_{0,i-1}} - \frac{H_0 z_{0,i}}{a_{0,i-1}} + \frac{H_0 z_{0,i+1}}{a_{0,i}} - \frac{H_0 z_{0,i}}{a_{0,i}} + F_{0,i} = 0. \tag{6}$$

After regrouping and denoting $A_{0,i} = \frac{H_0}{a_{0,i-1}}$ and $B_{0,i} = \frac{H_0}{a_{0,i}}$, Equation (6) can be written as [Idnurm, J. 2004]

$$A_{0,i} z_{0,i-1} - \left(A_{0,i} + B_{0,i}\right) z_{0,i} + B_{0,i} z_{0,i+1} + F_{0,i} = 0. \tag{7}$$

This formula ties together the ordinates of the three sequential nodal points of the cable. It is possible to compose as many formulas as the total number of nodal points is. However, one more equation must be described because the horizontal component of the internal force of the cable H_0 is also unknown. This can be done using the reactions of the cable's supports. First of all the vertical reaction of the cable's support may be presented as follows [Gimsing 1997]:

$$V_{0,0} = V_{0,0,LT} - H_0 \frac{z_{0,0} - z_{0,n+1}}{L_0} = \frac{\sum_{i=1}^{n} F_{0,i}(L - x_{0,i})}{L_0} - H_0 \frac{z_{0,0} - z_{0,n+1}}{L_0}, \tag{8}$$

where

- $V_{0,0}$ – initial vertical support reaction of the cable at the starting point;
- $V_{0,0,LT}$ – vertical support reaction of the horizontal simple beam (at the starting point), which has the same span and loads as the cable;
- $z_{0,0}$ – initial ordinate of the starting point of the cable;
- $z_{0,n+1}$ – initial ordinate of the end point of the cable;
- L_0 – initial horizontal distance between the starting point and the end point of the cable;
- $x_{0,i}$ – initial horizontal distance between the force $F_{0,i}$ and the starting point of the cable.

At the same time the vertical reaction of the cable's support is equal to the projection of the initial internal forces of the first cable segment on the coordinate *z*-axis:

$$V_{0,0} = S_{0,0,z} = H_0 \frac{z_{0,1} - z_{0,0}}{a_{0,0}}, \tag{9}$$

where

- $z_{0,1}$ – initial ordinate of the load $F_{0,1}$;
- $a_{0,0}$ – initial horizontal distance between the starting point of the cable and the load $F_{0,1}$.

After regrouping Equations (8) and (9), H_0 takes the following form [Idnurm, J. 2004]:

$$H_0 = \frac{a_{0,0}\sum_{i=1}^{n} F_{0,i}(L_0 - x_{0,i})}{L_0(z_{0,1} - z_{0,0}) + a_{0,0}(z_{0,0} - z_{0,n+1})}. \tag{10}$$

Finally, the ordinates of all the node points of the cable can be found by solving the linear system of equations based on Equation (7):

$$\begin{cases} A_{0,1}z_{0,0} - (A_{0,1} + B_{0,1})z_{0,1} + B_{0,1}z_{0,2} + F_{0,1} = 0 \\ A_{0,2}z_{0,1} - (A_{0,2} + B_{0,2})z_{0,2} + B_{0,2}z_{0,3} + F_{0,2} = 0 \\ \ldots \\ A_{0,n-1}z_{0,n-2} - (A_{0,n-1} + B_{0,n-1})z_{0,n-1} + B_{0,n-1}z_{0,n} + F_{0,n-1} = 0 \\ A_{0,n}z_{0,n-1} - (A_{0,n} + B_{0,n})z_{0,n} + B_{0,n}z_{0,n+1} + F_{0,n} = 0 \end{cases}. \tag{11}$$

If the horizontal distances between the node points (i.e. hangers) of the cable are equal $\left(A_0 = A_{0,i} = B_{0,i} = \frac{H_0}{a_0} \right)$, Equation (11) takes a simpler form:

$$\begin{cases} A_0 z_{0,0} - 2A_0 z_{0,1} + A_0 z_{0,2} + F_{0,1} = 0 \\ A_0 z_{0,1} - 2A_0 z_{0,2} + A_0 z_{0,3} + F_{0,2} = 0 \\ \ldots \\ A_0 z_{0,n-2} - 2A_0 z_{0,n-1} + A_0 z_{0,n} + F_{0,n-1} = 0 \\ A_0 z_{0,n-1} - 2A_0 z_{0,n} + A_0 z_{0,n+1} + F_{0,n} = 0 \end{cases}. \tag{12}$$

Based on the calculation results of Example 1, i.e. if both the horizontal distances between the hangers and the concentrated loads of the cable are equal, then:

- the shape of the cable in the initial balance does not depend on the values of the concentrated loads;
- the ordinates of the nodal points of the cable do not depend on the total span of the cable;
- previous researches have been shown that the nodal points of the cable, when the supports of the cable are at the same level, are located on the quadratic parabola [Kulbach 2007a; Idnurm, J. 2004; Gimsing 1997; Bangash 1999; Leonard 1988]; Example 1 showed that if the supports are at different levels the nodal points are located on the quadratic parabola as well.

Taking into account these inferences, it is possible to calculate the ordinate of the arbitrary node analytically if the ordinates of three points are known:

$$\begin{cases} z_{0,0} = \varphi \times x_{0,0}^2 + \omega \times x_{0,0} + \gamma \\ z_{0,i} = \varphi \times x_{0,i}^2 + \omega \times x_{0,i} + \gamma \\ z_{0,\mathrm{p}} = \varphi \times x_{0,p}^2 + \omega \times x_{0,p} + \gamma \\ z_{0,n+1} = \varphi \times x_{0,n+1}^2 + \omega \times x_{0,n+1} + \gamma \end{cases}, \tag{13}$$

where

$z_{0,0}$, $x_{0,0}$ – given initial ordinate and abscissa of the starting point of the cable;

$z_{0,n+1}$, $x_{0,n+1}$ – given initial ordinate and abscissa of the end point of the cable;

$z_{0,i}$, $x_{0,i}$ – given initial ordinate and abscissa of the random point of the cable;

$z_{0,\mathrm{p}}$, $x_{0,\mathrm{p}}$ – initial ordinate and abscissa in question in the observable point of the cable;

φ, ω, γ – constants of the parabolic function.

The initial ordinate in question in the observable point of the cable:

$$z_{0,\mathrm{p}} = z_{0,n+1} + \frac{(z_{0,0} - z_{0,n+1})(x_{0,\mathrm{p}}^2 - x_{0,n+1}^2)}{(x_{0,0}^2 - x_{0,n+1}^2)} + \left[\frac{(z_{0,i} - z_{0,n+1})(x_{0,0}^2 - x_{0,n+1}^2) - (z_{0,0} - z_{0,n+1})(x_{0,i}^2 - x_{0,n+1}^2)}{(x_{0,i} - x_{0,n+1})(x_{0,0}^2 - x_{0,n+1}^2) - (x_{0,0} - x_{0,n+1})(x_{0,i}^2 - x_{0,n+1}^2)} \right] \times \left[(x_{0,\mathrm{p}} - x_{0,n+1}) - \frac{(x_{0,\mathrm{p}}^2 - x_{0,n+1}^2)}{(x_{0,0} + x_{0,n+1})} \right]. \tag{14}$$

The solution is exact only if the observable point locates at the node of a string polygon. All the points of the cable locate on the quadratic parabola only in a continuous analysis (Figure 11). If the observable point locates between the two nodes using discrete analysis, then the ordinates of the adjacent nodes can be calculated as

$$\frac{z_{0,i-1} - z_{0,i}}{z_{0,\mathrm{p}} - z_{0,i}} = \frac{x_{0,i} - x_{0,i-1}}{x_{0,i} - x_{0,\mathrm{p}}}. \tag{15}$$

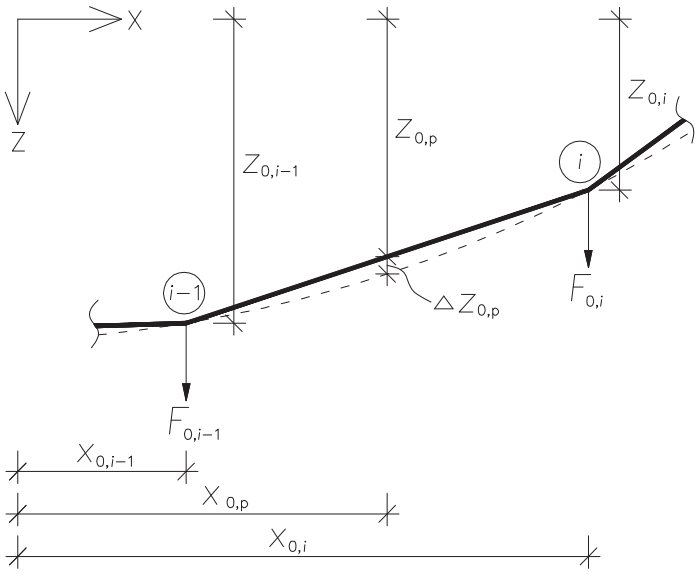

Figure 11. Differences between the continuous (dotted line) and the discrete design scheme

Example 1

Determine the internal forces of the cable in the initial balance illustrated in Figure E.1.1.

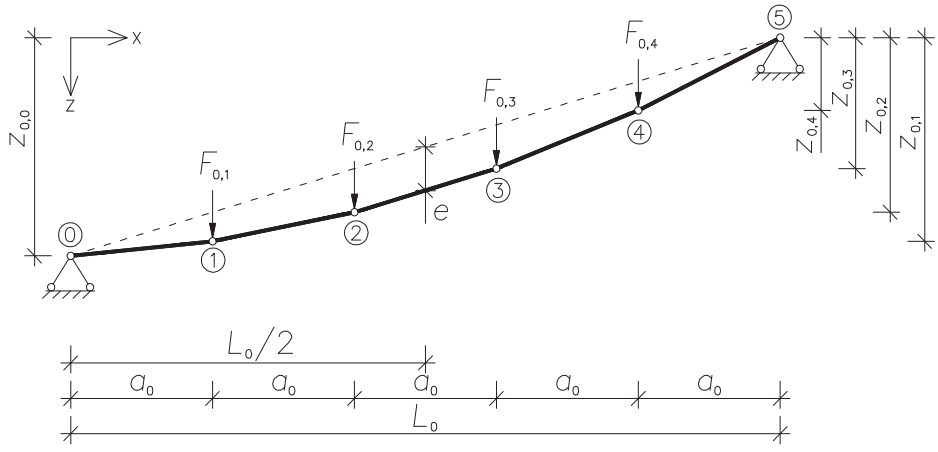

Figure E.1.1. Design scheme of Example 1

Source data:

- span: $L_0 = 50$ m;
- total amount of hangers: $n = 4$;
- horizontal distance between the hangers: $a_0 = 10$ m;
- ordinate of the starting point of the cable: $z_{0,0} = 15$ m;
- ordinate of the end point of the cable: $z_{0,5} = 0$;
- sag of the cable (in the middle): $e = 3$ m;
- initial nodal loads: $F_0 = F_{0,1} = F_{0,2} = F_{0,3} = F_{0,4} = 50$ kN.

The ordinate of node 3 is determined by

$$\frac{z_{0,0} + z_{0,5}}{2} + e = \frac{z_{0,2} + z_{0,3}}{2} \Rightarrow z_{0,3} = z_{0,0} + z_{0,5} + 2e - z_{0,2}.$$

The equilibrium conditions of the nodal points are obtained using Equation (12):

$$\begin{cases} A_0 z_{0,0} - 2A_0 z_{0,1} + A_0 z_{0,2} + F_0 = 0 \\ A_0 z_{0,1} - 2A_0 z_{0,2} + A_0 z_{0,3} + F_0 = 0 \\ z_{0,3} = z_{0,0} + z_{0,5} + 2e - z_{0,2} \\ A_0 z_{0,3} - 2A_0 z_{0,4} + A_0 z_{0,5} + F_0 = 0 \end{cases}.$$

The factor A_0 can be expressed from Equation (10):

$$A_0 = \frac{H_0}{a_0} = \frac{\sum_{i=1}^{n} F_{0,i}(L_0 - x_{0,i})}{L_0(z_{0,1} - z_{0,0}) + a_0(z_{0,0} - z_{0,n+1})} =$$

$$= \frac{F_0(L_0 - a_0) + F_0(L_0 - 2a_0) + F_0(L_0 - 3a_0) + F_0(L_0 - 4a_0)}{L_0(z_{0,1} - z_{0,0}) + a_0(z_{0,0} - z_{0,5})} =$$

$$= \frac{F_0(4L_0 - 10a_0)}{L_0(z_{0,1} - z_{0,0}) + a_0(z_{0,0} - z_{0,5})}.$$

Thus, the ordinates of the nodal points are

$$\begin{cases} z_{0,1} = \dfrac{12z_{0,0} + 10e}{15} = \dfrac{12\times 15 + 10\times 3}{15} = 14\ \text{m} \\ z_{0,2} = \dfrac{3z_{0,0} + 5e}{5} = \dfrac{3\times 15 + 5\times 3}{5} = 12\ \text{m} \\ z_{0,3} = \dfrac{2z_{0,0} + 5e}{5} = \dfrac{2\times 15 + 5\times 3}{5} = 9\ \text{m} \\ z_{0,4} = \dfrac{3z_{0,0} + 10e}{15} = \dfrac{3\times 15 + 10\times 3}{15} = 5\ \text{m} \end{cases}.$$

The horizontal component H_0 of the internal force of the cable can be calculated as

$$H_0 = a_0 A_0 = a_0 \frac{4F_0}{5z_{0,1} - 4z_{0,0} - z_{0,5} - 2e} = \frac{3F_0 L_0}{5e} = \frac{3\times 50\times 50}{5\times 3} = 500\ \text{kN}.$$

To examine the shape of the cable it can be assumed that the cable can be described analytically as follows: $z = \varphi\times x^2 + \omega\times x + \gamma$.

The constants of the quadratic equation using nodes 0, 2 and 5 are

$$\begin{cases} \varphi\times x_{0,0}^2 + \omega\times x_{0,0} + \gamma = z_{0,0} \\ \varphi\times x_{0,2}^2 + \omega\times x_{0,2} + \gamma = z_{0,2} \\ \varphi\times x_{0,5}^2 + \omega\times x_{0,5} + \gamma = z_{0,5} \end{cases} \Rightarrow \begin{cases} \varphi\times 0^2 + \omega\times 0 + \gamma = 15 \\ \varphi\times 20^2 + \omega\times 20 + \gamma = 12 \\ \varphi\times 50^2 + \omega\times 50 + \gamma = 0 \end{cases} \Rightarrow \begin{cases} \varphi = -1/200 \\ \omega = -1/20 \\ \gamma = 25 \end{cases}.$$

The analytical ordinates of the nodes 1, 3 and 4 using the calculated constants are

$$\begin{cases} z_{0,1} = \varphi\times x_{0,1}^2 + \omega\times x_{0,1} + \gamma = -\dfrac{1}{200}\times 10^2 - \dfrac{1}{20}\times 10 + 15 = 14\ \text{m} \\ z_{0,3} = \varphi\times x_{0,3}^2 + \omega\times x_{0,3} + \gamma = -\dfrac{1}{200}\times 30^2 - \dfrac{1}{20}\times 30 + 15 = 9\ \text{m} \\ z_{0,4} = \varphi\times x_{0,4}^2 + \omega\times x_{0,4} + \gamma = -\dfrac{1}{200}\times 40^2 - \dfrac{1}{20}\times 40 + 15 = 5\ \text{m} \end{cases}.$$

Consequently, the nodal points of the cable are located on the quadratic parabola.

2.2.2 Final balance of the cable

2.2.2.1 Exact equations of the cable in the final balance

After loading the cable with the additional loads ΔF_i, the nodes have displacements w_i and u_i (Figure 12). The condition of equilibrium in the final balance is

$$\vec{F}_i + \vec{S}_i + \vec{S}_{i-1} = 0, \tag{16}$$

where

$\vec{F}_i$ – final nodal load;

$\vec{S}_i$, $\vec{S}_{i-1}$ – final internal forces of the cable segments.

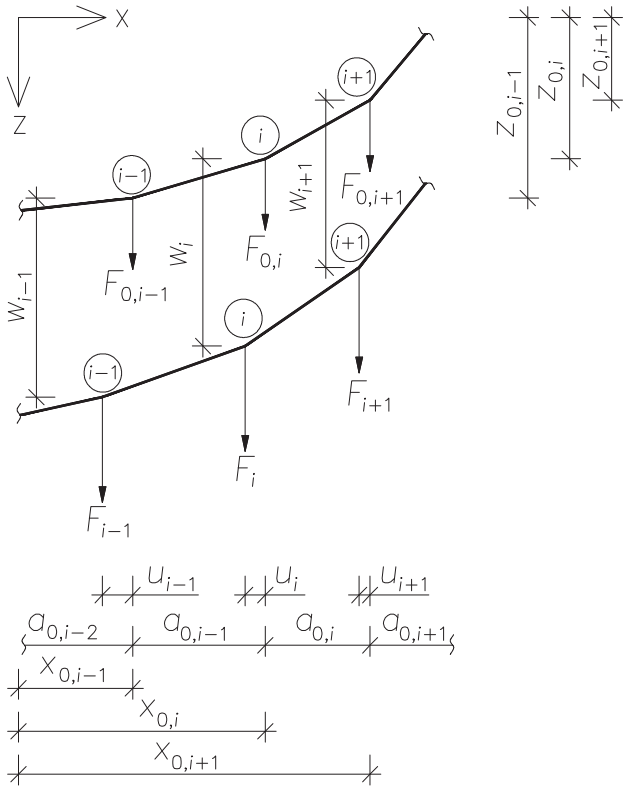

Figure 12. Final discrete scheme of the cable [Idnurm, J. 2004]

The total load F_i of the node in the final balance consists of the load in the initial balance $F_{0,i}$ and the complementary load ΔF_i [Kulbach, Õiger 1986]:

$$F_i = F_{0,i} + \Delta F_i. \tag{17}$$

As in Equation (5), the equilibrium of the node of the deformed cable can be expressed as follows:

$$F_i + H\frac{z_{0,i+1} + w_{i+1} - z_{0,i} - w_i}{a_{0,i} + u_{i+1} - u_i} + H\frac{z_{0,i-1} + w_{i-1} - z_{0,i} - w_i}{a_{0,i-1} + u_i - u_{i-1}} = 0, \tag{18}$$

where

F_i – final vertical nodal load (total);

H – projection of the final internal force of the cable on the coordinate x-axis (horizontal component);

u_{i-1}, u_i, u_{i+1} – horizontal displacements of the nodal points of the cable;

w_{i-1}, w_i, w_{i+1} – vertical displacements of the nodal points of the cable.

Additionally there is a need for extra equations to calculate H, w_i and u_i.

The relative deformation of the cable's segment can be found by using Hooke's law:

$$\begin{aligned}
\varepsilon_i &= \frac{\sigma_i}{E_\mathrm{c}} = \frac{1}{E_\mathrm{c}} \times \frac{S_i - S_{0,i}}{A_\mathrm{c}} = \frac{1}{E_\mathrm{c} A_\mathrm{c}} \left(\frac{H l_i}{a_i} - \frac{H_0 l_{0,i}}{a_{0,i}} \right) = \\
&= \frac{1}{E_\mathrm{c} A_\mathrm{c}} \left[\frac{H\sqrt{a_i^2 + \left(z_{i+1} - z_i\right)^2}}{a_i} - \frac{H_0\sqrt{a_{0,i}^2 + \left(z_{0,i+1} - z_{0,i}\right)^2}}{a_{0,i}} \right] = \\
&= \frac{1}{E_\mathrm{c} A_\mathrm{c}} \left[H\sqrt{1 + \left(\frac{z_{i+1} - z_i}{a_i} \right)^2} - H_0\sqrt{1 + \left(\frac{z_{0,i+1} - z_{0,i}}{a_{0,i}} \right)^2} \right] = \\
&= \frac{1}{E_\mathrm{c} A_\mathrm{c}} \left[H\sqrt{1 + \left(\frac{z_{0,i+1} + w_{i+1} - z_{0,i} - w_i}{a_{0,i} + u_{i+1} - u_i} \right)^2} - H_0\sqrt{1 + \left(\frac{z_{0,i+1} - z_{0,i}}{a_{0,i}} \right)^2} \right],
\end{aligned} \tag{19}$$

where

ε_i – strain of the cable segment;

σ_i – final stress of the cable segment;

E_c – modulus of elasticity of the cable;

A_c – cross-sectional area of the cable;

$S_{0,i}$, S_i – internal forces of the cable segment before and after lengthening;

$l_{0,i}$, l_i – length of the cable segment before and after lengthening;

a_i – final horizontal distance between the nodes of the cable (after lengthening).

The relative deformation can be also calculated using the displacements of the cable's nodal points:

$$\varepsilon_i = \frac{l_i}{l_{0,i}} - 1 = \frac{\sqrt{a_i^2 + \left(z_{i+1} - z_i\right)^2}}{\sqrt{a_{0,i}^2 + \left(z_{0,i+1} - z_{0,i}\right)^2}} - 1 = \\ = \frac{\sqrt{\left(a_{0,i} + u_{i+1} - u_i\right)^2 + \left(z_{0,i+1} + w_{i+1} - z_{0,i} - w_i\right)^2}}{\sqrt{a_{0,i}^2 + \left(z_{0,i+1} - z_{0,i}\right)^2}} - 1. \tag{20}$$

Equalising ε_i from Equations (19) and (20), we obtain the equation of the deformation compatibility in the form

$$\frac{1}{E_c A_c}\left[H\sqrt{1+\left(\frac{z_{0,i+1} + w_{i+1} - z_{0,i} - w_i}{a_{0,i} + u_{i+1} - u_i}\right)^2} - H_0\sqrt{1+\left(\frac{z_{0,i+1} - z_{0,i}}{a_{0,i}}\right)^2}\right] = \\ = \frac{\sqrt{\left(a_{0,i} + u_{i+1} - u_i\right)^2 + \left(z_{0,i+1} + w_{i+1} - z_{0,i} - w_i\right)^2}}{\sqrt{a_{0,i}^2 + \left(z_{0,i+1} - z_{0,i}\right)^2}} - 1. \tag{21}$$

Using Equations (18) and (21), it is possible to calculate w_i, u_i and H.

2.2.2.2 Simplified equations of the cable in the final balance

It is complicated to use exact analysis in the determination of the final balance because numerous cubic and quartic equations are needed to solve. Equations (18) and (21) can be simplified using numerical analysis.

Provided that $\left(u_{i+1} - u_i\right) << a_{0,i}$, Equation (18) takes the form of [Kulbach, Õiger 1986]

$$F_i + H\frac{z_{0,i+1} + w_{i+1} - z_{0,i} - w_i}{a_{0,i}} + H\frac{z_{0,i-1} + w_{i-1} - z_{0,i} - w_i}{a_{0,i-1}} = 0 \tag{22}$$

or [Idnurm, J. 2004]

$$\frac{H}{a_{0,i}}z_{0,i+1} - \frac{H}{a_{0,i}}z_{0,i} + \frac{H}{a_{0,i}}w_{i+1} - \frac{H}{a_{0,i}}w_i + \\ \frac{H}{a_{0,i-1}}z_{0,i-1} - \frac{H}{a_{0,i-1}}z_{0,i} + \frac{H}{a_{0,i-1}}w_{i-1} - \frac{H}{a_{0,i-1}}w_i + F_i = 0. \tag{23}$$

Regrouping the last expression and substituting $\frac{H}{a_{0,i-1}} = A_i$, $\frac{H}{a_{0,i}} = B_i$ and $\frac{H}{a_{0,i-1}} z_{0,i-1} - \frac{H}{a_{0,i-1}} z_{0,i} + \frac{H}{a_{0,i}} z_{0,i+1} - \frac{H}{a_{0,i}} z_{0,i} + F_i = C_i$, we can present Equation (23) similarly to Equation (7):

$$A_i w_{i-1} - (A_i + B_i) w_i + B_i w_{i+1} + C_i = 0. \tag{24}$$

The vertical displacements of each nodal point of the cable can be calculated from the system of equations based on Equation (24):

$$\begin{cases} A_1 w_0 - (A_1 + B_1) w_1 + B_1 w_2 + C_1 = 0 \\ A_2 w_1 - (A_2 + B_2) w_2 + B_2 w_3 + C_2 = 0 \\ \ldots \\ A_{n-1} w_{n-2} - (A_{n-1} + B_{n-1}) w_{n-1} + B_{n-1} w_n + C_{n-1} = 0 \\ A_n w_{n-1} - (A_n + B_n) w_n + B_n w_{n+1} + C_n = 0 \end{cases}. \tag{25}$$

If the horizontal distances between the hangers are equal, then

$$\begin{cases} A w_0 - 2A w_1 + A w_2 + C_1 = 0 \\ A w_1 - 2A w_2 + A w_3 + C_2 = 0 \\ \ldots \\ A w_{n-2} - 2A w_{n-1} + A w_n + C_{n-1} = 0 \\ A w_{n-1} - 2A w_n + A w_{n+1} + C_n = 0 \end{cases}. \tag{26}$$

Before the simplification of Equation (21), it can be expressed as follows:

$$t^4 \times D_{4,j} - t^3 \times D_{5,j} + t^2 \times D_{6,j} - t \times D_{7,j} + D_{8,j} = 0, \tag{27}$$

where

$t = a_{0,i} + (u_{i+1} - u_i)$;

$D_{1,j} = \left(z_{0,i+1} + w_{i+1} - z_{0,i} - w_i\right)^2$;

$D_{2,j} = \sqrt{a_{0,i}^2 + \left(z_{0,i+1} - z_{0,i}\right)^2}$;

$D_{3,j} = H_0 \sqrt{1 + \left(\frac{z_{0,i+1} - z_{0,i}}{a_{0,i}}\right)^2} - E_c A_c$;

$$D_{4,j} = \frac{\left(E_{\mathrm{c}} A_{\mathrm{c}}\right)^2}{D_{2,j}^2};$$

$$D_{5,j} = \frac{2HE_{\mathrm{c}} A_{\mathrm{c}}}{D_{2,j}};$$

$$D_{6,j} = H^2 + \left(E_{\mathrm{c}} A_{\mathrm{c}}\right)^2 \times \frac{D_{1,j}}{D_{2,j}^2} - D_{3,j}^2;$$

$$D_{7,j} = \frac{2HE_{\mathrm{c}} A_{\mathrm{c}} D_{1,j}}{D_{2,j}};$$

$$D_{8,j} = H^2 D_{1,j};$$

$$1 \le j \le n+1;$$

$$1 \le i \le n.$$

To calculate Equation (27) we assume that if $\beta << \alpha$, then the following relations can be used (a satisfying result is attained if $\frac{\beta}{\alpha} < 0{,}1$; see Table 3 and Figure 13):

1) $\left(\alpha+\beta\right)^3 = \alpha^3 + 3\alpha^2\beta + 3\alpha\beta^2 + \beta^3 \approx \alpha^3 + 3\alpha^2\beta + 3\alpha\beta^2 \Rightarrow$
$\Rightarrow \left[a_{0,i} + \left(u_{i+1} - u_i\right)\right]^3 \approx a_{0,i}^3 + 3a_{0,i}^2\left(u_{i+1} - u_i\right) + 3a_{0,i}\left(u_{i+1} - u_i\right)^2$ and

2) $\left(\alpha+\beta\right)^4 = \alpha^4 + 4\alpha^3\beta + 6\alpha^2\beta^2 + 4\alpha\beta^3 + \beta^4 \approx \alpha^4 + 4\alpha^3\beta + 6\alpha^2\beta^2 \Rightarrow$
$\Rightarrow \left[a_{0,i} + \left(u_{i+1} - u_i\right)\right]^4 \approx a_{0,i}^4 + 4a_{0,i}^3\left(u_{i+1} - u_i\right) + 6a_{0,i}^2\left(u_{i+1} - u_i\right),$

which leads us to the next formula:

$$u_{i+1} - u_i = D_{13,j}, \tag{28}$$

where

$$D_{10,j} = 6a_{0,i}^2 D_{4,j} - 3a_{0,i} D_{5,j} + D_{6,j};$$

$$D_{11,j} = 4a_{0,i}^3 D_{4,j} - 3a_{0,i}^2 D_{5,j} + 2a_{0,i} D_{6,j} - D_{7,j};$$

$$D_{12,j} = a_{0,i}^4 D_{4,j} - a_{0,i}^3 D_{5,j} + a_{0,i}^2 D_{6,j} - a_{0,i} D_{7,j} + D_{8,j};$$

$$D_{13,j} = \frac{-D_{11,j} + \sqrt{D_{11,j}^2 - 4D_{10,j}D_{12,j}}}{2D_{10,j}}.$$

Taking into account that [Kulbach, Õiger 1986]

$$\sum_{i=1}^{n}\left(u_{i+1}-u_i\right)=u_{n+1}-u_0, \tag{29}$$

we may write Equation (28) in the form of

$$u_{n+1}-u_0=\sum_{j=1}^{n+1}D_{13,j}, \tag{30}$$

where

u_0, u_{n+1} – horizontal displacements of the starting and end point of the cable.

Table 3. Comparison of the exact and the simplified analysis

α	β	$X_{1,1}$	$X_{1,2}$	$\frac{X_{1,2}}{X_{1,1}}\times 100\%$	$X_{2,1}$	$X_{2,2}$	$\frac{X_{2,2}}{X_{2,1}}\times 100\%$
1	1	8,0000	7,0000	87,50	16,0000	11,0000	68,75
1	0,9	6,8590	6,1300	89,37	13,0321	9,4600	72,59
1	0,8	5,8320	5,3200	91,22	10,4976	8,0400	76,59
1	0,7	4,9130	4,5700	93,02	8,3521	6,7400	80,70
1	0,6	4,0960	3,8800	94,73	6,5536	5,5600	84,84
1	0,5	3,3750	3,2500	96,30	5,0625	4,5000	88,89
1	0,4	2,7440	2,6800	97,67	3,8416	3,5600	92,67
1	0,3	2,1970	2,1700	98,77	2,8561	2,7400	95,94
1	0,2	1,7280	1,7200	99,54	2,0736	2,0400	98,38
1	0,1	1,3310	1,3300	99,92	1,4641	1,4600	99,72
1	0,09	1,2950	1,2943	99,94	1,4116	1,4086	99,79
1	0,08	1,2597	1,2592	99,96	1,3605	1,3584	99,85
1	0,07	1,2250	1,2247	99,97	1,3108	1,3094	99,89
1	0,06	1,1910	1,1908	99,98	1,2625	1,2616	99,93
1	0,05	1,1576	1,1575	99,99	1,2155	1,2150	99,96
1	0,04	1,1249	1,1248	99,99	1,1699	1,1696	99,98
1	0,03	1,0927	1,0927	100,00	1,1255	1,1254	99,99
1	0,02	1,0612	1,0612	100,00	1,0824	1,0824	100,00
1	0,01	1,0303	1,0303	100,00	1,0406	1,0406	100,00

where: $\begin{cases} X_{1,1}=\alpha^3+3\alpha^2\beta+3\alpha\beta^2+\beta^3=(\alpha+\beta)^3 \\ X_{1,2}=\alpha^3+3\alpha^2\beta+3\alpha\beta^2\approx(\alpha+\beta)^3 \end{cases}$

$\begin{cases} X_{2,1}=\alpha^4+4\alpha^3\beta+6\alpha^2\beta^2+4\alpha\beta^3+\beta^4=(\alpha+\beta)^4 \\ X_{2,2}=\alpha^4+4\alpha^3\beta+6\alpha^2\beta^2\approx(\alpha+\beta)^4 \end{cases}$

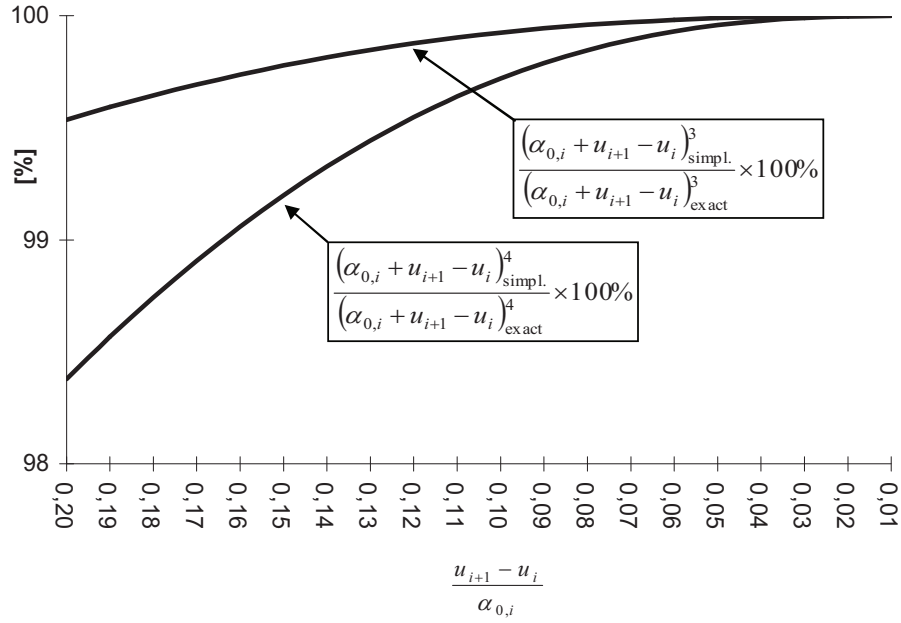

Figure 13. Ratio of simplified results to the exact calculation results

The final internal force of the cable and the displacements of the nodes can be found using the one- or two-level iterative process (respectively, steps 1…5 and 6…8 below). The solution algorithm is as follows:

1) Use F_i in Equation (10) and Equation (11) or (12) to calculate estimated H.
2) Use Equation (25) or (26) to calculate w_i.
3) Use Equation (30) to calculate $u_{n+1}-u_0$.
4) Compare the calculated $u_{n+1}-u_0$ to the exact value (e.g., if the supports are fixed, then $u_{n+1}-u_0=0$). If the difference between them is not small enough, modify the value of H and repeat the calculation from step 2.
5) Use Equation (28) to calculate u_i. The first level of the iterative process is completed.
6) The second level of the iterative process starts here. Take H and u_i from the first iterative process and use Equation (18) to calculate w_i.
7) Use Equations (30) and (28) to calculate corrected H and u_i.
8) Repeat steps 6 and 7 until H, u_i and w_i are converged to the required precision.

The full two-level iterative process (further: the second simplification) requires high computational efficiency, but if $(u_{i+1} - u_i)/a_{0,i} < 0{,}1$, this method leads to almost exact results.

If the deflections of the cable are relatively small (the experiments and the calculations showed that the vertical displacements should be less than $L/200$), it is accurate enough to use the one-level iterative process (further: the first simplification) to calculate the vertical deflections and the internal forces of the cable. It is not recommended to calculate the horizontal displacements of the cable's nodal points (except the cable's supports) using this method.

Example 2

Determine the final internal forces of the cable and the displacements of the nodal points described in Example 1 if every node has an additional load of $\Delta F = 100\,\text{kN}$ (Figure E.2.1). The cross-sectional area of the cable is $A_c = 2228\,\text{mm}^2$ and the modulus of elasticity $E_c = 1{,}25 \times 10^5\ \text{N/mm}^2$. Use both of the simplifications of the discrete analysis.

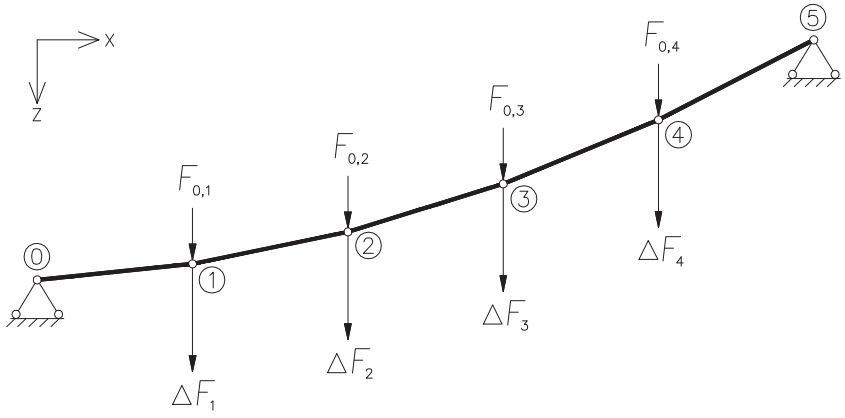

Figure E.2.1. Simplified design scheme of Example 2 (see also Figure E.1.1)

In consequence, the total final load at each nodal point is $F = F_1 = F_2 = F_3 = F_4 = 150$ kN.

At the first approximation the internal force of the cable can be calculated from Equation (12) using final loads (the equation is derived in Example 1):

$$H = \frac{3FL_0}{5e} = \frac{3 \times 150000 \times 50000}{5 \times 3000} = 1500000\ \text{N}.$$

The internal force of the cable calculated above is overvalued. Let us assume in the beginning that $H = 1400000\,\text{N}$. The exact value is found after the iteration.

The equilibrium conditions of the nodal points using Equation (26) are

$$\begin{cases} Aw_0 - 2Aw_1 + Aw_2 + C_1 = 0 \\ Aw_1 - 2Aw_2 + Aw_3 + C_2 = 0 \\ Aw_2 - 2Aw_3 + Aw_4 + C_3 = 0 \\ Aw_3 - 2Aw_4 + Aw_5 + C_4 = 0 \end{cases},$$

where $A = H/a_0$ and $C_i = (H/a_0) \times (z_{0,i-1} - z_{0,i} + z_{0,i+1} - z_{0,i}) + F_i$.

Constants of the system of equations:

$$\begin{cases} C_1 = (H/a_0) \times (z_{0,0} - 2z_{0,1} + z_{0,2}) + F \\ C_2 = (H/a_0) \times (z_{0,1} - 2z_{0,2} + z_{0,3}) + F \\ C_3 = (H/a_0) \times (z_{0,2} - 2z_{0,3} + z_{0,4}) + F \\ C_4 = (H/a_0) \times (z_{0,3} - 2z_{0,4} + z_{0,5}) + F \end{cases}.$$

The vertical displacements of the nodal points:

$$\begin{cases} w_1 = \dfrac{4C_1 + 3C_2 + 2C_3 + C_4}{5A} = \dfrac{4z_{0,0} - 5z_{0,1} + z_{0,5}}{5} + 2\dfrac{Fa_0}{H} \\ w_2 = \dfrac{3C_1 + 6C_2 + 4C_3 + 2C_4}{5A} = \dfrac{3z_{0,0} - 5z_{0,2} + 2z_{0,5}}{5} + 3\dfrac{Fa_0}{H} \\ w_3 = \dfrac{2C_1 + 4C_2 + 6C_3 + 3C_4}{5A} = \dfrac{2z_{0,0} - 5z_{0,3} + 3z_{0,5}}{5} + 3\dfrac{Fa_0}{H} \\ w_4 = \dfrac{C_1 + 2C_2 + 3C_3 + 4C_4}{5A} = \dfrac{z_{0,0} - 5z_{0,4} + 4z_{0,5}}{5} + 2\dfrac{Fa_0}{H} \end{cases} \Rightarrow$$

$$\Rightarrow \begin{cases} w_1 = \dfrac{4 \times 15000 - 5 \times 14000 + 0}{5} + 2 \times \dfrac{150000 \times 10000}{1400000} = 142{,}9 \text{ mm} \\ w_2 = \dfrac{3 \times 15000 - 5 \times 12000 + 0}{5} + 3 \times \dfrac{150000 \times 10000}{1400000} = 214{,}3 \text{ mm} \\ w_3 = \dfrac{2 \times 15000 - 5 \times 9000 + 0}{5} + 3 \times \dfrac{150000 \times 10000}{1400000} = 214{,}3 \text{ mm} \\ w_4 = \dfrac{15000 - 5 \times 5000 + 0}{5} + 2 \times \dfrac{150000 \times 10000}{1400000} = 142{,}9 \text{ mm} \end{cases}.$$

Placing H and w_i into Equation (30), $u_5 - u_0$ can be calculated. The numerical coefficients of this calculation are presented in Table E.2.1.

Table E.2.1. Numerical coefficients of Example 2 for calculating the difference between the horizontal displacements of the starting point and the end point of the cable

Symbol of the coeff.	**Nodal points of the cable**				
	***j* = 1**	***j* = 2**	***j* = 3**	***j* = 4**	***j* = 5**
$D_{1,j}$ =	7,35E+05	3,72E+06	9,00E+06	1,66E+07	2,64E+07
$D_{2,j}$ =	1,01E+04	1,02E+04	1,04E+04	1,08E+04	1,12E+04
$D_{3,j}$ =	-2,78E+08	-2,78E+08	-2,78E+08	-2,78E+08	-2,78E+08
$D_{4,j}$ =	7,68E+08	7,46E+08	7,12E+08	6,69E+08	6,21E+08
$D_{5,j}$ =	7,76E+10	7,65E+10	7,47E+10	7,24E+10	6,97E+10
$D_{6,j}$ =	-7,67E+16	-7,45E+16	-7,09E+16	-6,62E+16	-6,08E+16
$D_{7,j}$ =	5,70E+16	2,84E+17	6,72E+17	1,20E+18	1,84E+18
$D_{8,j}$ =	1,44E+18	7,29E+18	1,76E+19	3,25E+19	5,18E+19
$D_{10,j}$ =	3,82E+17	3,71E+17	3,54E+17	3,33E+17	3,09E+17
$D_{11,j}$ =	1,51E+21	1,47E+21	1,41E+21	1,33E+21	1,24E+21
$D_{12,j}$ =	-7,04E+22	-7,17E+22	-5,22E+22	-1,57E+22	3,31E+22
$D_{13,j}$ =	45,95	48,17	36,75	11,76	-26,79

The difference of the horizontal displacements of the cable's starting and end point:

$$u_5 - u_0 = \sum_{j=1}^{5} D_{13,j} = 45{,}95 + 48{,}17 + 36{,}75 + 11{,}76 - 26{,}79 = 115{,}8 \text{ mm}.$$

This result is inappropriate because the supports of the cable are fixed – after reducing H, the whole calculation must be repeated (iteration). The final results of the first simplification (also called the first phase of the iteration):

$$\begin{cases} H = 1297733 \text{ N} \\ w_1 = 311{,}7 \text{ mm}; u_1 = 55{,}2 \text{ mm} \\ w_2 = 467{,}6 \text{ mm}; u_2 = 115{,}2 \text{ mm} \\ w_3 = 467{,}6 \text{ mm}; u_3 = 147{,}8 \text{ mm} \\ w_4 = 311{,}7 \text{ mm}; u_4 = 120{,}4 \text{ mm} \end{cases}.$$

In the second phase of the iteration, Equation (18) must be used instead of Equation (22). This is possible because the estimated displacements of the nodal points are known.

After creating the system of equations using Equation (18)

$$\begin{cases} F_1 + H\dfrac{z_{0,2} + w_2 - z_{0,1} - w_1}{a_{0,1} + u_2 - u_1} + H\dfrac{z_{0,0} + w_0 - z_{0,1} - w_1}{a_{0,0} + u_1 - u_0} = 0 \\ F_2 + H\dfrac{z_{0,3} + w_3 - z_{0,2} - w_2}{a_{0,2} + u_3 - u_2} + H\dfrac{z_{0,1} + w_1 - z_{0,2} - w_2}{a_{0,1} + u_2 - u_1} = 0 \\ F_3 + H\dfrac{z_{0,4} + w_4 - z_{0,3} - w_3}{a_{0,3} + u_4 - u_3} + H\dfrac{z_{0,2} + w_2 - z_{0,3} - w_3}{a_{0,2} + u_3 - u_2} = 0 \\ F_4 + H\dfrac{z_{0,5} + w_5 - z_{0,4} - w_4}{a_{0,4} + u_5 - u_4} + H\dfrac{z_{0,3} + w_3 - z_{0,4} - w_4}{a_{0,3} + u_4 - u_3} = 0 \end{cases},$$

the corrected vertical displacements of the nodal points of the cable are

$$\begin{cases} w_1 = 297{,}7 \text{ mm} \\ w_2 = 432{,}3 \text{ mm} \\ w_3 = 412{,}4 \text{ mm} \\ w_4 = 257{,}8 \text{ mm} \end{cases}.$$

On the basis of values, using Equations (28) and (30), the internal force of the cable and the horizontal displacements of the nodes are as follows:

$$\begin{cases} H = 1211122 \text{ N} \\ u_1 = 51{,}1 \text{ mm} \\ u_2 = 103{,}9 \text{ mm} \\ u_3 = 127{,}0 \text{ mm} \\ u_4 = 96{,}2 \text{ mm} \end{cases}.$$

As these results are not the same as found before, the calculation must be repeated using the iteration.

The final results of the first and the second simplification are presented in Table E.2.2 and Figure E.2.2. Geometrically linear and non-linear behaviour of the cable under different loads is characterised in Figures E.2.3 and E.2.4 (the first simplification is used). Table E.2.3 shows the calculation results when the cable's modulus of elasticity is 125000 (version 1), 120000 (version 2) and 115000 MPa (version 3).

Table E.2.2. Final calculation results of Example 2

Parameter	First simplification		Second simplif.
	Value	Differ. from the second simplif. [%]	Value
H [N]	1297733	1,1	1284067
w_1 [mm]	311,7	-3,4	322,8
w_2 [mm]	467,6	-0,6	470,6
w_3 [mm]	467,6	3,3	452,8
w_4 [mm]	311,7	8,2	288,1
u_1 [mm]	55,2	-0,4	55,4
u_2 [mm]	115,2	1,5	113,5
u_3 [mm]	147,8	5,4	140,2
u_4 [mm]	120,4	11,0	108,5

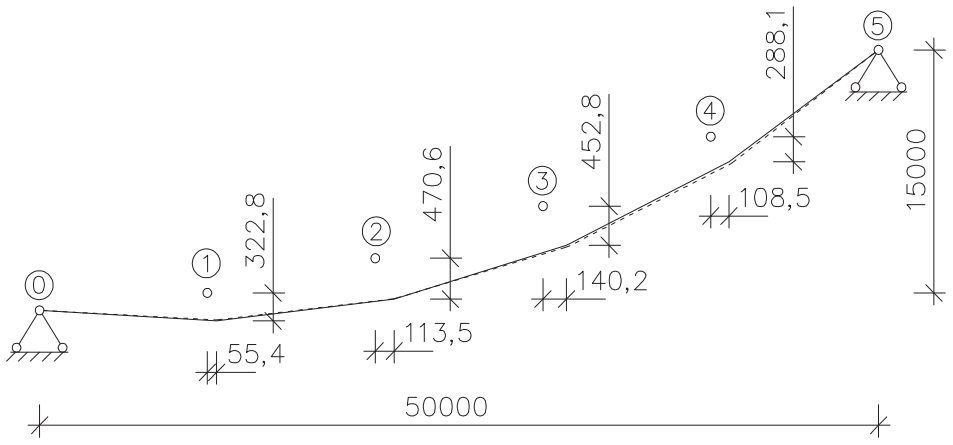

Figure E.2.2. Deformations of the cable of Example 2 using the first (dotted line) and the second simplified discrete analysis (dimensional numbers are presented for the second simplification); vertical displacements are enlarged 5 and horizontal 10 times

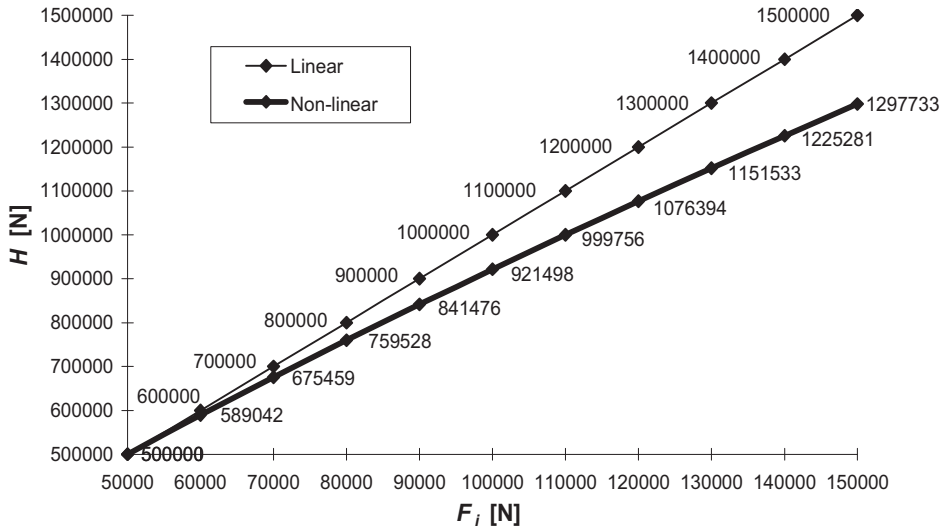

Figure E.2.3. Linear and non-linear dependences between the nodal load F_i and the horizontal component of the cable's internal force H of Example 2 (based on the first simplification)

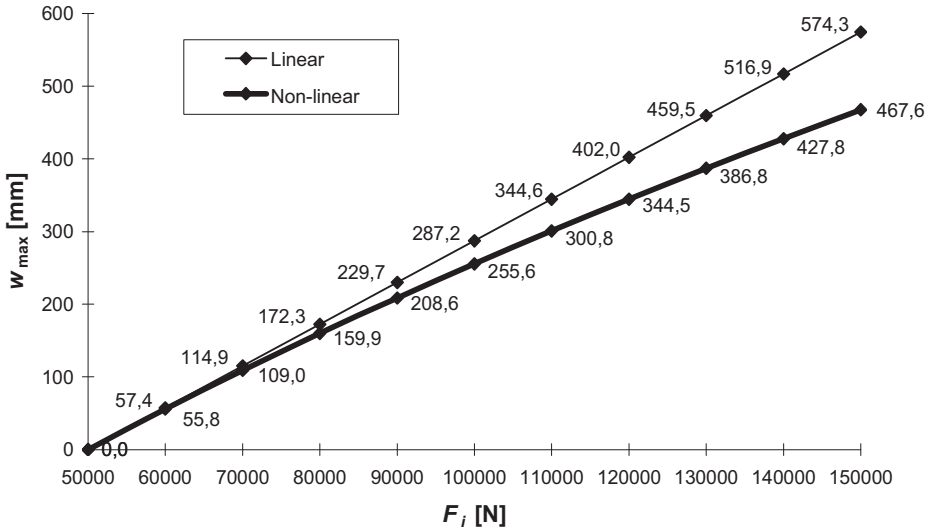

Figure E.2.4. Linear and non-linear dependences between the nodal load F_i and the maximum vertical deflection of the cable w_{max} of Example 2 (based on the first simplification)

Table E.2.3. Calculation results of the second simplification of Example 2 using different moduli of elasticity

Parameter	Version 1	Version 2		Version 3	
	Value	Value	$\frac{\text{Vers.2}}{\text{Vers.1}}$ [%]	Value	$\frac{\text{Vers.3}}{\text{Vers.1}}$ [%]
E [MPa]	125000	120000	-4,0	115000	-8,0
H [N]	1284067	1278233	-0,5	1272051	-0,9
w_1 [mm]	322,8	333,1	3,2	344,1	6,6
w_2 [mm]	470,6	485,5	3,2	501,5	6,6
w_3 [mm]	452,8	467,1	3,2	482,4	6,5
w_4 [mm]	288,1	297,1	3,1	306,8	6,5
u_1 [mm]	55,4	57,1	3,1	58,8	6,1
u_2 [mm]	113,5	117,0	3,1	120,7	6,3
u_3 [mm]	140,2	144,6	3,1	149,3	6,5
u_4 [mm]	108,5	111,9	3,1	115,6	6,5

2.2.2.3 Final balance of the cable if the support of the pylon is rigid

This section describes the structure that consists of two cables and one pylon. The nether support of the pylon can be rigid or hinged.

If the support of the pylon is rigid, then the horizontal components H_{I} and H_{II} of the internal forces of the cables are not equal (Figure 14a). The horizontal displacement of the pylon's top may be calculated as follows [Idnurm, J., Kiisa, Idnurm, S. 2009]:

$$u_{\mathrm{p}} = \frac{h_{\mathrm{p}}^3 \left(H_{\mathrm{II}} - H_{\mathrm{I}}\right)}{3E_{\mathrm{p}} I_{\mathrm{p}}}, \tag{31}$$

where

u_{p} – horizontal displacement of the pylon's top;

H_{I} – horizontal component of the internal force of the left cable;

H_{II} – horizontal component of the internal force of the right cable;

h_{p} – height of the pylon;

E_{p} – modulus of elasticity of the pylon;

I_{p} – moment of inertia of the pylon.

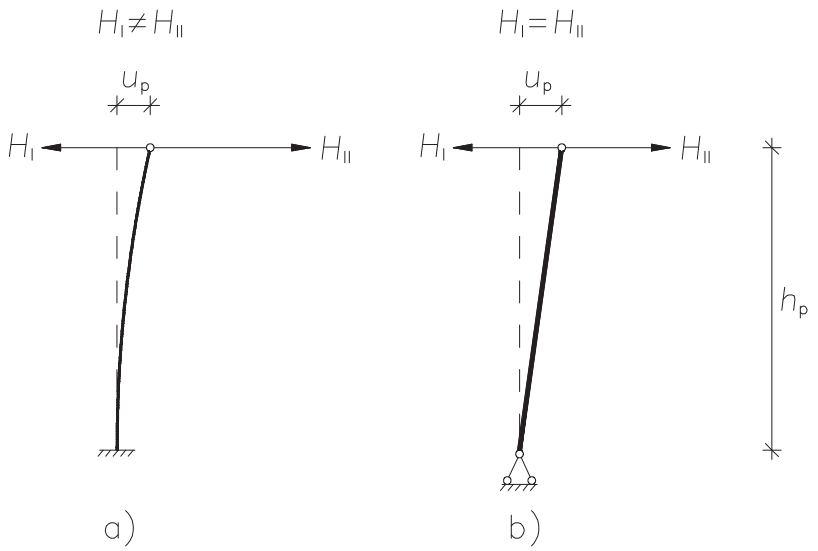

Figure 14. Design schemes of the pylon: a) fixed support; b) hinged support

There are many ways to calculate such structures. One possibility is to calculate both cables separately using the following iterative process:

1) Assume in the beginning that the pylon's top has no horizontal displacement, i.e. $u_p = 0$.
2) Calculate H_I and H_{II} separately using an algorithm described above.
3) Use Equation (31) to calculate corrected u_p.
4) Calculate H_I and H_{II} again using the corrected u_p.
5) If step 4 shows that H_I and H_{II} are not the same as calculated in step 2, change u_p until the purpose is achieved.

2.2.2.4 Final balance of the cable if the support of the pylon is a hinge

If the support of the pylon is a hinge (Figure 14b), then $H_I = H_{II}$ [Idnurm, J., Kiisa, Idnurm, S. 2009]. The following algorithm can be used:

1) Assume that the pylon's top has no horizontal displacement, i.e. $u_p = 0$.
2) Calculate H_I and H_{II} separately.
3) If $H_I \neq H_{II}$, change u_p until $H_I = H_{II}$.

Example 3

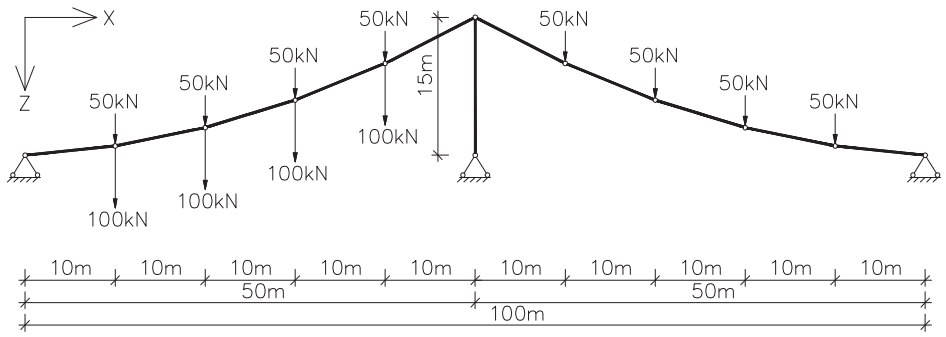

Figure E.3.1. Simplified design scheme of Example 3 (see also Figures E.1.1 and E.2.1)

Determine the final internal forces of the cable structure and the displacements of the nodal points described in Figure E.3.1 using the first simplification of the discrete analysis. The shape of the cable is the same as in Example 1. The cross-sectional area of the cable is $A_c = 2228\,\text{mm}^2$ and the modulus of elasticity $E_c = 1{,}22 \times 10^5\ \text{N/mm}^2$. All of the nodal points (4+4) are loaded by $F_0 = 50\,\text{kN}$ in the initial balance. In the final balance only the left cable is loaded by $\Delta F = 100\,\text{kN}$ at every node.

The total final load at each nodal point of the left cable is $F_\text{I} = 150$ kN and that of the right cable is $F_\text{II} = 50$ kN. It is clear that $H_\text{I} = H_\text{II} = H$. Basically two separate calculations must be done for both spans. The idea of the calculation is to find such H when the following condition is fulfilled: $u_{\text{I,p}} = u_{\text{II,p}}$. The operations that were made in Examples 1 and 2 are not repeated here.

Let us assume in the beginning that the horizontal component of the internal force of the cable is $H = 1400000\,\text{N}$ in the final balance. Using the calculation steps described in Examples 1 and 2 it is clear that

$$u_{\text{I,p}} + u_{\text{II,p}} = \sum_{j=1}^{5} D_{\text{I},13,j} + \sum_{j=1}^{5} D_{\text{II},13,j} = -131{,}94 + 545{,}37 = 413{,}4\ \text{mm}.$$

This result is inappropriate because of $u_{\text{I,p}} \neq u_{\text{II,p}}$. The final results appear when $H = 1022162\,\text{N}$:

$$u_{\text{I,p}} + u_{\text{II,p}} = -478{,}16 + 478{,}16 = 0{,}0\ \text{mm}.$$

The final results of Example 3 are presented in Table E.3.1 (to compare the differences, the results of the second simplification are also added).

Table E.3.1. Final calculation results of Example 3

Parameter	**First simplification**		**Second simplif.**
	Value	**Differ. from the second simplif. [%]**	**Value**
H [N]	1022162	4,1	981796
u_{p} [mm]	-478,2	0,0	-478,0
$w_{\mathrm{I},1}$ [mm]	935,0	-5,2	985,8
$w_{\mathrm{I},2}$ [mm]	1402,4	-1,9	1429,0
$w_{\mathrm{I},3}$ [mm]	1402,4	3,1	1359,6
$w_{\mathrm{I},4}$ [mm]	935,0	9,8	851,7
$u_{\mathrm{I},1}$ [mm]	68,9	1,9	67,6
$u_{\mathrm{I},2}$ [mm]	171,0	4,0	164,5
$u_{\mathrm{I},3}$ [mm]	192,9	17,8	163,7
$u_{\mathrm{I},4}$ [mm]	18,3	-	-31,3
$w_{\mathrm{II},1}$ [mm]	-1021,7	-4,1	-1065,2
$w_{\mathrm{II},2}$ [mm]	-1532,5	-4,1	-1597,5
$w_{\mathrm{II},3}$ [mm]	-1532,5	-3,6	-1590,5
$w_{\mathrm{II},4}$ [mm]	-1021,7	-2,8	-1051,1
$u_{\mathrm{II},1}$ [mm]	-4,2	-	10,6
$u_{\mathrm{II},2}$ [mm]	208,2	-8,8	228,4
$u_{\mathrm{II},3}$ [mm]	230,0	-6,7	246,5
$u_{\mathrm{II},4}$ [mm]	135,2	-5,3	142,8

2.3 Behaviour of the stiffening girder

The behaviour of the stiffening girder is described using the universal equation of the elastic curve. Afterwards using the derivatives, it is easy to calculate the bending moments and shear forces of the girder. This continuous method is used because it needs much less computational efficiency than the discrete method. This thesis is focused on three types of stiffening girders:

1) two-span continuous beam (Figure 15),
2) simple beam (Figure 16) and
3) two sequential simple beams (Figure 17).

If the girder is loaded by concentrated and distributed loads, the elastic curve of the girder takes the following form [Jürgenson 1985]:

$$w(x) = w_0 + \varphi_0 x + \sum_{k=1}^{n} P_k \frac{\left(x - x_{P,k}\right)^3}{6E_{\mathrm{g}}I_{\mathrm{g}}} \cdot \mathcal{H}\left(x - x_{P,k}\right) + \sum_{l=1}^{q} p_l \frac{\left(x - x_{p,l,1}\right)^4}{24E_{\mathrm{g}}I_{\mathrm{g}}} \cdot \mathcal{H}\left(x - x_{p,l,1}\right) - \sum_{l=1}^{q} p_l \frac{\left(x - x_{p,l,2}\right)^4}{24E_{\mathrm{g}}I_{\mathrm{g}}} \cdot \mathcal{H}\left(x - x_{p,l,2}\right), \tag{32}$$

where

- $w(x)$ – deflection of the stiffening girder at point x;
- w_0 – deflection of the stiffening girder at the starting point;
- φ_0 – angle of rotation of the stiffening girder at the starting point;
- P_k – concentrated load;
- p_l – distributed load;
- x – abscissa of the observable point on the stiffening girder;
- $x_{P,k}$ – abscissa of the point of application of the concentrated load;
- $x_{p,l,1}$ – abscissa of the starting point of application of the distributed load;
- $x_{p,l,2}$ – abscissa of the end point of application of the distributed load;
- n – total amount of concentrated loads;
- q – total amount of distributed loads;
- $E_{\mathrm{g}}I_{\mathrm{g}}$ – flexural rigidity of the stiffening girder;
- $\mathcal{H}(x - x_i)$ – *Heaviside*'s step function: $\mathcal{H}(x - x_i) = \begin{cases} 0, \text{ if } x < x_i \\ 1, \text{ if } x > x_i \end{cases}$.

2.3.1 Behaviour of the stiffening girder working as a two-span continuous beam

The design scheme of a two-span continuous beam is illustrated in Figure 15. To achieve clarity in the characterisation of the scheme, the concentrated forces P are divided into three groups: contact forces F from the hangers, imposed loads N and support reactions V.

The additional unknown parameters in Equation (32) are the support reactions of the girder, the deflection w_0 of the girder at the starting point and the angle of rotation φ_0 of the girder at the starting point.

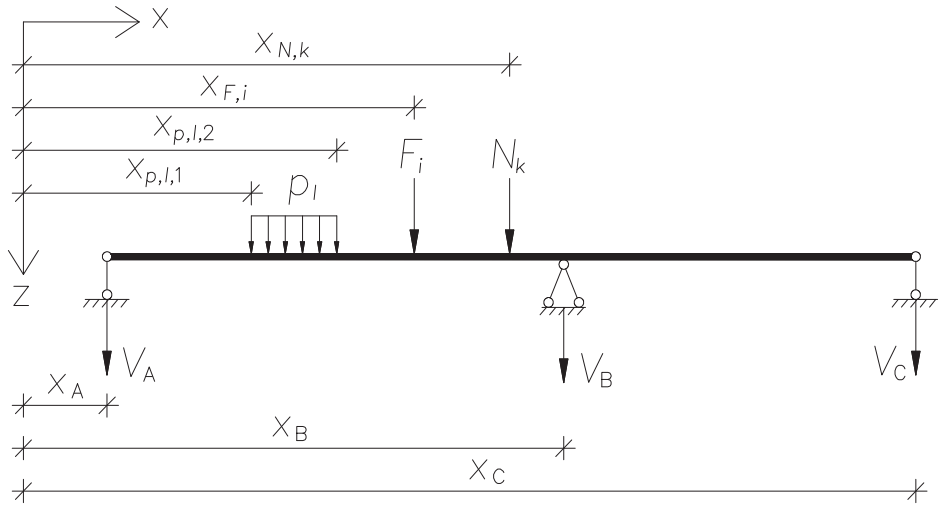

Figure 15. Design scheme of the stiffening girder – a two-span continuous beam

There is no deflection at the support C and φ_0 can be calculated from the following formula:

$$w(x_{\mathrm{C}}) = 0 + \varphi_0 x_{\mathrm{C}} + \sum_{k=1}^{n} P_k \frac{\left(x_{\mathrm{C}} - x_{P,k}\right)^3}{6E_{\mathrm{g}}I_{\mathrm{g}}} + \sum_{l=1}^{q} p_l \frac{\left(x_{\mathrm{C}} - x_{p,l,1}\right)^4}{24E_{\mathrm{g}}I_{\mathrm{g}}} - \sum_{l=1}^{q} p_l \frac{\left(x_{\mathrm{C}} - x_{p,l,2}\right)^4}{24E_{\mathrm{g}}I_{\mathrm{g}}} = 0, \tag{33}$$

where

$w(x_{\mathrm{C}})$ – deflection of the stiffening girder at support C (the end point of the girder);

x_{C} – abscissa of support C.

Having expressed φ_0 from Equation (33) it can be added to Equation (32) and the deflections of a two-span continuous beam can be presented as

$$w(x) = -\sum_{k=1}^{n} P_k \frac{\left(x_{\mathrm{C}} - x_{P,k}\right)^3 x}{6E_{\mathrm{g}}I_{\mathrm{g}}x_{\mathrm{C}}} - \sum_{l=1}^{q} p_l \frac{\left(x_{\mathrm{C}} - x_{p,l,1}\right)^4 x}{24E_{\mathrm{g}}I_{\mathrm{g}}x_{\mathrm{C}}} + \sum_{l=1}^{q} p_l \frac{\left(x_{\mathrm{C}} - x_{p,l,2}\right)^4 x}{24E_{\mathrm{g}}I_{\mathrm{g}}x_{\mathrm{C}}} + \sum_{k=1}^{n} P_k \frac{\left(x - x_{P,k}\right)^3}{6E_{\mathrm{g}}I_{\mathrm{g}}} \cdot \mathcal{H}\left(x - x_{P,k}\right) + \sum_{l=1}^{q} p_l \frac{\left(x - x_{p,l,1}\right)^4}{24E_{\mathrm{g}}I_{\mathrm{g}}} \cdot \mathcal{H}\left(x - x_{p,l,1}\right) - \sum_{l=1}^{q} p_l \frac{\left(x - x_{p,l,2}\right)^4}{24E_{\mathrm{g}}I_{\mathrm{g}}} \cdot \mathcal{H}\left(x - x_{p,l,2}\right). \tag{34}$$

Using the algebraic sum of the moments about the two supports (A and C) and the elastic curve at the support B it is possible to express all three vertical support reactions.

The sum of the moments about support A:

$$\sum_{k=1}^{r} N_k \left(x_{N,k} - x_{\mathrm{A}}\right) + \sum_{i=1}^{t} F_i \left(x_{F,i} - x_{\mathrm{A}}\right) + V_{\mathrm{C}} \left(x_{\mathrm{C}} - x_{\mathrm{A}}\right) + V_{\mathrm{B}} \left(x_{\mathrm{B}} - x_{\mathrm{A}}\right) + \sum_{l=1}^{q} p_l \left(x_{p,l,2} - x_{p,l,1}\right) \left(\frac{x_{p,l,2} + x_{p,l,1}}{2} - x_{\mathrm{A}} \right) = 0, \tag{35}$$

where

- N_k – concentrated imposed load;
- F_i – concentrated force from the hanger;
- V_{B} – vertical support reaction of support B of the stiffening girder;
- V_{C} – vertical support reaction of support C of the stiffening girder;
- $x_{N,k}$ – abscissa of the point of application of the concentrated imposed load;
- $x_{F,i}$ – abscissa of the point of application of the concentrated force from the hanger;
- x_{A} – abscissa of support A;
- x_{B} – abscissa of support B;
- r – total amount of imposed concentrated loads;
- t – total amount of hangers.

The sum of the moments about support C:

$$\sum_{k=1}^{r} N_k\left(x_{\mathrm{C}}-x_{N,k}\right)+\sum_{i=1}^{t} F_i\left(x_{\mathrm{C}}-x_{F,i}\right)+V_{\mathrm{A}}\left(x_{\mathrm{C}}-x_{\mathrm{A}}\right)+V_{\mathrm{B}}\left(x_{\mathrm{C}}-x_{\mathrm{B}}\right)+ \sum_{l=1}^{q} p_l\left(x_{p,l,2}-x_{p,l,1}\right)\left(x_{\mathrm{C}}-\frac{x_{p,l,2}+x_{p,l,1}}{2}\right)=0, \tag{36}$$

where

V_{A} – vertical support reaction of support A of the stiffening girder.

The third relation required can be derived from the equation of the elastic curve at the support B:

$$w(x_{\mathrm{B}})=-\sum_{k=1}^{r} N_k\frac{\left(x_{\mathrm{C}}-x_{N,k}\right)^3 x_{\mathrm{B}}}{6E_{\mathrm{g}}I_{\mathrm{g}}x_{\mathrm{C}}}-\sum_{i=1}^{t} F_i\frac{\left(x_{\mathrm{C}}-x_{F,i}\right)^3 x_{\mathrm{B}}}{6E_{\mathrm{g}}I_{\mathrm{g}}x_{\mathrm{C}}}- V_{\mathrm{A}}\frac{\left(x_{\mathrm{C}}-x_{\mathrm{A}}\right)^3 x_{\mathrm{B}}}{6E_{\mathrm{g}}I_{\mathrm{g}}x_{\mathrm{C}}}-V_{\mathrm{B}}\frac{\left(x_{\mathrm{C}}-x_{\mathrm{B}}\right)^3 x_{\mathrm{B}}}{6E_{\mathrm{g}}I_{\mathrm{g}}x_{\mathrm{C}}}-\sum_{l=1}^{q} p_l\frac{\left(x_{\mathrm{C}}-x_{p,l,1}\right)^4 x_{\mathrm{B}}}{24E_{\mathrm{g}}I_{\mathrm{g}}x_{\mathrm{C}}}+ \sum_{l=1}^{q} p_l\frac{\left(x_{\mathrm{C}}-x_{p,l,2}\right)^4 x_{\mathrm{B}}}{24E_{\mathrm{g}}I_{\mathrm{g}}x_{\mathrm{C}}}+\sum_{k=1}^{r} N_k\frac{\left(x_{\mathrm{B}}-x_{N,k}\right)^3}{6E_{\mathrm{g}}I_{\mathrm{g}}}\cdot\mathcal{H}\left(x_{\mathrm{B}}-x_{N,k}\right)+ \sum_{i=1}^{t} F_i\frac{\left(x_{\mathrm{B}}-x_{F,i}\right)^3}{6E_{\mathrm{g}}I_{\mathrm{g}}}\cdot\mathcal{H}\left(x_{\mathrm{B}}-x_{F,i}\right)+V_{\mathrm{A}}\frac{\left(x_{\mathrm{B}}-x_{\mathrm{A}}\right)^3}{6E_{\mathrm{g}}I_{\mathrm{g}}}+ \sum_{l=1}^{q} p_l\frac{\left(x_{\mathrm{B}}-x_{p,l,1}\right)^4}{24E_{\mathrm{g}}I_{\mathrm{g}}}\cdot\mathcal{H}\left(x_{\mathrm{B}}-x_{p,l,1}\right)-\sum_{l=1}^{q} p_l\frac{\left(x_{\mathrm{B}}-x_{p,l,2}\right)^4}{24E_{\mathrm{g}}I_{\mathrm{g}}}\cdot\mathcal{H}\left(x_{\mathrm{B}}-x_{p,l,2}\right)=0. \tag{37}$$

Taking into account Equations (35), (36) and (37), support reactions of the stiffening girder may be written in the following form:

$$V_{\mathrm{A}}=\left[\frac{\left(x_{\mathrm{C}}-x_{\mathrm{B}}\right)^{2}}{\left(x_{\mathrm{C}}-x_{\mathrm{A}}\right)^{3}x_{\mathrm{B}}-\left(x_{\mathrm{C}}-x_{\mathrm{A}}\right)\left(x_{\mathrm{C}}-x_{\mathrm{B}}\right)^{2}x_{\mathrm{B}}-\left(x_{\mathrm{B}}-x_{\mathrm{A}}\right)^{3}x_{\mathrm{C}}}\right]\times$$
$$\left[\sum_{k=1}^{r}N_{k}\left(x_{\mathrm{C}}-x_{N,k}\right)x_{\mathrm{B}}+\sum_{i=1}^{t}F_{i}\left(x_{\mathrm{C}}-x_{F,i}\right)x_{\mathrm{B}}+\right.$$
$$\sum_{l=1}^{q}p_{l}\left(x_{p,l,2}-x_{p,l,1}\right)x_{\mathrm{B}}\left(x_{\mathrm{C}}-\frac{x_{p,l,2}+x_{p,l,1}}{2}\right)-\sum_{k=1}^{r}N_{k}\frac{\left(x_{\mathrm{C}}-x_{N,k}\right)^{3}x_{\mathrm{B}}}{\left(x_{\mathrm{C}}-x_{\mathrm{B}}\right)^{2}}-$$
$$\sum_{i=1}^{t}F_{i}\frac{\left(x_{\mathrm{C}}-x_{F,i}\right)^{3}x_{\mathrm{B}}}{\left(x_{\mathrm{C}}-x_{\mathrm{B}}\right)^{2}}-\sum_{l=1}^{q}p_{l}\frac{\left(x_{\mathrm{C}}-x_{p,l,1}\right)^{4}x_{\mathrm{B}}}{4\left(x_{\mathrm{C}}-x_{\mathrm{B}}\right)^{2}}+\sum_{l=1}^{q}p_{l}\frac{\left(x_{\mathrm{C}}-x_{p,l,2}\right)^{4}x_{\mathrm{B}}}{4\left(x_{\mathrm{C}}-x_{\mathrm{B}}\right)^{2}}+$$
$$\sum_{k=1}^{r}N_{k}\frac{\left(x_{\mathrm{B}}-x_{N,k}\right)^{3}x_{\mathrm{C}}}{\left(x_{\mathrm{C}}-x_{\mathrm{B}}\right)^{2}}\cdot\mathcal{H}\left(x_{\mathrm{B}}-x_{N,k}\right)+\sum_{i=1}^{t}F_{i}\frac{\left(x_{\mathrm{B}}-x_{F,i}\right)^{3}x_{\mathrm{C}}}{\left(x_{\mathrm{C}}-x_{\mathrm{B}}\right)^{2}}\cdot\mathcal{H}\left(x_{\mathrm{B}}-x_{F,i}\right)+$$
$$\left.\sum_{l=1}^{q}p_{l}\frac{\left(x_{\mathrm{B}}-x_{p,l,1}\right)^{4}x_{\mathrm{C}}}{4\left(x_{\mathrm{C}}-x_{\mathrm{B}}\right)^{2}}\cdot\mathcal{H}\left(x_{\mathrm{B}}-x_{p,l,1}\right)-\sum_{l=1}^{q}p_{l}\frac{\left(x_{\mathrm{B}}-x_{p,l,2}\right)^{4}x_{\mathrm{C}}}{4\left(x_{\mathrm{C}}-x_{\mathrm{B}}\right)^{2}}\cdot\mathcal{H}\left(x_{\mathrm{B}}-x_{p,l,2}\right)\right],\tag{38}$$

$$V_{\mathrm{B}}=-\sum_{k=1}^{r}N_{k}\frac{\left(x_{\mathrm{C}}-x_{N,k}\right)}{\left(x_{\mathrm{C}}-x_{\mathrm{B}}\right)}-\sum_{i=1}^{t}F_{i}\frac{\left(x_{\mathrm{C}}-x_{F,i}\right)}{\left(x_{\mathrm{C}}-x_{\mathrm{B}}\right)}-$$
$$\sum_{l=1}^{q}p_{l}\frac{\left(x_{p,l,2}-x_{p,l,1}\right)}{\left(x_{\mathrm{C}}-x_{\mathrm{B}}\right)}\left(x_{\mathrm{C}}-\frac{x_{p,l,2}+x_{p,l,1}}{2}\right)-$$
$$\left[\frac{\left(x_{\mathrm{C}}-x_{\mathrm{A}}\right)\left(x_{\mathrm{C}}-x_{\mathrm{B}}\right)}{\left(x_{\mathrm{C}}-x_{\mathrm{A}}\right)^{3}x_{\mathrm{B}}-\left(x_{\mathrm{C}}-x_{\mathrm{A}}\right)\left(x_{\mathrm{C}}-x_{\mathrm{B}}\right)^{2}x_{\mathrm{B}}-\left(x_{\mathrm{B}}-x_{\mathrm{A}}\right)^{3}x_{\mathrm{C}}}\right]\times$$
$$\left[\sum_{k=1}^{r}N_{k}\left(x_{\mathrm{C}}-x_{N,k}\right)x_{\mathrm{B}}+\sum_{i=1}^{t}F_{i}\left(x_{\mathrm{C}}-x_{F,i}\right)x_{\mathrm{B}}+\right.$$
$$\sum_{l=1}^{q}p_{l}\left(x_{p,l,2}-x_{p,l,1}\right)x_{\mathrm{B}}\left(x_{\mathrm{C}}-\frac{x_{p,l,2}+x_{p,l,1}}{2}\right)-\sum_{k=1}^{r}N_{k}\frac{\left(x_{\mathrm{C}}-x_{N,k}\right)^{3}x_{\mathrm{B}}}{\left(x_{\mathrm{C}}-x_{\mathrm{B}}\right)^{2}}-$$
$$\sum_{i=1}^{t}F_{i}\frac{\left(x_{\mathrm{C}}-x_{F,i}\right)^{3}x_{\mathrm{B}}}{\left(x_{\mathrm{C}}-x_{\mathrm{B}}\right)^{2}}-\sum_{l=1}^{q}p_{l}\frac{\left(x_{\mathrm{C}}-x_{p,l,1}\right)^{4}x_{\mathrm{B}}}{4\left(x_{\mathrm{C}}-x_{\mathrm{B}}\right)^{2}}+\sum_{l=1}^{q}p_{l}\frac{\left(x_{\mathrm{C}}-x_{p,l,2}\right)^{4}x_{\mathrm{B}}}{4\left(x_{\mathrm{C}}-x_{\mathrm{B}}\right)^{2}}+$$
$$\sum_{k=1}^{r}N_{k}\frac{\left(x_{\mathrm{B}}-x_{N,k}\right)^{3}x_{\mathrm{C}}}{\left(x_{\mathrm{C}}-x_{\mathrm{B}}\right)^{2}}\cdot\mathcal{H}\left(x_{\mathrm{B}}-x_{N,k}\right)+\sum_{i=1}^{t}F_{i}\frac{\left(x_{\mathrm{B}}-x_{F,i}\right)^{3}x_{\mathrm{C}}}{\left(x_{\mathrm{C}}-x_{\mathrm{B}}\right)^{2}}\cdot\mathcal{H}\left(x_{\mathrm{B}}-x_{F,i}\right)+$$
$$\left.\sum_{l=1}^{q}p_{l}\frac{\left(x_{\mathrm{B}}-x_{p,l,1}\right)^{4}x_{\mathrm{C}}}{4\left(x_{\mathrm{C}}-x_{\mathrm{B}}\right)^{2}}\cdot\mathcal{H}\left(x_{\mathrm{B}}-x_{p,l,1}\right)-\sum_{l=1}^{q}p_{l}\frac{\left(x_{\mathrm{B}}-x_{p,l,2}\right)^{4}x_{\mathrm{C}}}{4\left(x_{\mathrm{C}}-x_{\mathrm{B}}\right)^{2}}\cdot\mathcal{H}\left(x_{\mathrm{B}}-x_{p,l,2}\right)\right],\tag{39}$$

$$
\begin{aligned}
V_{\mathrm{C}} = &-\sum_{k=1}^{r} N_k \frac{\left(x_{N,k}-x_{\mathrm{A}}\right)}{\left(x_{\mathrm{C}}-x_{\mathrm{A}}\right)} - \sum_{i=1}^{t} F_i \frac{\left(x_{F,i}-x_{\mathrm{A}}\right)}{\left(x_{\mathrm{C}}-x_{\mathrm{A}}\right)} - \\
&\sum_{l=1}^{q} p_l \frac{\left(x_{p,l,2}-x_{p,l,1}\right)}{\left(x_{\mathrm{C}}-x_{\mathrm{A}}\right)} \left(\frac{x_{p,l,2}+x_{p,l,1}}{2} - x_{\mathrm{A}} \right) + \\
&\sum_{k=1}^{r} N_k \frac{\left(x_{\mathrm{C}}-x_{N,k}\right)\left(x_{\mathrm{B}}-x_{\mathrm{A}}\right)}{\left(x_{\mathrm{C}}-x_{\mathrm{B}}\right)\left(x_{\mathrm{C}}-x_{\mathrm{A}}\right)} + \sum_{i=1}^{t} F_i \frac{\left(x_{\mathrm{C}}-x_{F,i}\right)\left(x_{\mathrm{B}}-x_{\mathrm{A}}\right)}{\left(x_{\mathrm{C}}-x_{\mathrm{B}}\right)\left(x_{\mathrm{C}}-x_{\mathrm{A}}\right)} + \\
&\sum_{l=1}^{q} p_l \frac{\left(x_{p,l,2}-x_{p,l,1}\right)\left(x_{\mathrm{B}}-x_{\mathrm{A}}\right)}{\left(x_{\mathrm{C}}-x_{\mathrm{B}}\right)\left(x_{\mathrm{C}}-x_{\mathrm{A}}\right)} \left(x_{\mathrm{C}} - \frac{x_{p,l,2}+x_{p,l,1}}{2} \right) + \\
&\left[\frac{\left(x_{\mathrm{B}}-x_{\mathrm{A}}\right)\left(x_{\mathrm{C}}-x_{\mathrm{B}}\right)}{\left(x_{\mathrm{C}}-x_{\mathrm{A}}\right)^3 x_{\mathrm{B}} - \left(x_{\mathrm{C}}-x_{\mathrm{A}}\right)\left(x_{\mathrm{C}}-x_{\mathrm{B}}\right)^2 x_{\mathrm{B}} - \left(x_{\mathrm{B}}-x_{\mathrm{A}}\right)^3 x_{\mathrm{C}}} \right] \times \\
&\left[\sum_{k=1}^{r} N_k \left(x_{\mathrm{C}}-x_{N,k}\right) x_{\mathrm{B}} + \sum_{i=1}^{t} F_i \left(x_{\mathrm{C}}-x_{F,i}\right) x_{\mathrm{B}} + \right. \\
&\sum_{l=1}^{q} p_l \left(x_{p,l,2}-x_{p,l,1}\right) x_{\mathrm{B}} \left(x_{\mathrm{C}} - \frac{x_{p,l,2}+x_{p,l,1}}{2} \right) - \sum_{k=1}^{r} N_k \frac{\left(x_{\mathrm{C}}-x_{N,k}\right)^3 x_{\mathrm{B}}}{\left(x_{\mathrm{C}}-x_{\mathrm{B}}\right)^2} - \\
&\sum_{i=1}^{t} F_i \frac{\left(x_{\mathrm{C}}-x_{F,i}\right)^3 x_{\mathrm{B}}}{\left(x_{\mathrm{C}}-x_{\mathrm{B}}\right)^2} - \sum_{l=1}^{q} p_l \frac{\left(x_{\mathrm{C}}-x_{p,l,1}\right)^4 x_{\mathrm{B}}}{4\left(x_{\mathrm{C}}-x_{\mathrm{B}}\right)^2} + \sum_{l=1}^{q} p_l \frac{\left(x_{\mathrm{C}}-x_{p,l,2}\right)^4 x_{\mathrm{B}}}{4\left(x_{\mathrm{C}}-x_{\mathrm{B}}\right)^2} + \\
&\sum_{k=1}^{r} N_k \frac{\left(x_{\mathrm{B}}-x_{N,k}\right)^3 x_{\mathrm{C}}}{\left(x_{\mathrm{C}}-x_{\mathrm{B}}\right)^2} \cdot \mathcal{H}\left(x_{\mathrm{B}}-x_{N,k}\right) + \sum_{i=1}^{t} F_i \frac{\left(x_{\mathrm{B}}-x_{F,i}\right)^3 x_{\mathrm{C}}}{\left(x_{\mathrm{C}}-x_{\mathrm{B}}\right)^2} \cdot \mathcal{H}\left(x_{\mathrm{B}}-x_{F,i}\right) + \\
&\left. \sum_{l=1}^{q} p_l \frac{\left(x_{\mathrm{B}}-x_{p,l,1}\right)^4 x_{\mathrm{C}}}{4\left(x_{\mathrm{C}}-x_{\mathrm{B}}\right)^2} \cdot \mathcal{H}\left(x_{\mathrm{B}}-x_{p,l,1}\right) - \sum_{l=1}^{q} p_l \frac{\left(x_{\mathrm{B}}-x_{p,l,2}\right)^4 x_{\mathrm{C}}}{4\left(x_{\mathrm{C}}-x_{\mathrm{B}}\right)^2} \cdot \mathcal{H}\left(x_{\mathrm{B}}-x_{p,l,2}\right) \right].
\end{aligned}
\tag{40}
$$

Using Equations (34), (38), (39) and (40), it is possible to calculate deflections of the two-span continuous beam.

2.3.2 Behaviour of the stiffening girder working as a simple beam

If the stiffening girder is not supported at the pylon, then the design scheme is a simple beam (Figure 16).

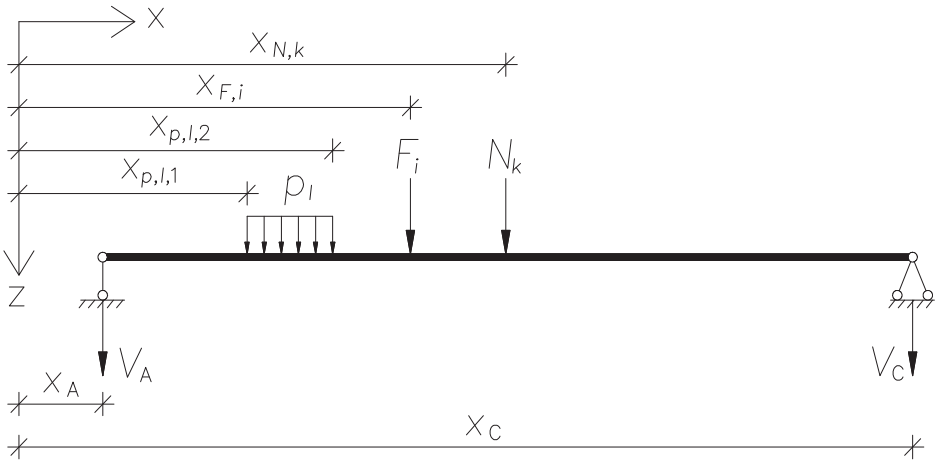

Figure 16. Design scheme of the stiffening girder – a simple beam

The elastic curve of the girder can be calculated using Equation (34). The support reactions are

$$V_A = -\sum_{k=1}^{r} N_k \frac{\left(x_C - x_{N,k}\right)}{\left(x_C - x_A\right)} - \sum_{i=1}^{t} F_i \frac{\left(x_C - x_{F,i}\right)}{\left(x_C - x_A\right)} - \sum_{l=1}^{q} p_l \frac{\left(x_{p,l,2} - x_{p,l,1}\right)}{\left(x_C - x_A\right)} \left(x_C - \frac{x_{p,l,2} + x_{p,l,1}}{2} \right) \tag{41}$$

and

$$V_C = \sum_{k=1}^{r} N_k \frac{\left(x_{N,k} - x_A\right)}{\left(x_C - x_A\right)} - \sum_{i=1}^{t} F_i \frac{\left(x_{F,i} - x_A\right)}{\left(x_C - x_A\right)} - \sum_{l=1}^{q} p_l \frac{\left(x_{p,l,2} - x_{p,l,1}\right)}{\left(x_C - x_A\right)} \left(\frac{x_{p,l,2} + x_{p,l,1}}{2} - x_A \right). \tag{42}$$

2.3.3 Behaviour of the stiffening girder working as two simple beams

The intermediate support can also be a hinge and then the stiffening girder works as two sequential simple beams (Figure 17).

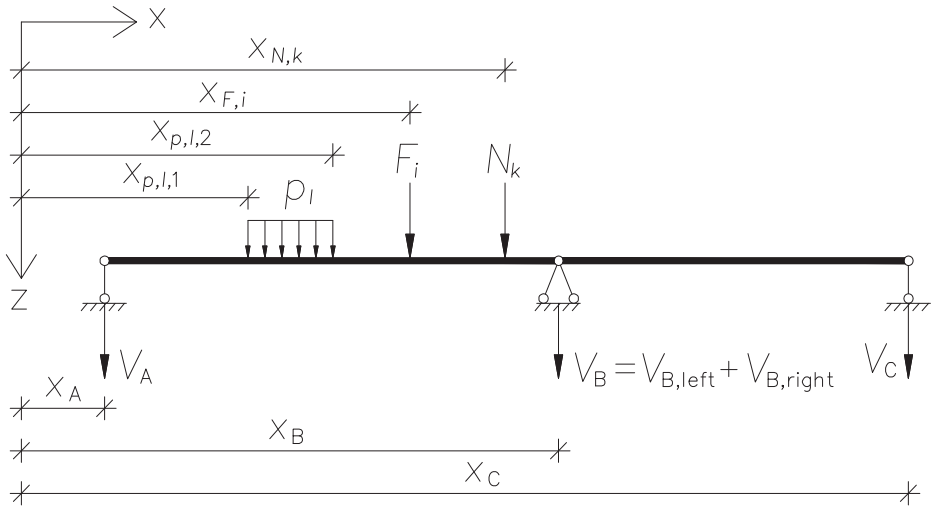

Figure 17. Design scheme of the stiffening girder – two simple beams

The elastic curve of the left section of the girder (segment A-B):

$$w(x) = -\sum_{k=1}^{n} P_k \frac{\left(x_\mathrm{B} - x_{P,k}\right)^3 x}{6E_\mathrm{g}I_\mathrm{g}x_\mathrm{B}} \cdot \mathcal{H}\left(x_\mathrm{B} - x_{P,k}\right) -$$

$$\left[\sum_{l=1}^{q} p_l \frac{\left(x_\mathrm{B} - x_{p,l,1}\right)^4 x}{24E_\mathrm{g}I_\mathrm{g}x_\mathrm{B}} - \sum_{l=1}^{q} p_l \frac{\left(x_\mathrm{B} - x_{p,l,2}\right)^4 x}{24E_\mathrm{g}I_\mathrm{g}x_\mathrm{B}}\right] \cdot \mathcal{H}\left(x_\mathrm{B} - x_{p,l,1}\right) \cdot \mathcal{H}\left(x_\mathrm{B} - x_{p,l,2}\right) -$$

$$\sum_{l=1}^{q} p_l \frac{\left(x_\mathrm{B} - x_{p,l,1}\right)^4 x}{24E_\mathrm{g}I_\mathrm{g}x_\mathrm{B}} \cdot \mathcal{H}\left(x_\mathrm{B} - x_{p,l,1}\right) \cdot \mathcal{H}\left(x_{p,l,2} - x_\mathrm{B}\right) +$$

$$\sum_{k=1}^{n} P_k \frac{\left(x - x_{P,k}\right)^3}{6E_\mathrm{g}I_\mathrm{g}} \cdot \mathcal{H}\left(x - x_{P,k}\right) \cdot \mathcal{H}\left(x_\mathrm{B} - x_{p,k}\right) + \left[\sum_{l=1}^{q} p_l \frac{\left(x - x_{p,l,1}\right)^4}{24E_\mathrm{g}I_\mathrm{g}} \cdot \mathcal{H}\left(x - x_{p,l,1}\right) -\right.$$

$$\left.\sum_{l=1}^{q} p_l \frac{\left(x - x_{p,l,2}\right)^4}{24E_\mathrm{g}I_\mathrm{g}} \cdot \mathcal{H}\left(x - x_{p,l,2}\right)\right] \cdot \mathcal{H}\left(x_\mathrm{B} - x_{p,l,2}\right) +$$

$$\sum_{l=1}^{q} p_l \frac{\left(x - x_{p,l,1}\right)^4}{24E_\mathrm{g}I_\mathrm{g}} \cdot \mathcal{H}\left(x - x_{p,l,1}\right) \cdot \mathcal{H}\left(x_\mathrm{B} - x_{p,l,1}\right) \cdot \mathcal{H}\left(x_{p,l,2} - x_\mathrm{B}\right). \tag{43}$$

The elastic curve of the right section of the girder (segment B-C):

$$w(x)=-\sum_{k=1}^{n}P_k\frac{\left(x_{\mathrm{C}}-x_{P,k}\right)^3x}{6E_{\mathrm{g}}I_{\mathrm{g}}x_{\mathrm{C}}}\cdot\mathcal{H}\left(x_{P,k}-x_{\mathrm{B}}\right)-$$
$$\left[\sum_{l=1}^{q}p_l\frac{\left(x_{\mathrm{C}}-x_{p,l,1}\right)^4x}{24E_{\mathrm{g}}I_{\mathrm{g}}x_{\mathrm{C}}}-\sum_{l=1}^{q}p_l\frac{\left(x_{\mathrm{C}}-x_{p,l,2}\right)^4x}{24E_{\mathrm{g}}I_{\mathrm{g}}x_{\mathrm{C}}}\right]\cdot\mathcal{H}\left(x_{p,l,1}-x_{\mathrm{B}}\right)+$$
$$\sum_{k=1}^{n}P_k\frac{\left(x-x_{P,k}\right)^3}{6E_{\mathrm{g}}I_{\mathrm{g}}}\cdot\mathcal{H}\left(x-x_{P,k}\right)\cdot\mathcal{H}\left(x_{P,k}-x_{\mathrm{B}}\right)+\left[\sum_{l=1}^{q}p_l\frac{\left(x-x_{p,l,1}\right)^4}{24E_{\mathrm{g}}I_{\mathrm{g}}}\cdot\mathcal{H}\left(x-x_{p,l,1}\right)-\right.$$
$$\left.\sum_{l=1}^{q}p_l\frac{\left(x-x_{p,l,2}\right)^4}{24E_{\mathrm{g}}I_{\mathrm{g}}}\cdot\mathcal{H}\left(x-x_{p,l,2}\right)\right]\cdot\mathcal{H}\left(x_{p,l,1}-x_{\mathrm{B}}\right). \tag{44}$$

The support reactions V_{A}, $V_{\mathrm{B}}=V_{\mathrm{B,left}}+V_{\mathrm{B,right}}$ and V_{C} can be calculated as follows:

$$V_{\mathrm{A}}=-\sum_{k=1}^{r}N_k\frac{\left(x_{\mathrm{B}}-x_{N,k}\right)}{\left(x_{\mathrm{B}}-x_{\mathrm{A}}\right)}\cdot\mathcal{H}\left(x_{\mathrm{B}}-x_{N,k}\right)-\sum_{i=1}^{t}F_i\frac{\left(x_{\mathrm{B}}-x_{F,i}\right)}{\left(x_{\mathrm{B}}-x_{\mathrm{A}}\right)}\cdot\mathcal{H}\left(x_{\mathrm{B}}-x_{F,i}\right)-$$
$$\sum_{l=1}^{q}p_l\frac{\left(x_{p,l,2}-x_{p,l,1}\right)}{\left(x_{\mathrm{B}}-x_{\mathrm{A}}\right)}\left(x_{\mathrm{B}}-\frac{x_{p,l,2}+x_{p,l,1}}{2}\right)\cdot\mathcal{H}\left(x_{\mathrm{B}}-x_{p,l,2}\right)\cdot\mathcal{H}\left(x_{\mathrm{B}}-x_{p,l,1}\right)- \tag{45}$$
$$\sum_{l=1}^{q}p_l\frac{\left(x_{\mathrm{B}}-x_{p,l,1}\right)}{\left(x_{\mathrm{B}}-x_{\mathrm{A}}\right)}\left(\frac{x_{\mathrm{B}}-x_{p,l,1}}{2}\right)\cdot\mathcal{H}\left(x_{p,l,2}-x_{\mathrm{B}}\right)\cdot\mathcal{H}\left(x_{\mathrm{B}}-x_{p,l,1}\right),$$

$$V_{\mathrm{B,left}}=-\sum_{k=1}^{r}N_k\frac{\left(x_{N,k}-x_{\mathrm{A}}\right)}{\left(x_{\mathrm{B}}-x_{\mathrm{A}}\right)}\cdot\mathcal{H}\left(x_{\mathrm{B}}-x_{N,k}\right)-\sum_{i=1}^{t}F_i\frac{\left(x_{F,i}-x_{\mathrm{A}}\right)}{\left(x_{\mathrm{B}}-x_{\mathrm{A}}\right)}\cdot\mathcal{H}\left(x_{\mathrm{B}}-x_{F,i}\right)-$$
$$\sum_{l=1}^{q}p_l\frac{\left(x_{p,l,2}-x_{p,l,1}\right)}{\left(x_{\mathrm{B}}-x_{\mathrm{A}}\right)}\left(\frac{x_{p,l,2}+x_{p,l,1}}{2}-x_{\mathrm{A}}\right)\cdot\mathcal{H}\left(x_{\mathrm{B}}-x_{p,l,2}\right)\cdot\mathcal{H}\left(x_{\mathrm{B}}-x_{p,l,1}\right)- \tag{46}$$
$$\sum_{l=1}^{q}p_l\frac{\left(x_{\mathrm{B}}-x_{p,l,1}\right)}{\left(x_{\mathrm{B}}-x_{\mathrm{A}}\right)}\left(\frac{x_{\mathrm{B}}+x_{p,l,1}}{2}-x_{\mathrm{A}}\right)\cdot\mathcal{H}\left(x_{p,l,2}-x_{\mathrm{B}}\right)\cdot\mathcal{H}\left(x_{\mathrm{B}}-x_{p,l,1}\right),$$

$$V_{\mathrm{B,right}} = -\sum_{k=1}^{r} N_k \frac{\left(x_{N,k} - x_{\mathrm{B}}\right)}{\left(x_{\mathrm{C}} - x_{\mathrm{B}}\right)} \cdot \mathcal{H}\left(x_{N,k} - x_{\mathrm{B}}\right) - \sum_{i=1}^{t} F_i \frac{\left(x_{F,i} - x_{\mathrm{B}}\right)}{\left(x_{\mathrm{C}} - x_{\mathrm{B}}\right)} \cdot \mathcal{H}\left(x_{F,i} - x_{\mathrm{B}}\right) -$$
$$\sum_{l=1}^{q} p_l \frac{\left(x_{p,l,2} - x_{p,l,1}\right)}{\left(x_{\mathrm{C}} - x_{\mathrm{B}}\right)} \left(x_{\mathrm{C}} - \frac{x_{p,l,2} + x_{p,l,1}}{2} \right) \cdot \mathcal{H}\left(x_{p,l,2} - x_{\mathrm{B}}\right) \cdot \mathcal{H}\left(x_{p,l,1} - x_{\mathrm{B}}\right) - \tag{47}$$
$$\sum_{l=1}^{q} p_l \frac{\left(x_{p,l,2} - x_{\mathrm{B}}\right)}{\left(x_{\mathrm{C}} - x_{\mathrm{B}}\right)} \left(x_{\mathrm{C}} - \frac{x_{p,l,2} + x_{\mathrm{B}}}{2} \right) \cdot \mathcal{H}\left(x_{p,l,2} - x_{\mathrm{B}}\right) \cdot \mathcal{H}\left(x_{\mathrm{B}} - x_{p,l,1}\right),$$

$$V_{\mathrm{C}} = -\sum_{k=1}^{r} N_k \frac{\left(x_{N,k} - x_{\mathrm{B}}\right)}{\left(x_{\mathrm{C}} - x_{\mathrm{B}}\right)} \cdot \mathcal{H}\left(x_{N,k} - x_{\mathrm{B}}\right) - \sum_{i=1}^{t} F_i \frac{\left(x_{F,i} - x_{\mathrm{B}}\right)}{\left(x_{\mathrm{C}} - x_{\mathrm{B}}\right)} \cdot \mathcal{H}\left(x_{F,i} - x_{\mathrm{B}}\right) -$$
$$\sum_{l=1}^{q} p_l \frac{\left(x_{p,l,2} - x_{p,l,1}\right)}{\left(x_{\mathrm{C}} - x_{\mathrm{B}}\right)} \left(\frac{x_{p,l,2} + x_{p,l,1}}{2} - x_{\mathrm{B}} \right) \cdot \mathcal{H}\left(x_{p,l,2} - x_{\mathrm{B}}\right) \cdot \mathcal{H}\left(x_{p,l,1} - x_{\mathrm{B}}\right) - \tag{48}$$
$$\sum_{l=1}^{q} p_l \frac{\left(x_{p,l,2} - x_{\mathrm{B}}\right)}{\left(x_{\mathrm{C}} - x_{\mathrm{B}}\right)} \left(\frac{x_{p,l,2} - x_{\mathrm{B}}}{2} \right) \cdot \mathcal{H}\left(x_{p,l,2} - x_{\mathrm{B}}\right) \cdot \mathcal{H}\left(x_{\mathrm{B}} - x_{p,l,1}\right).$$

2.4 Behaviour of the girder-stiffened cable

The method of the design of the girder-stiffened cable worked out in this thesis is based on an algorithm where the cable and the stiffening girder are calculated separately. The algorithm uses an iterative process and the conceptual steps of the calculation are as follows:

1) The first step is to find the shape and the inside force of the cable in the initial balance.
2) The inside force of the cable, the displacements of the cable's nodal points and the horizontal displacement of the pylon's top must be calculated using the whole dead load of the structure. At this stage the stiffening girder is suspended to the cable. This state is taken as the initial balance for the next stage.
3) The imposed load has effect on the stiffening girder – the girder and the cable work together from now on. The inside forces of the hangers (i.e. contact forces) must be assumed and it must be taken into account that most of the imposed load is carried by the cable [Idnurm, J. 2004; Kirsanov 1981]. The initial contact forces are calculated, provided that the cable has approximately 90% of the bridge's total load. The contact forces are redistributed during the iteration. After finding all the deflections and inside forces of the structure the elongation of the hangers can be calculated [Rohusaar 2005]:

$$\Delta l_{\mathrm{h},i} = \frac{\Delta F_{\mathrm{h},i} l_{\mathrm{h},i}}{E_{\mathrm{h},i} A_{\mathrm{h},i}}, \tag{49}$$

where

$\Delta l_{\mathrm{h},i}$ – lengthening of the hanger;
$l_{\mathrm{h},i}$ – initial length of the hanger;
$\Delta F_{\mathrm{h},i}$ – change of the internal force of the hanger;
$E_{\mathrm{h},i}$ – modulus of elasticity of the hanger;
$A_{\mathrm{h},i}$ – cross-sectional area of the hanger.

4) The final step is to evaluate if the assumed inside forces of the hangers were right. The following requirement should be satisfied:

$$\sum_{i=1}^{n} \left| w_{\mathrm{g},i} - w_{\mathrm{c},i} - \Delta l_{\mathrm{h},i} \right| \approx 0, \tag{50}$$

where

$w_{\mathrm{g},i}$ – vertical deflection of the stiffening girder at the point where the hanger is connected;

$w_{c,i}$ – vertical deflection of the cable at the point where the same hanger is connected.

If this condition is not satisfied, the contact forces must be corrected and the calculation must be repeated until Equation (50) is assured.

Example 4

Determine the final internal forces and the deflections of the girder-stiffened cable structure described in Figure E.4.1 using the first simplification of the discrete analysis. The moment of inertia of the girder is $I_g = 4{,}49 \times 10^9$ mm^4 and the modulus of elasticity $E_g = 2{,}06 \times 10^5$ N/mm^2. The modulus of elasticity of the cable is $E_c = 1{,}19 \times 10^5$ N/mm^2.

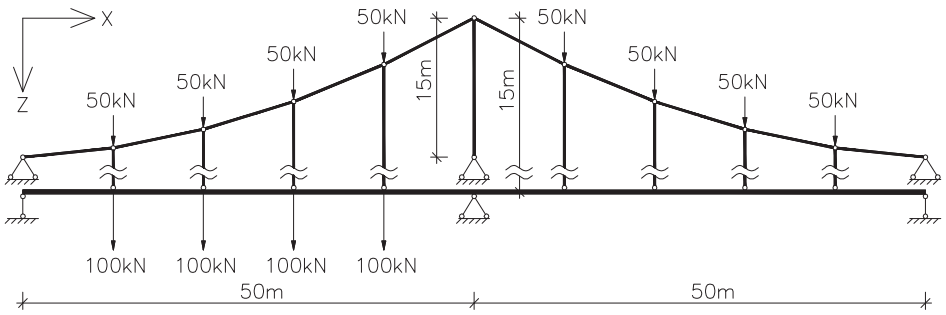

Figure E.4.1. Simplified design scheme of Example 4 (see also Figures E.1.1, E.2.1 and E.3.1)

In the initial balance the cable is loaded only (50 kN at every nodal point) and the stiffening girder is not. Later, when the additional load 100 kN appears, the cable and the girder work together. It is hard to predict the partition of the loads between the girder and the cable. Let us assume in the beginning that the total final load is $F_{I,c,i} = 80\,\text{kN}$ (including the load in the initial balance) for every nodal point of the left cable and $F_{II,c,i} = 60\,\text{kN}$ for the right cable. Thus, for the left span of the girder the contact load from the hangers is $F_{I,g,i} = -(80 - 50) = -30\,\text{kN}$ and for the right span $F_{II,g,i} = -(60 - 50) = -10\,\text{kN}$.

Using the calculation steps described in Example 3, the horizontal component of the internal force of the cable and the vertical displacements of the nodal points can be calculated (see Table E.4.1).

To calculate the support reaction V_A of the stiffening girder, Equation (38) takes the form of

$$V_{\mathrm{A}}=\left[\frac{\left(x_{\mathrm{C}}-x_{\mathrm{B}}\right)^{2}}{\left(x_{\mathrm{C}}-x_{\mathrm{A}}\right)^{3}x_{\mathrm{B}}-\left(x_{\mathrm{C}}-x_{\mathrm{A}}\right)\left(x_{\mathrm{C}}-x_{\mathrm{B}}\right)^{2}x_{\mathrm{B}}-\left(x_{\mathrm{B}}-x_{\mathrm{A}}\right)^{3}x_{\mathrm{C}}}\right]\times$$
$$\left[\sum_{k=1}^{r}N_{k}\left(x_{\mathrm{C}}-x_{N,k}\right)x_{\mathrm{B}}+\sum_{i=1}^{t}F_{i}\left(x_{\mathrm{C}}-x_{F,i}\right)x_{\mathrm{B}}-\right.$$
$$\sum_{k=1}^{r}N_{k}\frac{\left(x_{\mathrm{C}}-x_{N,k}\right)^{3}x_{\mathrm{B}}}{\left(x_{\mathrm{C}}-x_{\mathrm{B}}\right)^{2}}-\sum_{i=1}^{t}F_{i}\frac{\left(x_{\mathrm{C}}-x_{F,i}\right)^{3}x_{\mathrm{B}}}{\left(x_{\mathrm{C}}-x_{\mathrm{B}}\right)^{2}}+$$
$$\left.\sum_{k=1}^{r}N_{k}\frac{\left(x_{\mathrm{B}}-x_{N,k}\right)^{3}x_{\mathrm{C}}}{\left(x_{\mathrm{C}}-x_{\mathrm{B}}\right)^{2}}\cdot\mathcal{H}\left(x_{\mathrm{B}}-x_{N,k}\right)+\sum_{i=1}^{t}F_{i}\frac{\left(x_{\mathrm{B}}-x_{F,i}\right)^{3}x_{\mathrm{C}}}{\left(x_{\mathrm{C}}-x_{\mathrm{B}}\right)^{2}}\cdot\mathcal{H}\left(x_{\mathrm{B}}-x_{F,i}\right)\right],$$

which leads to the next result:

$$V_{\mathrm{A}}=\left[\frac{(100-50)^{2}}{(100-0)^{3}\times50-(100-0)\times(100-50)^{2}\times50-(50-0)^{3}\times100}\right]\times$$
$$[100\times(100-10)\times50+100\times(100-20)\times50+100\times(100-30)\times50+$$
$$100\times(100-40)\times50+(-30)\times(100-10)\times50+(-30)\times(100-20)\times50+$$
$$(-30)\times(100-30)\times50+(-30)\times(100-40)\times50+(-10)\times(100-60)\times50+$$
$$(-10)\times(100-70)\times50+(-10)\times(100-80)\times50+(-10)\times(100-90)\times50-$$
$$100\times\frac{(100-10)^{3}\times50}{(100-50)^{2}}-100\times\frac{(100-20)^{3}\times50}{(100-50)^{2}}-100\times\frac{(100-30)^{3}\times50}{(100-50)^{2}}-$$
$$100\times\frac{(100-40)^{3}\times50}{(100-50)^{2}}-(-30)\times\frac{(100-10)^{3}\times50}{(100-50)^{2}}-(-30)\times\frac{(100-20)^{3}\times50}{(100-50)^{2}}-$$
$$(-30)\times\frac{(100-30)^{3}\times50}{(100-50)^{2}}-(-30)\times\frac{(100-40)^{3}\times50}{(100-50)^{2}}-(-10)\times\frac{(100-60)^{3}\times50}{(100-50)^{2}}-$$
$$(-10)\times\frac{(100-70)^{3}\times50}{(100-50)^{2}}-(-10)\times\frac{(100-80)^{3}\times50}{(100-50)^{2}}-(-10)\times\frac{(100-90)^{3}\times50}{(100-50)^{2}}+$$
$$100\times\frac{(50-10)^{3}\times100}{(100-50)^{2}}+100\times\frac{(50-20)^{3}\times100}{(100-50)^{2}}+100\times\frac{(50-30)^{3}\times100}{(100-50)^{2}}+$$
$$100\times\frac{(50-40)^{3}\times100}{(100-50)^{2}}+(-30)\times\frac{(50-10)^{3}\times100}{(100-50)^{2}}+(-30)\times\frac{(50-20)^{3}\times100}{(100-50)^{2}}+$$
$$(-30)\times\frac{(50-30)^{3}\times100}{(100-50)^{2}}+(-30)\times\frac{(50-40)^{3}\times100}{(100-50)^{2}}\Bigg]=-122\ \mathrm{kN}.$$

Similarly, the other support reactions $V_{\mathrm{B}} = -156\,\mathrm{kN}$ and $V_{\mathrm{C}} = 38\,\mathrm{kN}$ using Equations (39) and (40) can be found.

From Equation (34) it is possible to find the deflections of the girder at the points where the hangers are connected. For example, if $x = 20\,\mathrm{m},$ then

$$w(x) = \frac{1}{6E_{\mathrm{g}}I_{\mathrm{g}}}\left[-\sum_{k=1}^{n} P_k \frac{\left(x_{\mathrm{C}} - x_{P,k}\right)^3 x}{x_{\mathrm{C}}} + \sum_{k=1}^{n} P_k \left(x - x_{P,k}\right)^3 \cdot \mathcal{H}\left(x - x_{P,k}\right)\right] \Rightarrow$$

$$\Rightarrow w(20) = w_{\mathrm{I,g,2}} = \frac{1}{6 \times 206000000 \times 0{,}004491802543} \times$$

$$\left[-(-122) \times \frac{(100-0)^3 \times 20}{100} - (-156) \times \frac{(100-50)^3 \times 20}{100} - 38 \times \frac{(100-100)^3 \times 20}{100} - \right.$$

$$(-30) \times \frac{(100-10)^3 \times 20}{100} - (-30) \times \frac{(100-20)^3 \times 20}{100} - (-30) \times \frac{(100-30)^3 \times 20}{100} -$$

$$(-30) \times \frac{(100-40)^3 \times 20}{100} - (-10) \times \frac{(100-60)^3 \times 20}{100} - (-10) \times \frac{(100-70)^3 \times 20}{100} -$$

$$(-10) \times \frac{(100-80)^3 \times 20}{100} - (-10) \times \frac{(100-90)^3 \times 20}{100} - 100 \times \frac{(100-10)^3 \times 20}{100} -$$

$$100 \times \frac{(100-20)^3 \times 20}{100} - 100 \times \frac{(100-30)^3 \times 20}{100} - 100 \times \frac{(100-40)^3 \times 20}{100} +$$

$$\left.(-122) \times (20-0)^3 + (-30) \times (20-10)^3 + 100 \times (20-10)^3\right] =$$

$$= 0{,}4312\,\mathrm{m} = 431{,}2\,\mathrm{mm}.$$

Equation (49) provides us the elongations of the hangers. For instance, the elongation of the fourth hanger from the left is

$$\Delta l_{\mathrm{I,h,4}} = \frac{30000 \times 10000}{206000 \times \dfrac{\pi \times 75^2}{4}} = 0{,}33\,\mathrm{mm}.$$

Other calculation results are presented in Table E.4.1. The evaluation of the calculations must be done using Equation (50):

$$\sum_{i=1}^{n} \left| w_{\mathrm{g},i} - w_{\mathrm{c},i} - \Delta l_{\mathrm{h},i} \right| = 832{,}7\,\mathrm{mm} \neq 0,$$

which means that the internal forces of the hangers must be corrected and the calculation steps should be repeated.

Table E.4.1. Tentative and final calculation results of Example 4

Description of the element		**Deformation [mm]**	
Element name	**Symbol**	**Tentative**	**Final**
Left cable	$w_{\mathrm{I,c,1}}$	348,8	288,2
	$w_{\mathrm{I,c,2}}$	523,3	451,7
	$w_{\mathrm{I,c,3}}$	523,3	432,5
	$w_{\mathrm{I,c,4}}$	348,8	249,4
Right cable	$w_{\mathrm{II,c,1}}$	-238,4	-178,9
	$w_{\mathrm{II,c,2}}$	-357,6	-255,2
	$w_{\mathrm{II,c,3}}$	-357,6	-236,0
	$w_{\mathrm{II,c,4}}$	-238,4	-140,3
Left beam	$w_{\mathrm{I,g,1}}$	275,2	288,2
	$w_{\mathrm{I,g,2}}$	431,2	451,8
	$w_{\mathrm{I,g,3}}$	411,8	432,7
	$w_{\mathrm{I,g,4}}$	236,3	249,6
Right beam	$w_{\mathrm{II,g,1}}$	-167,2	-178,8
	$w_{\mathrm{II,g,2}}$	-236,7	-255,2
	$w_{\mathrm{II,g,3}}$	-217,2	-236,0
	$w_{\mathrm{II,g,4}}$	-128,3	-140,3
Left hangers	$\Delta l_{\mathrm{I,h,1}}$	0,03	0,03
	$\Delta l_{\mathrm{I,h,2}}$	0,10	0,10
	$\Delta l_{\mathrm{I,h,3}}$	0,20	0,19
	$\Delta l_{\mathrm{I,h,4}}$	0,33	0,24
Right hangers	$\Delta l_{\mathrm{II,h,1}}$	0,11	0,11
	$\Delta l_{\mathrm{II,h,2}}$	0,07	0,07
	$\Delta l_{\mathrm{II,h,3}}$	0,03	0,04
	$\Delta l_{\mathrm{II,h,4}}$	0,01	0,02
Pylon's top	u_{p}	-150,8	-114,9

The final internal forces and the support reactions after the iteration (the final deformations are presented in Table E.4.1) are

$$\begin{cases} H = 672187 \text{ N} \\ F_{\text{I,c,1}} = 75595 \text{ N } (F_{\text{I,g,1}} = 25595 \text{ N}) \\ F_{\text{I,c,2}} = 79506 \text{ N } (F_{\text{I,g,2}} = 29506 \text{ N}) \\ F_{\text{I,c,3}} = 78234 \text{ N } (F_{\text{I,g,3}} = 28234 \text{ N}) \\ F_{\text{I,c,4}} = 71673 \text{ N } (F_{\text{I,g,4}} = 21673 \text{ N}) \\ F_{\text{II,c,1}} = 60319 \text{ N } (F_{\text{II,g,1}} = 10319 \text{ N}) \\ F_{\text{II,c,2}} = 60800 \text{ N } (F_{\text{II,g,2}} = 10800 \text{ N}) \\ F_{\text{II,c,3}} = 62071 \text{ N } (F_{\text{II,g,3}} = 12071 \text{ N}) \\ F_{\text{II,c,4}} = 64229 \text{ N } (F_{\text{II,g,4}} = 14229 \text{ N}) \\ V_{\text{A}} = \text{-}127647 \text{ N} \\ V_{\text{B}} = \text{-}163481 \text{ N} \\ V_{\text{C}} = 43555 \text{ N} \end{cases}.$$

The bending moments and the shear forces of the stiffening girder:

$$M(x) = E_{\text{g}} I_{\text{g}} w''(x) = \sum_{k=1}^{n} P_k \left(x - x_{P,k}\right) \cdot \mathcal{H}\left(x - x_{P,k}\right);$$

$$Q(x) = E_{\text{g}} I_{\text{g}} w'''(x) = \sum_{k=1}^{n} P_k \cdot \mathcal{H}\left(x - x_{P,k}\right).$$

For example:

$$M(20) = -127{,}647 \times 20 + \left(-25{,}595\right) \times 10 + 100 \times 10 = -1808{,}890 \text{ kNm};$$
$$Q_{\text{left}}(20) = -127{,}647 + \left(-25{,}595\right) + 100 = -53{,}242 \text{ kN};$$
$$Q_{\text{right}}(20) = -127{,}647 + \left(-25{,}595\right) + 100 + (-29{,}506) + 100 = 17{,}252 \text{ kN}.$$

The curves of the bending moment and the shear force of the stiffening girder are illustrated in Figures E.4.2 and E.4.3.

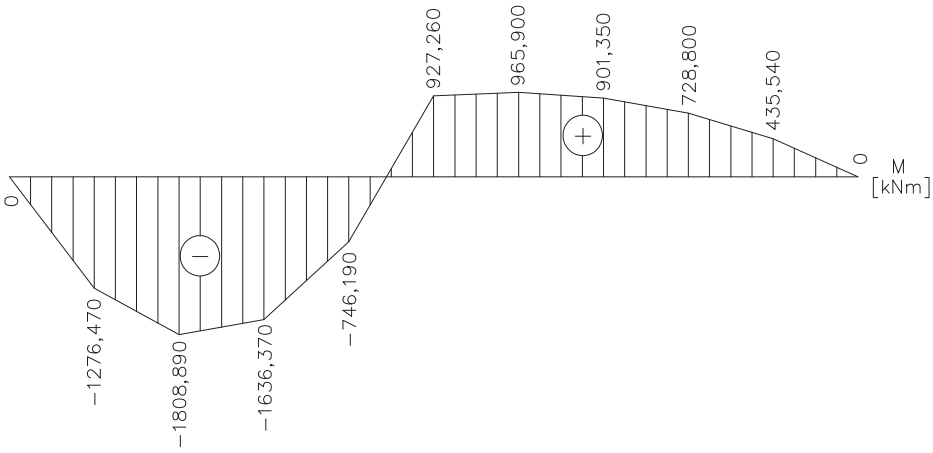

Figure E.4.2. Bending moments of the stiffening girder of Example 4

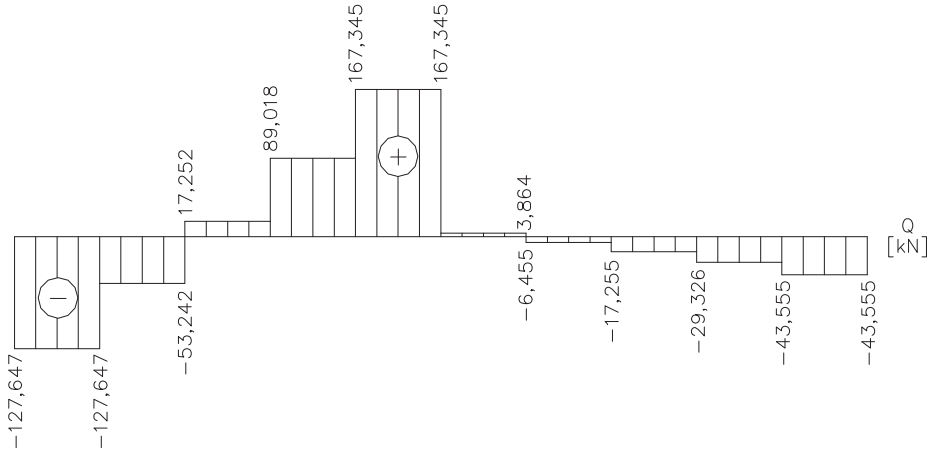

Figure E.4.3. Shear forces of the stiffening girder of Example 4

3. EXPERIMENTAL INVESTIGATION

3.1 Purpose of the experiment

The main idea of the experimental investigation is to verify the numerical discrete design method for the single-pylon suspension bridge. The exact dimensioning and optimising of the structure is not the purpose at this point. The initial parameters of the structure were selected from the previous studies of the author [Kiisa 2003, 2004].

3.2 Description of the test model

The structure under observation is a single-pylon pedestrian suspension bridge (Figure 18 and Appendix 1). The stiffening girder works as a two-span continuous beam (2×50 m). The pylon with the height of 15 m is situated in the middle of the bridge and the connection to the ground is a hinge. The bridge has two parallel main cables which are anchored to the ground separately from the stiffening girder. The main parameters of the bridge are presented in Table 4.

Table 4. Parameters of the bridge and the test model [Dolidze 1975; Pitlyuk 1971; Tärno 2003]

Parameter		Bridge	Coeff.	Test model
Overall dim.	Total length	100 m	α	4000 mm
	Left span	50 m	α	2000 mm
	Right span	50 m	α	2000 mm
	Pylon's height *	15 m	α	600 mm
Cable	Cross-sect. area	2228 mm^2	α^2	3,565 mm^2 **
	Mod. of elasticity	$(1{,}18...1{,}25)\times10^5$ MPa ***	1	$(1{,}18...1{,}25)\times10^5$ MPa ***
Stiff. girder	Mom. of inertia	44918×10^5 mm^4	α^4	11499 mm^4 ****
	Mod. of elasticity	$2{,}06\times10^5$ MPa	1	$2{,}06\times10^5$ MPa
Hangers	Diameter	75 mm	α	3 mm
	Mod. of elasticity	$2{,}06\times10^5$ MPa	1	$2{,}06\times10^5$ MPa

Comments:

* The height of the pylon is given from the stiffening girder.

** The total diameter of the cable is approximately 3 mm.

*** Variation of the modulus of elasticity is described below.

**** The stiffening girder is a round steel section with a diameter of 22 mm.

The scale of the model is $\alpha = 1/25 = 0{,}04$. To reduce the number of the complicated joints and to increase the measurement accuracy the model is coplanar (only vertical loads are used). To increase the stability of the model the A-shaped pylon is used. The model's supports (pylon, stiffening girder, cable) to the bearing frame are predicted to be non-deforming. The characterisation of the model is presented in Figure 19 and in Table 4.

Figure 18. View of the test model

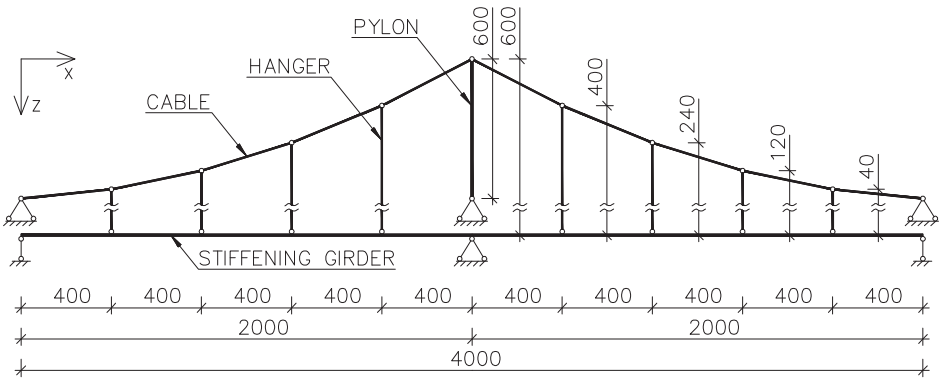

Figure 19. Simplified design scheme of the test model

3.3 Loads and load combinations

In the testing process only the vertical loads were used (imposed and dead load). The imposed loads were applied to both of the spans and to one span (Figure 20). Only the static concentrated loads were applied.

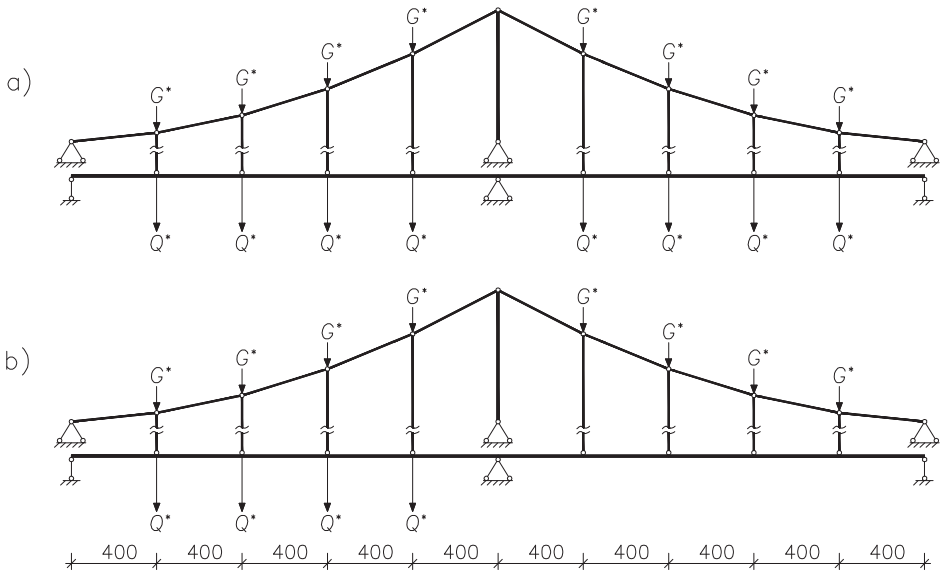

Figure 20. Load combinations of the test model (the same loads used while testing the cable without the stiffening girder): a) imposed loads Q applied to both of the spans (in addition to the dead load G*); b) imposed loads Q* applied to one span*

Using the scale of the model 1:25, the weight of the structure decreased 25^3 times, but the cross-sectional area of the elements only 25^2 times. The stresses from the dead load were 25 times smaller than in a real structure because of this. Additional loads must be used to compensate this difference, considering at the same time the assistant structures of the test model. For instance, in the initial balance of the real structure the nodal load of the cable is $G = 50\,\text{kN}$, which means $G^* = 50 \times 10^3 / 25^2 = 80\,\text{N} = 8155\,\text{g}$ for the test model (Table 5). But the dead load of this section of the model is only 390 g and that means an additional load of $8155 - 390 = 7765\,\text{g}$ must be used.

Concentrated imposed loads were applied to the stiffening girder at the points where the hangers are connected. The value of the imposed load is $Q = 100\,\text{kN}$ in the real structure and $Q^* = 100 \times 10^3 / 25^2 = 160\,\text{N} = 16310\,\text{g}$ in the model.

Table 5. Loads of the bridge and the test model [Dolidze 1975; Pitlyuk 1971; Tärno 2003]

Load type	**Load of the bridge**	**Coeff.**	**Load of the test model**
Dead load	$G = 50$ kN	α^2	$G^* = 80$ N
Imposed load	$Q = 100$ kN		$Q^* = 160$ N

The model was tested in the following stages:

1) The initial balance – only the cable was loaded by the dead load of the stiffening girder, hangers and the cable itself. In this stage the sections of the girder were connected to the hangers, but the girder was not contiguous.
2) The final balance – the stiffening girder was working with the cables under the loads.

On analogy, the cable without the girder was loaded to acquire more information for comparisons.

3.4 Measuring devices

The scheme of the measuring devices is illustrated in Figure 21 (see also Appendix 1). The following measuring devices were used:

1) Maksimov's gauge (the accuracy of 0,1 mm) – 8 devices to measure vertical deflections of the stiffening girder;
2) dial gauge (0,01 mm) – for measuring the horizontal displacements of the pylon's top;
3) strain gauge (10^{-6}) – two devices are connected to the end point of both cables.

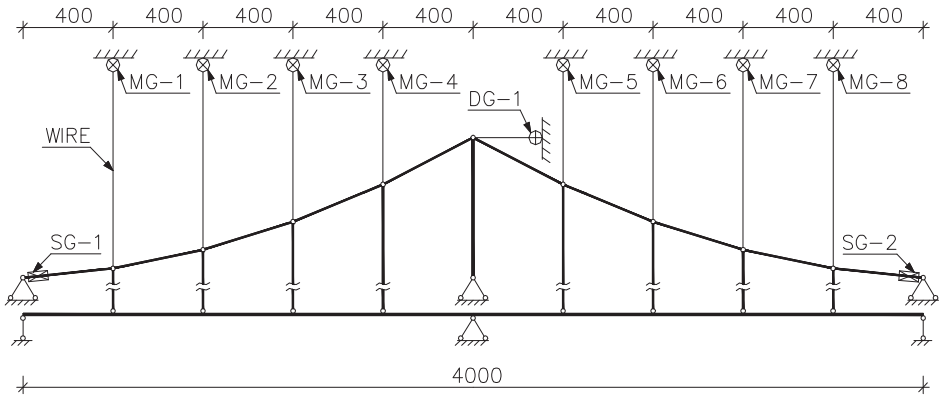

Figure 21. Scheme of the measuring devices (MG – Maksimov's gauge; DG – dial gauge; SG – strain gauge)

3.5 Experimental results

A compendious overview of the tests is described in Table 6. Every test was repeated for five times to ensure reliability of the results (the pause between the tests was five minutes).

Table 6. Simplified description of the tests

Symbol of the test	Load-bearing structure	Location of the dead load	Location of the imposed load
T-1.1	Cable	In both spans	In both spans
T-1.2	Cable	In both spans	In one span
T-2.1	Cable + stiffening girder	In both spans	In both spans
T-2.2	Cable + stiffening girder	In both spans	In one span

In the comparison of the experimental and calculated results it was most complicated to deal with the variable modulus of elasticity of the cable during the loading. When the internal force of the cable changed in the range of 800 and 2000 N, the modulus of elasticity changed between 1,18...1,25 N/mm^2 (Figure 22). The reason of this was the seven-wire strand with non-parallel wires. This choice was purposeful, to obtain larger deflections of the cable and to increase the accuracy of the measuring. In the theoretical calculations different moduli were used in different load steps.

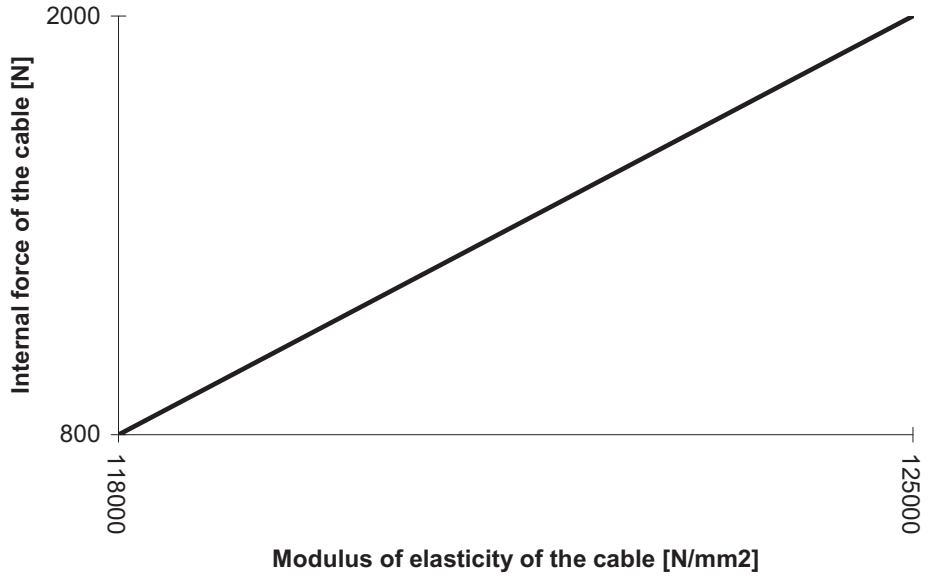

Figure 22. Dependence between the internal force and the modulus of elasticity of the cable

The test results verified the credibility of the test model. The results of each test varied at a maximum of ±1% from the average, being mostly between –0,2% and +0,2%. The average difference between single test results and mean results was 0,0%. That was the main reason why the tests were repeated only for five times. The vertical displacements of the nodal points were between 2,8…55,0 mm, i.e. the relative error of the measuring device was maximally $0{,}1/2{,}8\times100\% \approx 3{,}6\%$. Detailed test results are presented in Appendix 2.

The test results were compared with the calculated results. The calculated results are based on the first simplification of the discrete analysis. The reason is that the first simplification needs much less computational efficiency than the second one and the difference of the results between these two simplifications are almost the same as the relative errors of the measuring devices. The difference of the single results of the tests and the calculations were between +2,2...–12,6%. The measured results (the deflection of the cable, the internal force of the cable and the horizontal displacement of the pylon's top) were on average –4,4% smaller than the calculations predicted, proving well that the numerical calculation method worked out in this thesis is applicable. The results of the tests (R_E) and calculations (R_C) are summarised and compared ($\Delta R_{E/C}$) in Tables 7…12. The differences between the experimental results and the theoretical calculations of the maximum vertical displacements of the cable's nodal points are illustrated in Figure 23.

Table 7. Horizontal components of the cable's internal force (without a stiffening girder)

Symbol of the measuring device	**Experimental results (R_E), calculated results (R_C) and their differences ($\Delta R_{E/C}$)**					
	T-1.1			**T-1.2**		
	R_E [N]	**R_C [N]**	**$\Delta R_{E/C}$ [%]**	**R_E [N]**	**R_C [N]**	**$\Delta R_{E/C}$ [%]**
SG-1	1916,1	2076,4	-7,7	1494,5	1635,5	-8,6
SG-2	1959,2	2076,4	-5,6	1594,1	1635,5	-2,5

Table 8. Vertical displacements of the cable's nodal points (without a stiffening girder)

Symbol of the measuring device	**Experimental results (R_E), calculated results (R_C) and their differences ($\Delta R_{E/C}$)**					
	T-1.1			**T-1.2**		
	R_E [mm]	**R_C [mm]**	**$\Delta R_{E/C}$ [%]**	**R_E [mm]**	**R_C [mm]**	**$\Delta R_{E/C}$ [%]**
MG-1	12,5	12,5	0,1	37,5	37,4	0,2
MG-2	18,2	18,7	-2,6	55,0	56,1	-2,0
MG-3	18,0	18,7	-4,0	52,8	56,1	-5,9
MG-4	11,7	12,5	-6,2	33,5	37,4	-10,4
MG-5	12,0	12,5	-3,9	-35,7	-40,9	-12,6
MG-6	18,6	18,7	-0,6	-55,2	-61,3	-10,0
MG-7	19,0	18,7	1,5	-56,6	-61,3	-7,7
MG-8	12,6	12,5	0,6	-37,6	-40,9	-7,9

Table 9. Horizontal displacements of the pylon's top (without a stiffening girder)

Symbol of the measuring device	Experimental results (R_E), calculated results (R_C) and their differences ($\Delta R_{E/C}$)					
	T-1.1			T-1.2		
	R_E [mm]	R_C [mm]	$\Delta R_{E/C}$ [%]	R_E [mm]	R_C [mm]	$\Delta R_{E/C}$ [%]
DG-1	0,0	0,0	0,0	19,2	19,1	0,3

Table 10. Horizontal components of the cable's internal force (with a stiffening girder)

Symbol of the measuring device	Experimental results (R_E), calculated results (R_C) and their differences ($\Delta R_{E/C}$)					
	T-2.1			T-2.2		
	R_E [N]	R_C [N]	$\Delta R_{E/C}$ [%]	R_E [N]	R_C [N]	$\Delta R_{E/C}$ [%]
SG-1	1216,2	1287,2	-5,5	1050,0	1075,5	-2,4
SG-2	1221,7	1287,2	-5,1	1037,3	1075,5	-3,6

Table 11. Vertical displacements of the cable's nodal points (with a stiffening girder)

Symbol of the measuring device	Experimental results (R_E), calculated results (R_C) and their differences ($\Delta R_{E/C}$)					
	T-2.1			T-2.2		
	R_E [mm]	R_C [mm]	$\Delta R_{E/C}$ [%]	R_E [mm]	R_C [mm]	$\Delta R_{E/C}$ [%]
MG-1	5,7	6,2	-7,4	11,1	11,5	-3,5
MG-2	8,5	9,0	-6,1	16,9	18,1	-6,5
MG-3	7,3	7,4	-1,7	16,6	17,3	-4,2
MG-4	3,0	3,0	2,2	9,8	10,0	-2,3
MG-5	2,8	3,0	-4,2	-6,9	-7,2	-4,0
MG-6	7,1	7,4	-4,8	-9,4	-10,2	-7,5
MG-7	8,5	9,0	-5,8	-8,7	-9,4	-7,5
MG-8	5,6	6,2	-9,9	-5,3	-5,6	-5,0

Table 12. Horizontal displacements of the pylon's top (with a stiffening girder)

Symbol of the measuring device	Experimental results (R_E), calculated results (R_C) and their differences ($\Delta R_{E/C}$)					
	T-2.1			T-2.2		
	R_E [mm]	R_C [mm]	$\Delta R_{E/C}$ [%]	R_E [mm]	R_C [mm]	$\Delta R_{E/C}$ [%]
DG-1	0,0	0,0	0,0	4,4	4,6	-4,9

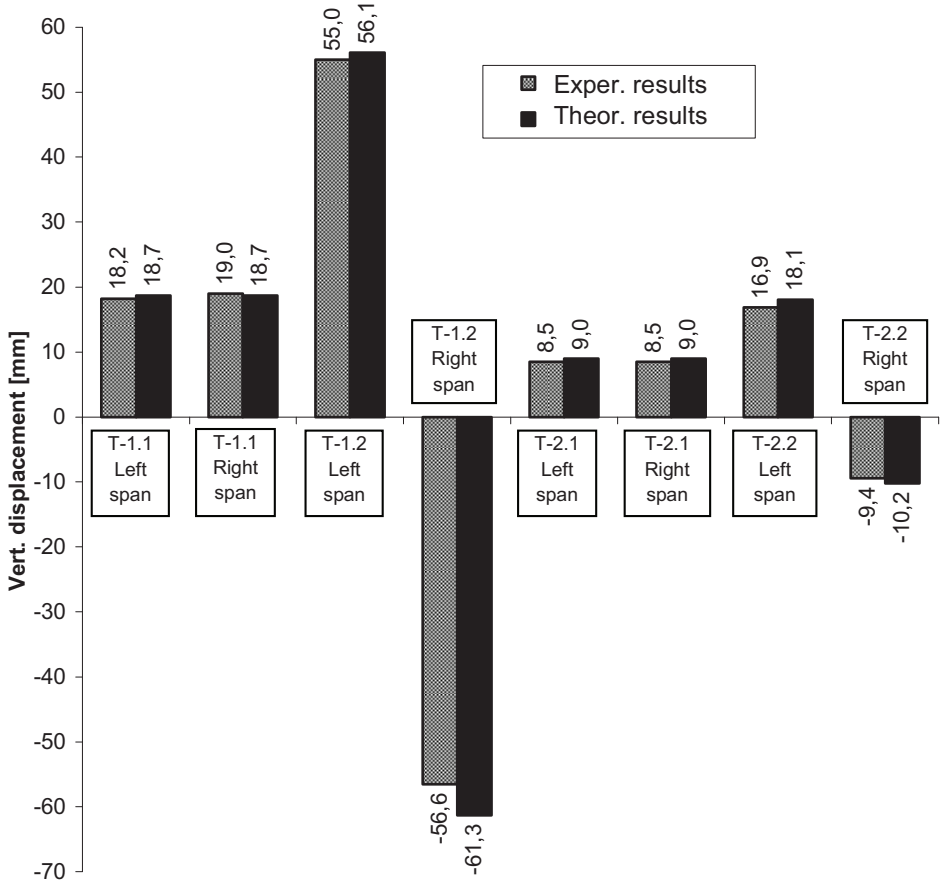

Figure 23. Differences between experimental results and theoretical calculations of the maximum vertical displacements of the cable's nodal points (the loads are characterised in Figure 20 and Tables 5…6)

CONCLUSION AND RECOMMENDATIONS FOR FURTHER RESEARCH

In this thesis an algorithm has been worked out to calculate the internal forces and deformations of a statically loaded single-pylon suspension bridge, using discrete and, to a small extent, continuous mathematical structures. Analytic and numerical methods of discrete analysis are used to calculate the cable. The behaviour of the stiffening girder is described using continuous analysis. The calculation examples are added to illustrate and explain the theoretical part and a model test in scale 1:25 has been carried out to check the validity of the developed calculation method.

It is complicated to use an exact analysis of the cable because numerous cubic and quartic equations are needed to be solved and no usable analytic solutions are available. Therefore, simplifications have been made and two numerical methods worked out in this thesis.

The following simplifications have been made to calculate the cable:

a) In the conditions of equilibrium of the cable's nodal points: $a_{0,i} + (u_{i+1} - u_i) \approx a_{0,i}$.

b) In the equations of the relative deformation of the cable's segments: $\left[a_{0,i} + (u_{i+1} - u_i)\right]^3 \approx a_{0,i}^3 + 3a_{0,i}^2(u_{i+1} - u_i) + 3a_{0,i}(u_{i+1} - u_i)^2$ and $\left[a_{0,i} + (u_{i+1} - u_i)\right]^4 \approx a_{0,i}^4 + 4a_{0,i}^3(u_{i+1} - u_i) + 6a_{0,i}^2(u_{i+1} - u_i)^2$.

Conclusions based on the calculation methods:

- The one-level iterative process uses both of the simplifications described above. If the vertical deflection of the cable is relatively small (experiments and the calculations showed that it should be less than $L/200$), it is accurate enough to use this method to calculate the vertical deflections and the internal forces of the cable. It is not recommended to calculate the horizontal displacements of the cable's nodal points (except the cable's supports) using this method.
- The full two-level iterative process worked out in this thesis uses simplifications only in the equations of the relative deformation of the cable's segments. If $(u_{i+1} - u_i)/a_{0,i} < 0{,}1$, this method leads to almost exact results. The disadvantage of this method is that it requires high computational efficiency.
- The variable modulus of elasticity of the cable should be taken into account. If the modulus changes during the loading only in the range of some percent, the variability of the calculation results of the internal

forces and the deflections are in the same magnitude with the calculation accuracy and the effect can be neglected.

Conclusions resulting from the load-testing:

- The test results verified the credibility of the test model. The results of each test varied at a maximum of ±1% from the average, being mostly between –0,2% and +0,2%. The average difference between single test results and mean results was 0,0%.
- The difference of the single results of the tests and the calculations were between +2,2...–12,6%. The measured results (the deflection of the cable, the internal force of the cable and the horizontal displacement of the pylon's top) were on average –4,4% smaller than the calculations predicted, proving well that the numerical calculation method worked out in this thesis is applicable.

Recommendations for further research:

- It is inconvenient to determine the internal forces of the hangers in the case of unsymmetrical loads at the bridge deck. An algorithm should be developed to make this process as effective as possible.
- It is complicated to use the exact analytical discrete analysis because of numerous quartic equations. The computer software should be improved to solve this problem.

The greatest advantage of the discrete analysis is that it is easy to describe different load types and load combinations. The most important disadvantage is the necessity to calculate difficult systems of equations and very often these systems converge slowly. Because of the high accuracy of the calculations and the fast development of digital computers, discrete analysis has a substantial role in the calculations of the long-span cable-supported structures.

REFERENCES

Aare, J., Kulbach, V. 1984. Accurate and Approximate Analysis of Statical Behaviour of Suspension Bridges. – Journal of Structural Mechanics, vol 17 (no 3), p. 1-12.

Bangash, M. Y. H. 1999. Suspension and Cable-Stayed Bridges: Prototype Bridge Structures. London: Thomas Telford Publishing.

Breuer, S., Zwas, G. 1993. Numerical mathematics – a laboratory approach. Cambridge: Cambridge University Press.

Chapra, S. C., Raymond, R. P. 2006. Numerical methods for engineers. Fifth edition. New York: McGraw-Hill.

Chen, W.-F., Duan, L. 1999. Bridge Engineering Handbook. Florida: CRC Press LCL.

Fürst, A., Marti, P., Ganz, H. R. 2001. Bending of stay cables. – Structural Engineering International, vol 11 (no 1), p. 42–46.

Gimsing, N. J. 1997. Cable Supported Bridges: Concept and Design. Second edition. Chichester: John Wiley & Sons.

Grigorjeva, T., Juozapaitis, A., Kamaitis, Z. 2004. Structural analysis of suspension bridges with varying rigidity of main cables. *In:* Proceedings of the 8th International Conference Modern Building Materials, Structures and Techniques. Vilnius: Technika, p. 469–472.

Grigorjeva, T., Juozapaitis, A., Kamaitis, Z. 2006. Simplified engineering design method of suspension bridges with rigid cables under action symmetrical and asymmetrical loads. – The Baltic Journal of Road and Bridge Engineering, vol 1 (no 1), p. 11–20.

Grigorjeva, T., Juozapaitis, A., Kamaitis, Z. 2010. Influence of construction method on the behaviour of suspension bridges with main rigid cables. *In:* Proceedings of the 10th International Conference Modern Building Materials, Structures and Techniques. Vilnius: Technika, p. 628–634.

Grigorjeva, T., Juozapaitis, A., Kamaitis, Z. 2010. Static analysis and simplified design of suspension bridges having various rigidity of cables. – Journal of Civil Engineering and Management, vol 16 (no 3), p. 363–371.

Idnurm, J. 2004. Discrete Analysis of Cable-Supported Bridges. Tallinn: TUT Press.

Idnurm, J., Kiisa, M., Idnurm, S. 2009. Discrete analysis for classical and single-pylon suspension bridges. *In:* Proceedings of the Twelfth International Conference on Civil, Structural and Environmental Engineering Computing. Stirlingshire: Civil-Comp Press, paper 218.

Janno, J. 2008. Arvutusmeetodid. Tallinn: TTÜ Kirjastus.

Juozopaitis, A., Idnurm, S., Kaklauskas, G., Idnurm, J., Gribniak, V. 2010. Non-linear analysis of suspension bridges with flexible and rigid cables. – Journal of Civil Engineering and Management, vol 16 (no 1), p. 149–154.

Jürgenson, A. 1985. Tugevusõpetus. Tallinn: Valgus.
Kiisa, M. 2003. Ühe pülooniga Tartu jalakäijate rippsilla töö uurimine. (*Bakalaureusetöö Tallinna Tehnikaülikoolis*).
Kiisa, M. 2005. Ühe pülooniga jalakäijate rippsilla töö eksperimentaalne uurimine. (*Magistritöö Tallinna Tehnikaülikoolis*).
Kirs, J., Arjassov, G. 1999. Sissejuhatus lõplike elementide meetodisse: I osa. Tallinn: TTÜ Kirjastus.
Kivi, E. 2009. Structural Behavior of Cable-Stayed Suspension Bridge Structure. Tallinn: TUT Press.
Kulbach, V. 2007. Cable Structures: Design and Static Analysis. Tallinn: Estonian Academy Publishers.
Kulbach, V. 2007. Kaabelkonstruktsioonidest Eestis ja maailmas Tallinna Tehnikaülikooli uurimistööde taustal. – Teadusmõte Eestis (IV): tehnikateadused (II). Tallinn: Eesti Teaduste Akadeemia, lk 49–63.
Lahe, A. 1998. Lõplike elementide meetod. Tallinn: TTÜ Kirjastus.
Lensen, H., Kruus, M. 2006. Diskreetne matemaatika. Kolmas, parandatud ja täiendatud trükk. Tallinn: TTÜ Kirjastus.
Leonard, J. W. 1988. Tension Structures – Behavior & Analysis. New York: R. R. Donnelley & Sons Company.
Lovasz, L., Pelikan, J., Vesztergombi, K. 2003. Discrete mathematics: elementary and beyond. New York: Springer-Verlag New York, Inc.
Matve, H. 1978. Sillad läbi aegade. Tallinn: Valgus.
Palm, R. 2003. Diskreetse matemaatika elemendid. Tartu: Tartu Ülikooli Kirjastuse trükikoda.
Rohusaar, J. 2005. Tugevusõpetus ehitajatele. Tallinn: Tallinna Tehnikakõrgkool.
Tang, M.-C. 2010. The story of world record spans. – Civil Engineering, March 2010, p. 57–63.
Tärno, Ü. 2003. Ehituslike ruumstruktuuride mudelkatsetused. Tallinn: TTÜ Kirjastus.
Vaarmann, O. 2005. Arvutusmeetodid. Tallinn: TTÜ Kirjastus.
Virola, J. 1999. Maailma suurimad sillad. – Keskkonnatehnika, nr 5, lk 30–38.
Virola, J. 1999. Maailma suurimad sillad (II). – Keskkonnatehnika, nr 6, lk 38–42.
Virola, J. 2002. Akashi-Kaikyo – möödunud aastatuhande suurim. – Keskkonnatehnika, nr 3, lk 20–24.
Virola, J. 2002. Kolm Tacoma silda. – Keskkonnatehnika, nr 6, lk 16–19.
Õiger, K. 1992. Actual Behaviour, Analysis and Design of Thin Saddle-Shaped Shell Roofs. Tampere: Tampere University of Technology.

Долидзе, Д. Е. 1975. Испытание конструкций и сооружений. Москва: Высшая школа.
Кирсанов, Н. М. 1981. Висячие и вантовые конструкции. Москва: Стройиздат.

Кульбах, В. 1973. Анализ статической работы предварительно напряженных сетчатых висячих покрытий с деформируемым контуром. Таллин: Таллинский Политехнический Институт.
Кульбах, В., Ыйгер, К. 1986. Статический расчет висячих систем. Таллин: Таллинский Политехнический Институт.
Мянд, У. 1974. Определение основных параметров седловидных висячих покрытий. Таллин: Таллинский Политехнический Институт.
Питлюк, Д. А. 1971. Испытание строительных конструкций на моделях. Ленинград: Издательство литературы по строительству.
Равасоо, А. 1971. Исследование работы висячих покрытий гиперболо-параболической формы. 1971. Таллин: Таллинский Политехнический Институт.
Тальвик, А. 1982. Исследование статической работы висячего покрытия с контуром из прямолинейных стержней. Таллин: Таллинский Политехнический Институт.
Тальвик, И. 1990. Определение динамических характеристик и ветровых нагрузок седловидных висячих покрытий. Таллин: Таллинский Политехнический Институт.
Энгельбрехт, Ю. 1968. Расчет и исследование работы висячих покрытий отрицательной кривизны с перекрестной сеткой тросов. Таллин: Таллинский Политехнический Институт.

AUTHOR'S PUBLICATIONS

Kiisa, M., Idnurm, J., Idnurm, S. 2011. Discrete analysis of the elastic cable. – The Baltic Journal of Road and Bridge Engineering. *(Accepted for publishing on 21.04.2011)*

Kiisa, M. 2010. Kaabli mittelineaarne analüüs *(Non-linear Analysis of the Cable)*. – Tallinna Tehnikakõrgkooli Toimetised, no 13, p. 57–67.

Kiisa, M., Idnurm, J., Idnurm, S. 2009. Discrete analysis for single pylon suspension bridges. – Engineering Structures and Technologies, vol 1 (no 4), p. 166–171.

Idnurm, J., Kiisa, M., Idnurm, S. 2009. Discrete analysis for classical and single-pylon suspension bridges. *In:* Proceedings of the Twelfth International Conference on Civil, Structural and Environmental Engineering Computing. Stirlingshire: Civil-Comp Press, paper 218.

Kiisa, M. 2006. Vantsilla mudeli katsetamine *(Experimental Investigation of the Cable-Stayed Bridge)*. – Tallinna Tehnikakõrgkooli Toimetised, no 9, p. 33–39.

APPENDIX 1

Photos of the test model

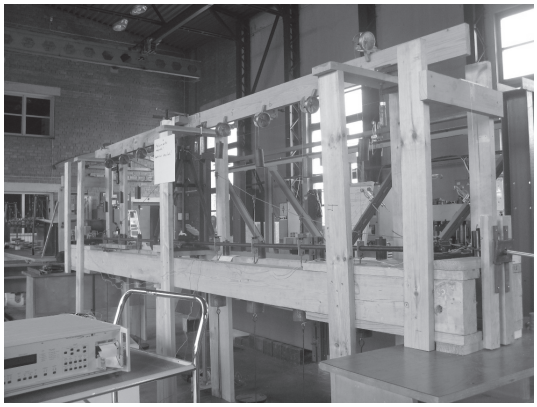

Figure A.1.1. Overview of the model

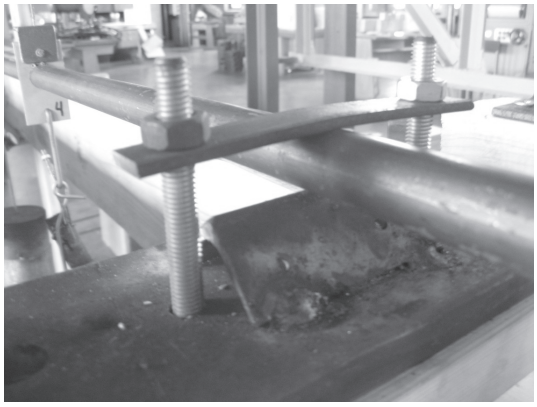

Figure A.1.2. Support of the stiffening girder (in the middle)

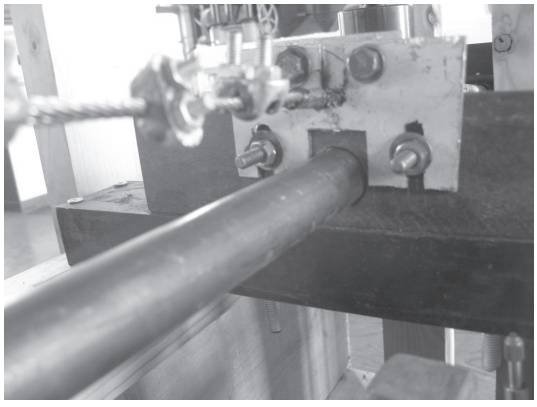

Figure A.1.3. Support of the stiffening girder (at the start and the end)

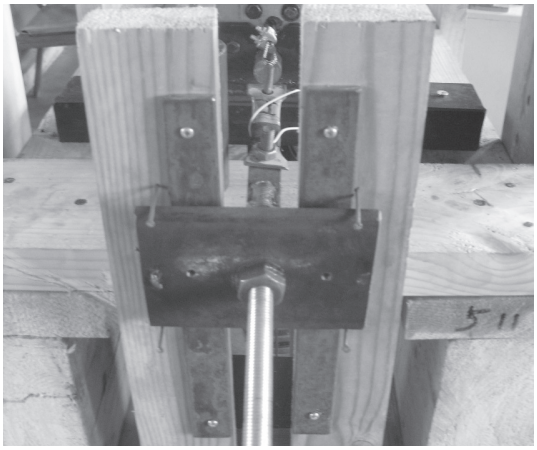

Figure A.1.4. Foundation of the cable

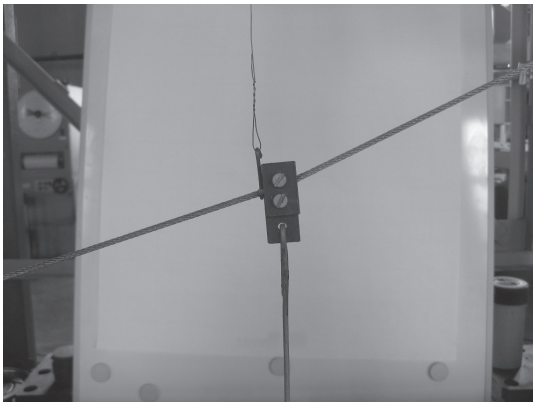

Figure A.1.5. Connection of the hanger and the cable

Figure A.1.6. Measurement of the deflections of the bearing frame

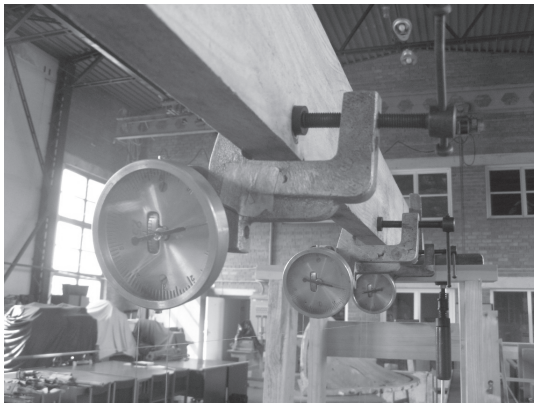

Figure A.1.7. Maksimov's gauges for measuring the vertical deflections of the cable

Figure A.1.8. Dial gauge for measuring the horizontal displacements of the pylon

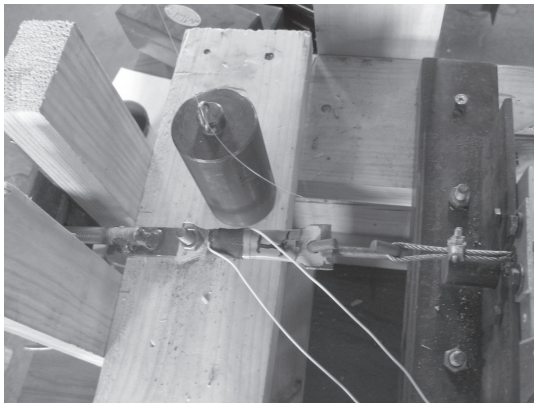

Figure A.1.9. Ttrain gauges for measuring the elongation of the cable

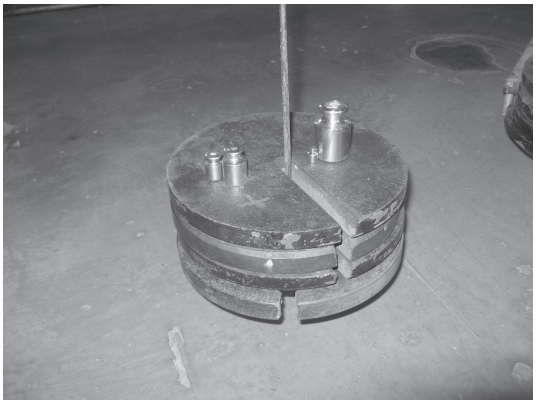

Figure A.1.10. Loading of the test model

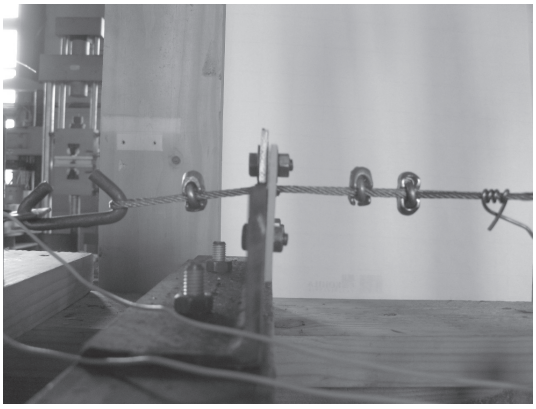

Figure A.1.11. Large deformations of the cable without the stiffening girder

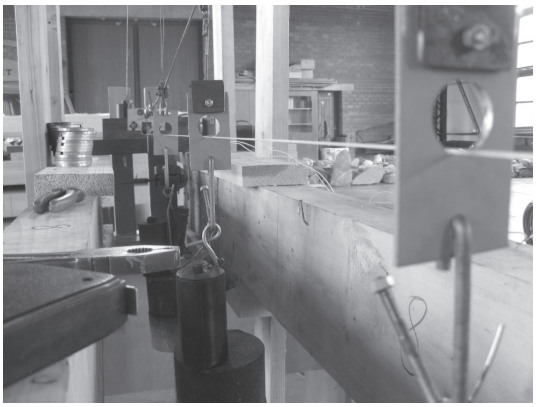

Figure A.1.12. Regulation of the test model

Figure A.1.13. Deformed stiffening girder in the unloaded span

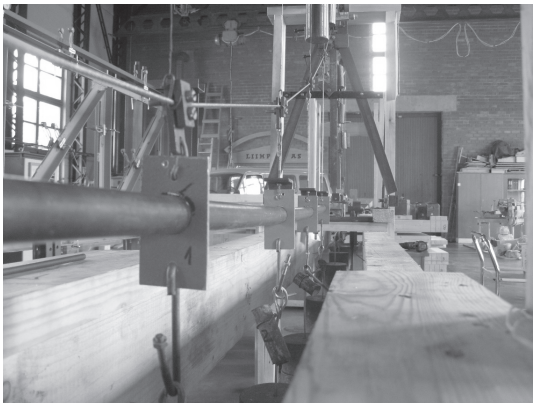

Figure A.1.14. Deformed stiffening girder in the loaded span

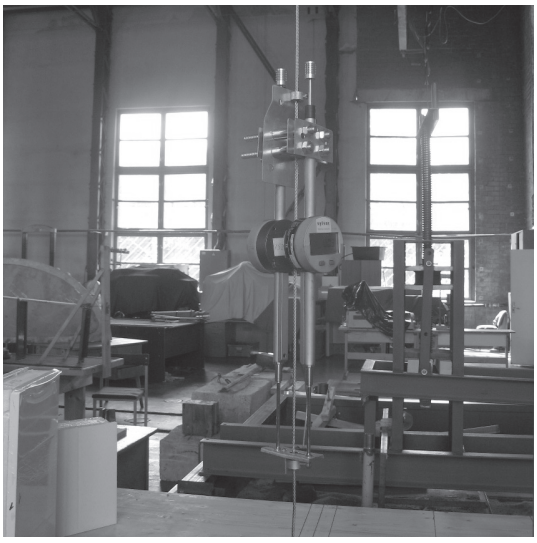

Figure A.1.15. Testing of the cable's modulus of elasticity

APPENDIX 2

Results of the load tests

*Table A.2.1. Results of the load test T-1.1**

Symbol of the meas. device	Test 1		Test 2		Test 3		Test 4		Test 5		Aver. result
	Test result	Differ. from aver. result [%]	Test result	Differ. from aver. result [%]	Test result	Differ. from aver. result [%]	Test result	Differ. from aver. result [%]	Test result	Differ. from aver. result [%]	
SG-1	165	-0,1	165	-0,1	165	-0,1	165	-0,1	166	0,5	165,2
SG-2	188	-0,3	188	-0,3	189	0,2	189	0,2	189	0,2	188,6
MG-1	12,5	0,2	12,45	-0,2	12,4	-0,6	12,55	0,6	12,5	0,2	12,48
MG-2	18,25	0,2	18,15	-0,3	18,15	-0,3	18,3	0,5	18,2	-0,1	18,21
MG-3	18,0	0,3	17,95	0,0	17,85	-0,6	18,0	0,3	17,95	0,0	17,95
MG-4	11,65	-0,3	11,7	0,1	11,7	0,1	11,7	0,1	11,7	0,1	11,69
MG-5	11,95	-0,3	12,05	0,6	12,05	0,6	11,9	-0,7	11,95	-0,3	11,98
MG-6	18,7	0,5	18,65	0,3	18,7	0,5	18,45	-0,8	18,5	-0,5	18,60
MG-7	19,1	0,6	19,05	0,4	19,0	0,1	18,8	-0,9	18,95	-0,2	18,98
MG-8	12,65	0,8	12,6	0,4	12,55	0,0	12,45	-0,8	12,5	-0,4	12,55
DG-1	-0,01	-	-0,01	-	-0,03	-	0,03	-	0,01	-	0,00

* The description of the test model and the loads (load combinations) are presented in Figures 18…20 and Tables 4…6

*Table A.2.2. Results of the load test T-1.2**

Symbol of the meas. device	Test 1		Test 2		Test 3		Test 4		Test 5		Aver. result
	Test result	Differ. from aver. result [%]	Test result	Differ. from aver. result [%]	Test result	Differ. from aver. result [%]	Test result	Differ. from aver. result [%]	Test result	Differ. from aver. result [%]	
SG-1	102	-0,8	102	-0,8	103	0,2	103	0,2	104	1,2	102,8
SG-2	128	-0,9	128	-0,9	130	0,6	130	0,6	130	0,6	129,2
MG-1	37,4	-0,2	37,5	0,1	37,45	0,0	37,5	0,1	37,45	0,0	37,46
MG-2	55,0	0,0	54,95	-0,1	55,0	0,0	55,0	0,0	54,95	-0,1	54,98
MG-3	52,8	0,0	52,75	-0,1	52,8	0,0	52,8	0,0	52,75	-0,1	52,78
MG-4	33,55	0,1	33,5	-0,1	33,55	0,1	33,5	-0,1	33,5	-0,1	33,52
MG-5	-35,75	0,1	-35,7	0,0	-35,7	0,0	-35,7	0,0	-35,7	0,0	-35,71
MG-6	-55,15	-0,1	-55,2	0,0	-55,2	0,0	-55,2	0,0	-55,25	0,1	-55,20
MG-7	-56,55	0,0	-56,6	0,1	-56,55	0,0	-56,55	0,0	-56,55	0,0	-56,56
MG-8	-37,6	-0,1	-37,65	0,1	-37,65	0,1	-37,6	-0,1	-37,6	-0,1	-37,62
DG-1	19,24	0,3	19,24	0,3	19,12	-0,4	19,23	0,2	19,11	-0,4	19,19

* The description of the test model and the loads (load combinations) are presented in Figures 18…20 and Tables 4…6

*Table A.2.3. Results of the load test T-2.1**

Symbol of the meas. device	Test 1		Test 2		Test 3		Test 4		Test 5		Aver. result
	Test result	Differ. from aver. result [%]	Test result	Differ. from aver. result [%]	Test result	Differ. from aver. result [%]	Test result	Differ. from aver. result [%]	Test result	Differ. from aver. result [%]	
SG-1	62	0,6	62	0,6	62	0,6	61	-1,0	61	-1,0	61,6
SG-2	69	0,6	68	-0,9	69	0,6	69	0,6	68	-0,9	68,6
MG-1	5,7	-0,3	5,7	-0,3	5,7	-0,3	5,75	0,5	5,75	0,5	5,72
MG-2	8,45	-0,2	8,45	-0,2	8,45	-0,2	8,5	0,4	8,5	0,4	8,47
MG-3	7,25	-0,5	7,25	-0,5	7,25	-0,5	7,35	0,8	7,35	0,8	7,29
MG-4	3,0	-0,7	3,0	-0,7	3,0	-0,7	3,05	1,0	3,05	1,0	3,02
MG-5	2,85	0,7	2,85	0,7	2,85	0,7	2,8	-1,1	2,8	-1,1	2,83
MG-6	7,1	0,6	7,1	0,6	7,1	0,6	7,0	-0,8	7,0	-0,8	7,06
MG-7	8,55	0,7	8,55	0,7	8,55	0,7	8,4	-1,1	8,4	-1,1	8,49
MG-8	5,6	0,5	5,6	0,5	5,55	-0,4	5,55	-0,4	5,55	-0,4	5,57
DG-1	0,01	-	0,01	-	0,02	-	0,05	-	0,05	-	0,03

* The description of the test model and the loads (load combinations) are presented in Figures 18…20 and Tables 4…6

*Table A.2.4. Results of the load test T-2.2**

Symbol of the meas. device	Test 1		Test 2		Test 3		Test 4		Test 5		Aver. result
	Test result	Differ. from aver. result [%]	Test result	Differ. from aver. result [%]	Test result	Differ. from aver. result [%]	Test result	Differ. from aver. result [%]	Test result	Differ. from aver. result [%]	
SG-1	37	0,0	37	0,0	37	0,0	37	0,0	37	0,0	37,0
SG-2	39	1,0	39	1,0	39	1,0	38	-1,6	38	-1,6	38,6
MG-1	11,05	-0,6	11,15	0,3	11,1	-0,2	11,2	0,7	11,1	-0,2	11,12
MG-2	16,9	0,1	16,9	0,1	16,85	-0,2	16,9	0,1	16,9	0,1	16,89
MG-3	16,6	0,2	16,55	-0,1	16,55	-0,1	16,55	-0,1	16,6	0,2	16,57
MG-4	9,75	0,0	9,75	0,0	9,75	0,0	9,75	0,0	9,75	0,0	9,75
MG-5	-6,85	-0,3	-6,85	-0,3	-6,9	0,4	-6,85	-0,3	-6,9	0,4	-6,87
MG-6	-9,4	-0,4	-9,4	-0,4	-9,45	0,1	-9,45	0,1	-9,5	0,6	-9,44
MG-7	-8,7	-0,3	-8,75	0,2	-8,7	-0,3	-8,7	-0,3	-8,8	0,8	-8,73
MG-8	-5,3	-0,6	-5,3	-0,6	-5,35	0,4	-5,35	0,4	-5,35	0,4	-5,33
DG-1	4,37	0,0	4,37	0,0	4,36	-0,2	4,36	-0,2	4,38	0,3	4,37

* The description of the test model and the loads (load combinations) are presented in Figures 18…20 and Tables 4…6

APPENDIX A

Curriculum Vitae

1. Personal data

Name: Martti Kiisa
Date and place of birth: 28.10.1979, Tallinn
Nationality: Estonian

2. Contact information

Address: Pärnu Road 62, Tallinn 10135
Phone: +372 5299321
E-mail: martti.kiisa@mail.ee

3. Education

Educational institution	*Graduation year*	*Education (field of study/degree)*
Tallinn University of Technology	2005	Construction engineering / Master of Sciences
Tallinn University of Technology	2003	Construction engineering / Bachelor of Sciences

4. Language competence/skills

Language	*Level*
Estonian	Native language
English	Average skills
Russian	Average skills
German	Basic skills

5. Professional Employment

Period	*Organisation*	*Position*
2005– to date	Estonian Road Administration	Chief specialist of bridges
2003– to date	Tallinn University of Applied Sciences	2009– Associate Professor 2004–2009 Lecturer 2003–2004 Assistant
2000–2003	Tesman AS	Work superintendet

6. Publications

Kiisa, M., Idnurm, J., Idnurm, S. 2011. Discrete analysis of the elastic cable. – The Baltic Journal of Road and Bridge Engineering. *(Accepted for publishing on 21.04.2011)*

Kiisa, M. 2010. Kaabli mittelineaarne analüüs *(Non-linear Analysis of the Cable)*. – Tallinna Tehnikakõrgkooli Toimetised, no 13, p. 57–67.

Kiisa, M., Idnurm, J., Idnurm, S. 2009. Discrete analysis for single pylon suspension bridges. – Engineering Structures and Technologies, vol 1 (no 4), p. 166–171.

Idnurm, J., Kiisa, M., Idnurm, S. 2009. Discrete analysis for classical and single-pylon suspension bridges. *In:* Proceedings of the Twelfth International Conference on Civil, Structural and Environmental Engineering Computing. Stirlingshire: Civil-Comp Press, paper 218.

Kiisa, M. 2006. Vantsilla mudeli katsetamine *(Experimental Investigation of the Cable-Stayed Bridge)*. – Tallinna Tehnikakõrgkooli Toimetised, no 9, p. 33–39.

7. Defended theses

Year	*Level*	*Thesis*
2005	Master's thesis	The Experimental Study of the Single-Pylon Pedestrian Suspension Bridge
2003	Bachelor's thesis	The Investigation of the Single-Pylon Pedestrian Suspension Bridge in Tartu

8. Main areas of scientific work

Non-linear discrete analysis of the cable-supported structures.

APPENDIX B

Elulookirjeldus

1. Isikuandmed

Ees- ja perekonnanimi: Martti Kiisa
Sünniaeg ja -koht: 28.10.1979, Tallinn
Kodakondsus: Eesti

2. Kontaktandmed

Aadress: Pärnu mnt 62, Tallinn 10135
Telefon: +372 5299321
E-post: martti.kiisa@mail.ee

3. Hariduskäik

Õppeasutus	*Lõpetamise aeg*	*Haridus (eriala/kraad)*
Tallinna Tehnikaülikool	2005	Ehitustehnika / tehnikateaduste magister
Tallinna Tehnikaülikool	2003	Ehitustehnika / tehnikateaduste bakalaureus

4. Keelteoskus

Keel	*Tase*
Eesti	Emakeel
Inglise	Kesktase
Vene	Kesktase
Saksa	Algtase

5. Teenistuskäik

Töötamise aeg	*Tööandja nimetus*	*Ametikoht*
2005– tänaseni	Maanteeamet	Sildade peaspetsialist
2003– tänaseni	Tallinna Tehnikakõrgkool	2009– Dotsent 2004–2009 Lektor 2003–2004 Assistent
2000–2003	Tesman AS	Töödejuhataja

6. Publikatsioonid

Kiisa, M., Idnurm, J., Idnurm, S. 2011. Discrete analysis of the elastic cable. – The Baltic Journal of Road and Bridge Engineering. *(Kinnitus avaldamiseks: 21.04.2011)*

Kiisa, M. 2010. Kaabli mittelineaarne analüüs. – Tallinna Tehnikakõrgkooli Toimetised, nr 13, lk 57–67.

Kiisa, M., Idnurm, J., Idnurm, S. 2009. Discrete analysis for single pylon suspension bridges. – Engineering Structures and Technologies, vol 1 (no 4), p. 166–171.

Idnurm, J., Kiisa, M., Idnurm, S. 2009. Discrete analysis for classical and single-pylon suspension bridges. *In:* Proceedings of the Twelfth International Conference on Civil, Structural and Environmental Engineering Computing. Stirlingshire: Civil-Comp Press, paper 218.

Kiisa, M. 2006. Vantsilla mudeli katsetamine. – Tallinna Tehnikakõrgkooli Toimetised, nr 9, lk 33–39.

7. Kaitstud lõputööd

Aasta	*Lõputöö tase*	*Lõputöö pealkiri*
2005	Magistritöö	Ühe pülooniga jalakäijate rippsilla töö eksperimentaalne uurimine
2003	Bakalaureusetöö	Ühe pülooniga Tartu jalakäijate rippsilla töö uurimine

8. Teadustöö põhisuunad

Kaabeltoestatud konstruktsioonide mittelineaarne diskreetne analüüs.

ABSTRACT

The present thesis is a continuation of the research on cable-supported structures (roofs, hoisting masts, bridges), which started at the end of the 1950s at Tallinn University of Technology.

The aim of the doctoral thesis is to present an algorithm to calculate the internal forces and deformations of a statically loaded single-pylon suspension bridge by use of discrete and, to a small extent, continuous mathematical structures. Although discrete analysis requires high computational efficiency, it is possible to consider more precisely the complicated load combinations and types. It is complicated to use an analytic discrete analysis because numerous cubic and quartic equations are needed to be solved. Therefore, simplifications have been made here and two numerical methods worked out.

Suspension bridges are structures with the longest span worldwide. Structures like these have usually large deformations and to obtain sufficiently precise calculation results, it is inevitable to consider geometric non-linearity. The thesis is focused on the classical suspension bridges where the main cables are anchored in the ground, the hangers are vertical and the main cables are stiffened only by stiffening girders.

In addition, the thesis includes calculation examples to illustrate and explain the theoretical part. A model test in scale 1:25 has been carried out to check the validity of the developed calculation method.

Keywords: discrete analysis, geometrical non-linearity, cable-supported structure, suspension bridge, load test

RESÜMEE

Käesolev doktoritöö on jätkuks Tallinna Tehnikaülikoolis 1950ndate lõpus alanud kaabeltoestatud konstruktsioonidega (katused, tõstemastid, sillad) seotud uurimistöödele.

Töö põhieesmärgiks on välja töötada meetod arvutamaks staatiliselt koormatud ühe pülooniga rippsilla sisejõude ja deformatsioone kasutades diskreetseid ja vähesel määral ka pidevaid matemaatilisi struktuure. Kuigi diskreetne analüüs nõuab suurt arvutusjõudlust, on sellega võimalik täpselt arvesse võtta keerulisi koormusi ja nende kombinatsioone. Analüütilist diskreetset analüüsi on keeruline kasutada, kuna tuleb lahendada suurel hulgal kolmanda ja neljanda astme võrrandeid. Siinkohal on tehtud lihtsustusi ja välja töötatud kaks numbrilist meetodit probleemi lahendamiseks.

Rippsillad on suurima sildeavaga ehitised maailmas. Sellistes ehitus-konstruktsioonides esinevad suured deformatsioonid ja täpsete arvutustulemuste saamiseks on geomeetriliselt mittelineaarse käitumise arvessevõtmine hädavajalik. Töös on keskendutud klassikalistele rippsildadele, mille peakaablid on ankurdatud eraldi maasse, riputid on vertikaalsed ja peakaablid on jäigastatud jäikustaladega.

Teoreetilise lahenduskäigu illustreerimiseks on töösse lisatud ka arvutusnäited ja läbi on viidud mudelkatsetus mõõtkavas 1:25 kontrollimaks arendatud arvutusmeetodit.

Märksõnad: diskreetne analüüs, geomeetriline mittelineaarsus, kaabeltoestatud konstruktsioon, rippsild, koormustest

DISSERTATIONS DEFENDED AT TALLINN UNIVERSITY OF TECHNOLOGY ON *CIVIL ENGINEERING*

1. **Heino Mölder**. Cycle of investigations to improve the efficiency and reliability of activated sludge process in sewage treatment plants. 1992.

2. **Stellian Grabko**. Structure and properties of oil-shale Portland cement concrete. 1993.

3. **Kent Arvidsson**. Analysis of interacting systems of shear walls, coupled shear walls and frames in multi-storey buildings. 1996.

4. **Andrus Aavik**. Methodical basis for the evaluation of pavement structural strength in Estonian Pavement Management System (EPMS). 2003.

5. **Priit Vilba**. Unstiffened welded thin-walled metal girder under uniform loading. 2003.

6. **Irene Lill.** Evaluation of Labour Management Strategies in Construction. 2004.

7. **Juhan Idnurm**. Discrete analysis of cable-supported bridges. 2004.

8. **Arvo Iital**. Monitoring of Surface Water Quality in Small Agricultural Watersheds. Methodology and optimization of monitoring network. 2005.

9. **Liis Sipelgas**. Application of satellite data for monitoring the marine environment. 2006.

10. **Ott Koppel**. Infrastruktuuri arvestus vertikaalselt integreeritud raudtee-ettevõtja korral: hinnakujunduse aspekt (Eesti peamise raudtee-ettevõtja näitel). 2006.

11. **Targo Kalamees**. Hygrothermal criteria for design and simulation of buildings. 2006.

12. **Raido Puust**. Probabilistic leak detection in pipe networks using the SCEM-UA algorithm. 2007.

13. **Sergei Zub**. Combined treatment of sulfate-rich molasses wastewater from yeast industry. Technology optimization. 2007.

14. **Alvina Reihan**. Analysis of long-term river runoff trends and climate change impact on water resources in Estonia. 2008.

15. **Ain Valdmann**. On the coastal zone management of the city of Tallinn under natural and anthropogenic pressure. 2008.

16. **Ira Didenkulova**. Long wave dynamics in the coastal zone. 2008.

17. **Alvar Toode**. DHW consumption, consumption profiles and their influence on dimensioning of a district heating network. 2008.

18. **Annely Kuu**. Biological diversity of agricultural soils in Estonia. 2008.

19. **Andres Tolli**. Hiina konteinerveod läbi Eesti Venemaale ja Hiinasse tagasisaadetavate tühjade konteinerite arvu vähendamise võimalused. 2008.

20. **Heiki Onton**. Investigation of the causes of deterioration of old reinforced concrete constructions and possibilities of their restoration. 2008.

21. **Harri Moora**. Life cycle assessment as a decision support tool for system optimisation – the case of waste management in Estonia. 2009.

22. **Andres Kask**. Lithohydrodynamic processes in the Tallinn Bay area. 2009.

23. **Loreta Kelpšaitė**. Changing properties of wind waves and vessel wakes on the eastern coast of the Baltic Sea. 2009.

24. **Dmitry Kurennoy.** Analysis of the properties of fast ferry wakes in the context of coastal management. 2009.

25. **Egon Kivi**. Structural behavior of cable-stayed suspension bridge structure. 2009.

26. **Madis Ratassepp**. Wave scattering at discontinuities in plates and pipes. 2010.

27. **Tiia Pedusaar**. Management of lake Ülemiste, a drinking water reservoir. 2010.

28. **Karin Pachel**. Water resources, sustainable use and integrated management in Estonia. 2010.

29. **Andrus Räämet**. Spatio-temporal variability of the Baltic Sea wave fields. 2010.

30. **Alar Just**. Structural fire design of timber frame assemblies insulated by glass wool and covered by gypsum plasterboards. 2010.

31. **Toomas Liiv**. Experimental Analysis of Boundary Layer Dynamics in Plunging Breaking Wave. 2011.